Changes in archaeal and bacterial community composition following entombment in halite crystals

Tom J. C. Huby

A thesis submitted for degree of MSc by Dissertation

Department of Biological Sciences

University of Essex

October 2018

Summary

The general aim of this project was to identify whether microorganisms from salt-saturated brines are preferentially entombed inside halite brine inclusions. This involved direct comparison of microbial communities (Archaea and Bacteria) in *in-situ* brine and halite samples collected from Trapani Salterns in Sicily, as well as, comparison between parent brines and experimentally-entombed halite communities over a course of 21-weeks.

Quantification of archaeal and bacterial numbers showed that Archaea are exceptionally more abundant in both brine and halite, and that Bacteria are about 0.25% of the overall community in both conditions. Remarkably, few differences were observed in terms of abundance and community structure between communities in 21-week-old halite and those found in the parent brines. Evidently, all organisms of a mixed microbial community are entombed equally and most that are trapped in this way are capable of surviving inside halite for short to moderate lengths of time. This is presumably due to a complex web of interspecies interactions, co-operations and the sharing of usable metabolites.

Nevertheless, some organisms are poor survivors inside halite and showed a decrease in their relative abundance in halite. In this study, this was highlighted by the decreased abundance of *Haloquadratum, Candidatus* Nanosalina and Cyanobacteria VII inside halite.

Finally, comparisons made between communities from different Pond (brine) origins showed some significant differences and suggests that communities in halite can vary considerably depending on the environmental conditions (e.g. ionic composition and water activity) at the point of halite precipitation.

Acknowledgements

First and foremost, I would like to give a huge thank you to my supervisor Dr. Terry McGenity, for providing me with the opportunity to work on this fantastic project, and for his continued patience, support and kind offerings of over-ripened office fruit.

Secondly, I would like to thank Dr. Boyd McKew and Dr. Dave Clark, for their invaluable help and contribution to this project. Without their participation, I might not have had any sequencing data to work with, and would likely have been lost in a sea of bioinformatics, statistics, and botched attempts at using R.

Thirdly, I would like to say a big thank you to the inhabitants of 5.28 for making my time spent in the lab so enjoyable, in particular Shivani Patel (for her weird ways and mad laughter) and both Claudia Saenz and Duncan Sweeney (for nights I don't quite remember, but know that I had fun).

I would also like to give thanks to Farid Benyahia for his consistent support in the lab, and to John Green and Tania Cresswell-Maynard for their technical support.

Lastly, I would like to give a special thank you to my parents, grandparents and girlfriend for their continued encouragement, and for putting up with me in my grumpiest of moments.

Fieldwork was supported by funds from the European Cooperation in Science and Technology (COST) Action CA15103, "Uncovering the Mediterranean salt giant (MEDSALT)".

Contents

1 Introduction

Over the past several decades our understanding of life in extreme environments has progressed considerably. Further advances in culture-independent techniques and the discovery of new extremophilic organisms have expanded dramatically the list of known microbial habitats. Microbial life has been found to thrive in environments at the polar extremes of temperature, pH, salinity, pressure and radiation, and subsequent study of these organisms has revealed a diversity of biochemical mechanisms that organisms have adopted to live in seemingly inhospitable conditions (Seckbach et al., 2015).

The central focus of this Introduction is to discuss the features of the extremely halophilic Archaea (class Halobacteria) that enable them to dominate in aerobic hypersaline brines, contribute to the formation of halite crystals, and which enable some to survive for long-periods of time inside halite brine inclusions.

1.1 Halotolerance vs Halophily: Adaptation to Salt-stress

Halophiles, by a basic definition, are organisms that can grow and thrive in environments containing high salt (NaCl) concentrations. Halophilic representatives can be found in each of the three domains of life (Bacteria, Eukarya and Archaea) and can be characterised based on their salt requirement for growth: extreme halophiles (growth between 2.5–5.2 M salt), borderline extreme halophiles (growth between 1.5-4.0 M salt), moderate halophiles (growth between 0.5-2.5 M salt) and finally halotolerant organisms that can survive over a range of salt concentrations but do not show an obligate need for salt in order to grow (Kushner, 1978; Oren, 2008). While it is convenient to characterise microbes in this way, many variations in salt tolerance and salt requirements exist, and so not all organisms fit neatly into these categories.

As the salinity of an environment increases, water availability decreases and internal water is lost from the cell as a consequence of osmosis. In response to high solute concentrations in their surroundings, halophiles and halotolerant organisms have adaptation mechanisms that enable them to cope with changes in osmotic pressure and water activity (a_w) (Grant, 2004). Since biological membranes are permeable to water and small ions, cells are generally unable to maintain an internal water activity higher than that of the surrounding brine or they risk rapid water loss (Oren, 1999). To sustain turgor pressure and combat lethal water loss, the cellular cytoplasm of halophilic or halotolerant organisms is maintained iso-osmotic with the surrounding environment. Two fundamentally different osmo-regulatory strategies exist that serve this purpose: (1) the exclusion of salt and the *de-novo* biosynthesis or accumulation (from

surrounding environment) of organic osmolytes / compatible solutes, or (2) the intracellular accumulation of high concentrations of inorganic ions (mostly K^+ and Cl^-) (Oren, 1999).

A compatible solute or osmolyte is a substance accumulated inside the cell to balance osmotic pressure that is compatible with cellular metabolism (Antón, 2011). Compatible solutes provide a means of short-term protection from fluctuations in salinity and many have also been shown to have a stabilising effect on cellular proteins (Yancey, 2005). Consequently, this strategy is widely used by both halotolerant and halophilic organisms alike (with the exception of most extreme halophiles that adopt the "salt-in" strategy). There exists a wide array of organic compatible solutes that are utilised by organisms spanning all three domains; for instance the accumulation of glycine betaine and the synthesis of ectoine or hydroxyectoine are often associated with halophilic bacteria of diverse phylogenetic affiliations (Imhoff & Rodriguez-Valera, 1984; Roberts *et al.*, 2005). Glycerol is known to be the primary osmolyte in many eukaryotic cells, such as the extremely salt tolerant fungus *Hortaea werneckii* (Kogej *et al.*, 2007) and in the halophilic green alga genus *Dunaliella* (Ben-Amotz & Avron, 1973). β-amino acids such as β-glutamate, β-glutamine and N^{ε}-acetyl-β-lysine are utilised by halotolerant and halophilic methanogens (Sowers & Gunsalus, 1995).

The synthesis and accumulation of osmotic solutes is energetically costly. In hypersaline environments, where salt-stress is persistent, the amount of energy needed to maintain low intracellular ion concentrations alongside solute production is thought to greatly exceed the energy requirements for growth and repair (Oren, 1999). Consequently, most microbes that have adapted to life at extreme salt concentrations (2.5 to 5.2 M NaCl) carry out an alternative method of osmoregulation – "salting-in". In brief, this strategy involves the extrusion of Na^+ and accumulation of K^+, largely driven by a proton electrochemical gradient across the cytoplasmic membrane (Oren, 1999). Cells that accumulate high concentrations of KCl have enzymes and other internal machinery that are adapted to remain functional at high ionic strengths. This is often represented by an acidic proteome containing a large excess of acidic amino acids (mainly glutamic and aspartic acids) on the surface and fewer hydrophobic amino acids (Tadeo *et al.*, 2009). As a consequence of this adaptation, organisms that salt-in are often obligate halophiles, which have a minimum salt requirement in order to maintain enzymatic and structural integrity. Examples of microbes that have adapted in this way are limited to a small number of halophilic groups: Archaea of the class Halobacteria and a few Bacteria: the aerobic *Salinibacter* (Bacteroidetes) and the anaerobic halophilic fermentative Halanaerobiales (Firmicutes) (Oren, 2011).

While there are two distinctly different mechanisms of osmoregulation, it is often difficult to make assumptions of the adaptations and ecological range of an organism based on phylogeny alone.

It is highly likely that delineation between extreme and moderate halophiles is considerably more nuanced than suggested. Many moderate halophiles have been shown to have acidic proteomes, and some acidic proteomes can function in the absence of high cytoplasmic salt concentrations (Deole *et al.*, 2013; Oren, 2013). Also, despite previously thought as obligate extreme halophiles, some haloarchaeal species (e.g. *Haladaptatus paucihalophilus*) have been isolated from relatively low salinity environments and possess functional genes for the synthesis and transport of compatible solutes such as trehalose and glycine-betaine (Purdy *et al.*, 2004; Savage *et al.*, 2007; Youssef *et al.*, 2014). Furthermore, phylogenetic analysis performed by Youssef *et al.* (2014) suggested that trehalose synthesis is likely an ancestral trait of the haloarchaea, and that the absence of such trait is representative of gene loss events that occurred as haloarchaea adapted to a more consistent hypersaline environment.

1.2 Classification and Phylogeny of Haloarchaea

Halophilic microbial inhabitants of hypersaline brines become trapped inside halite as NaCl precipitates (approaching saturation ~5.2 M NaCl). The central focus of this section and ensuing review shall concentrate on the dominant organisms present inside halite crystals and other hypersaline environments; the extremely halophilic archaea belonging to the class of Halobacteria (Phylum *Euryarchaeaota)* (Grant, 2001). The unofficial term “Haloarchaea” is commonly used to refer to organisms of this class as well as to distinguish the placement of the otherwise titled Halobacteria within the archaeal domain. The Halobacteria are one of the most studied groups of Archaea and as written by Oren (2014) “the halophilic archaea provide an excellent example of how changing concepts on prokaryote taxonomy and development of new methods have influenced the way in which the taxonomy of a single group is treated.” In May 2017, there were 57 recognised genera and 233 species (Arahal *et al.*, 2017) within the class Halobacteria*;* a huge increase when compared to 1997 when there were only 9 recognised genera and 28 recognised species at the time in which minimal standards for their description were proposed (Oren *et al.*, 1997). Previously, the hierarchy comprised of a single order (the *Halobacteriales* (Grant & Larsen, 1989) and family (the *Halobacteriaceae* (Gibbons, 1974)), organised according to 16S rRNA gene sequence similarity as well as morphological and physiological characteristics. Over the years, many amendments to the phylogeny of the *Halobacteriaceae* have occurred, resulting in the assignment of species to novel genera. Only recently however, the hierarchical ordering of the class Halobacteria has been revised further. Gupta *et al.* (2015) compared protein coding sequences within haloarchaeal genomes and found discrete molecular markers, in the form of conserved signature indels and conserved sequence proteins, that could be used in addition to the 16S rRNA gene comparisons to further

differentiate unique groups of haloarchaea. Consequently, members of the class Halobacteria have since been reorganised to include two new orders (the *Haloferacales* and *Natrialbales*) and two new families (the *Haloferacaceae* and *Natrialbaceae)* (Gupta *et al.*, 2015; Oren & Ventosa, 2016). Using the same molecular method, additional proposals have suggested a reappraisal of the *Halobacteriales,* to include the novel families *Haloarculaceae* and *Halococcaceae,* as well as the division of *Haloferacales* to include the two novel families *Haloferacaceae* and *Halorubraceae* (Gupta *et al.*, 2016) (Figure 1.1)

Despite the distinction of new phylogenetic clades, there are a number common phenotypic characteristics shared between genera. Most haloarchaea are obligate extreme halophiles that grow optimally at salt concentrations above 2.5 M and lyse when placed in pure water. Many cells are pigmented red-orange in colour due to the high content of photoprotective 50-carbon bacterioruberin carotenoids in their cell membrane (Oren, 2009a). Most haloarchaea have an aerobic heterotrophic lifestyle (but see Section 1.4 for consideration of other modes of haloarchaeal growth), and at optimum conditions appear are either pleomorphic or appear as rods, cocci or as flat squares in the case of *Haloquadratum walsybi* (Burns *et al.*, 2004).

Haloarchaeal membranes are generally formed of C_{20}:C_{20} diether lipids (but also C_{20}:C_{25} and C_{25}:C_{25}) that form a bilayer similar to that of most bacteria and eukarya but are hardier, and less permeable to ions due to the increased chemical stability of their ether linkages and tight packing between phytanyl side chains (De Rosa *et al.*, 1983; Kellermann *et al.*, 2016). The low permeability of archaeal membranes is thought to have arisen as a mechanism to deal with chronic energy stress. By limiting the futile cycling of ions, archaeal membranes are able to reduce the amount of energy lost during the maintenance of a chemiosmotic potential (Valentine, 2007). This in turn reduces the maintenance energy of archaeal cells and thus is exceptionally advantageous in the face of extreme environmental conditions and in the context of long-term survival in halite.

Haloarchaeal cells have only a single membrane and are therefore constantly required to synchronise their membrane lipid composition with the ever-changing external conditions of their environment in order to uphold their role as a protective barrier against toxic cation concentrations, UV radiation and desiccation (for a comprehensive review of such changes see Kellermann *et al.* (2016)). In addition to the membrane, the cellular envelopes of haloarchaea also include an exceptionally diverse array of cell wall structures, which surround the cell and contribute to cell shape and osmoprotection (Albers & Meyer, 2011). Some examples include: the cocci *Halococcus morrhuae* which has a thick sulphated heteropolysaccharide cell wall, the rod *Halobacterium salinarum R1* which has a surface-layer (S-layer) cell wall structure, and finally the ultra-thin square-shaped *Haloquadratum walsbyi*

which, in addition to its S-layer, secretes a large protein (9159 amino acids in length) known as Halomucin as an additional defensive barrier (against desiccation and phage predation) (Albers & Meyer, 2011; Zenke *et al.*, 2015).

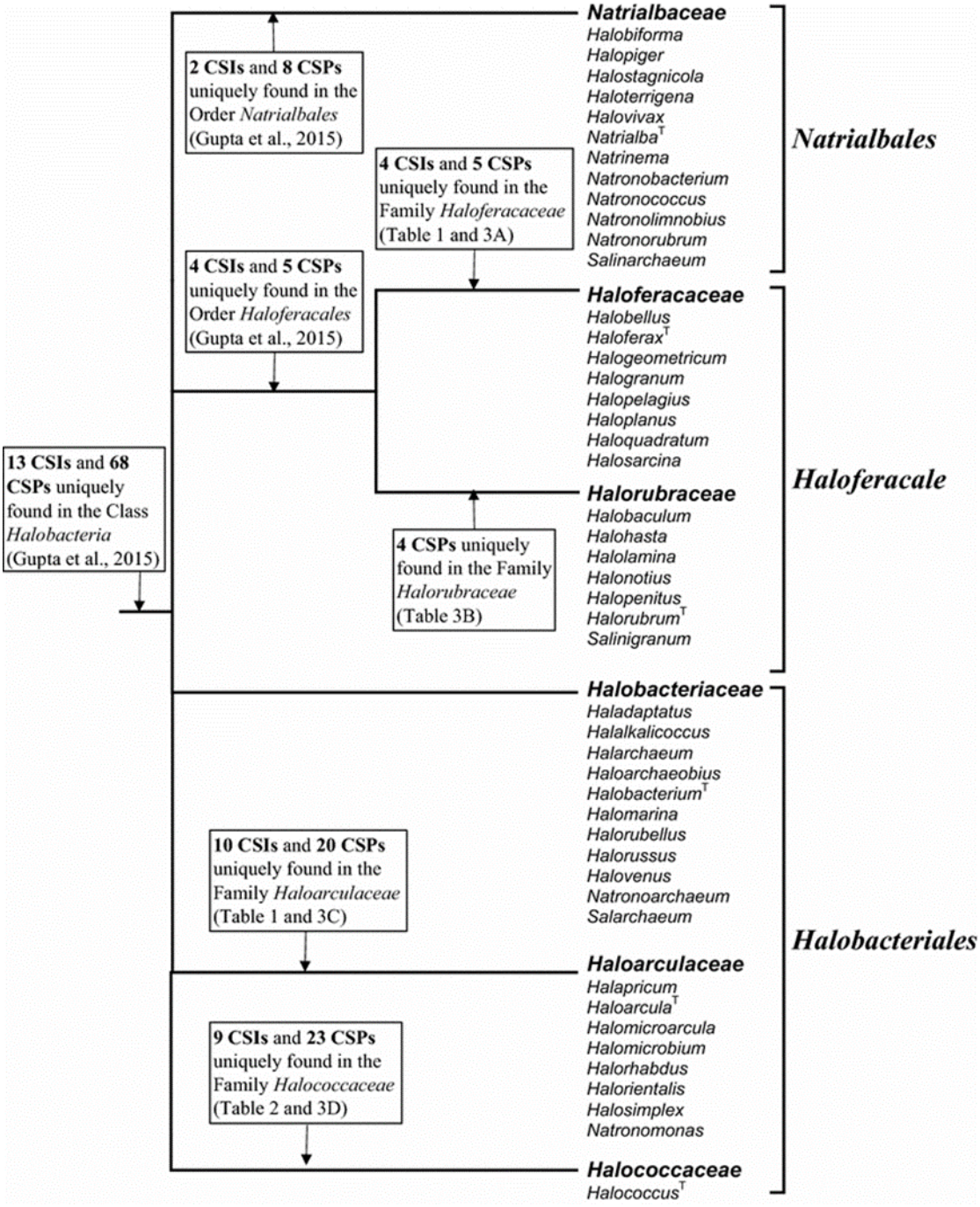

Figure 1.1: A summary of the recently proposed ordering of the Halobacteria (Gupta *et al.*, 2015, 2016)**.** The diagram, taken from Gupta (2016), depicts the reappraisal of families from the class Halobacteria as described in the two studies. Hierarchy is arranged according to the distribution of conserved signature insertion/deletions (CSIs) and signature proteins (CSPs).

1.3 Hypersaline Environments Inhabited by Haloarchaea

Hypersaline environments are loosely defined as environments with a salt concentration above that of seawater (3.5 %). For the purpose of this section however, I will refer to hypersaline environments as those that are subject to evaporative concentration with salinity above 10% through to saturation (~ 34%) (McGenity & Oren, 2012). There are two distinct sub-groups of hypersaline environments that can be distinguished based on ionic composition as shown in Table 1.1. Thalassohaline environments, such as coastal salterns, lagoons and certain inland salt lakes, arise through evaporation, and have an ionic composition proportional to seawater (Na^+ and Cl^- as the predominant ions). In contrast, athalassohaline environments such as the Dead Sea, alkaline soda lakes and some deep-sea hypersaline anoxic lakes (DHAL) arise through different means and have ionic compositions determined by the surrounding geology (McGenity & Oren, 2012).

Much of our understanding of prokaryotic diversity in thalassohaline environments has come from the study of coastal salterns. Multi-pond solar salterns are used to manufacture salt from sea water and are comprised of a succession of shallow man-made pools subjected to evaporation. Salterns provide a model system to study the effect of salinity on microbial community dynamics. In each successive pool the brine is concentrated further, until the final crystallizer pool where salt is harvested. Studies investigating these systems have shown a negative relationship between rising salinity and species diversity (Benlloch *et al.*, 2002; Baati *et al.*, 2010a; Boujelben *et al.*, 2012). In intermediate salinity ponds (22-32%) there are diverse microbial communities of halophilic chemo-organotrophic bacteria (often *Alpha*- or *Gammaproteobacteria*) and Archaea (Halobacteria*)*, as well as oxygenic phototrophic species of Cyanobacteria and green algae such as *Dunaliella salina* (Benlloch *et al.*, 2002). However, at salt concentrations approaching saturation (32-37%) there is often a shift in community structure as many species are unable to survive. In saltern crystallizer ponds, Haloarchaeal species are seen to dominate and co-exist with abundant populations of the halophilic bacterium *Salinibacter ruber,* as well as members of the ubiquitous Nanohaloarchaea (Antón *et al.*, 2000; Benlloch *et al.*, 2002; Casamayor *et al.*, 2002; Ghai *et al.*, 2011; Narasingarao *et al.*, 2012).

Also prevalent in hypersaline environments are diverse communities of phages that outnumber both archaeal and bacterial cells from ten to a hundred-fold (Atanasova *et al.*, 2015). With only a few cellular predators around, phages play an significant role in the microbial loop of hypersaline environments, as lysis of infected halophilic microbial cells results in the release of cellular materials (i.e. nucleic acids, proteins and lipids) that are then used as substrates by other community members (Guixa-Boixareu *et al.*, 1996; Quadri *et al.*, 2016). Many haloarchaeoviruses are thought to also have a mutualistic association with their hosts, by

facilitating genetic exchange they promote variation amongst haloarchaeal populations which in turn enables adaptation to changing environmental conditions and drives speciation (Luk *et al.*, 2014).

Haloarchaeal communities at high salinities differ between locations and are largely influenced by the physico-chemical conditions of the environment they inhabit. For instance, the Dead Sea is an extensively studied hypersaline environment containing approximately 34 % salt. The "sea" is rather an inland athalassohaline salt lake noted for its unusual ionic composition. Due to extensive evaporation, the precipitation of halite from the water column has resulted in a decrease in Na^+ concentrations and the formation of an environment dominated by high concentrations of divalent cations such as Mg^{2+} and Ca^{2+}(Bodaker *et al.*, 2010). The $MgCl_2$ and $CaCl_2$ salts that arise in such conditions are exceptionally chaotropic (disordering/entropy inducing) and as such are toxic in the absence of compensating kosmotropes (Williams & Hallsworth, 2009). In the Dead Sea such effects are off-set by sufficient concentrations of kosmotropic Na^+, however the continued precipitation of NaCl is leading to a gradual increase in the ratio of Mg^{2+}:Na^+ ions and an increasingly chaotropic environment (Bodaker *et al.*, 2009).

Life in the Dead Sea consists of a small latent community of haloarchaea (Bodaker *et al.*, 2009). Occasionally however, rainy winters dilute the upper proportion of the water column resulting in the temporary formation of dense blooms of *Dunaliella* algae (Oren & Shilo, 1982; Oren *et al.*, 1995). Glycerol produced by *Dunaliella* as an osmotic compatible solute is thought to play a significant role in the carbon cycling of hypersaline environments and act as an important carbon and energy source for the nascent haloarchaeal population. The breakdown of glycerol by haloarchaea often produces pyruvate, acetate and D-lactate that are further metabolised aerobically by many of the same organisms (Oren & Gurevich, 1994). Consequently, glycerol from *Dunaliella* in turn gives rise to blooms of red-pigmented haloarchaea.

Oxygen is poorly soluble in salt-saturated brines and can easily become a limiting factor for the development of haloarchaea, which generally live aerobic heterotrophic lifestyles. Some haloarchaeal representatives (such as the flat, square *Haloquadratum walsbyi*) can overcome such limitations by producing gas vesicles, which alongside their flat morphology, enable them to migrate towards, maintain their position and enhance O_2-diffusion at the oxygen-rich surface (Andrei *et al.*, 2012). Alternatively, many haloarchaea are facultative anaerobes able to grow anaerobically in oxygen-limited conditions by utilising alternative electron acceptors such as nitrate, dimethylsulfoxide (DMSO), trimethylamine N-oxide (TMAO) or fumarate. A limited few members such as *Halobacterium salinarum* have also shown able to grow using alternative terminal electron acceptors and/or the anaerobic fermentation of L-arginine to citrulline (Oren, 2006).

Previous understanding of haloarchaea has presented them primarily as obligate aerobic chemo-organotrophs that have a minimum requirement of salt to function. However, in recent years, studies have provided examples that contradict such assumptions and suggest that their ecological niche and diverse means of energy generation have been greatly under-estimated. For instance, the isolation of haloarchaea from salinities close to that of sea-water (Purdy *et al.*, 2004), and the recorded ability of *Haladaptatus paucihalophilus* (Savage *et al.*, 2007) to remain viable in pure water. More recently, research has unearthed novel isolates that show a preference for low-oxygen or anoxic environments. *Halorhabdus tiamatea* isolated from a deep-sea hypersaline anoxic lake in the Red Sea demonstrated a preference for microaerophilic conditions, and is thought to grow by the anaerobic degradation (primarily fermentation) of polysaccharides (Antunes *et al.*, 2008; Werner *et al.*, 2014). Furthermore, Sorokin *et al.* (2016a) discovered and isolated the first obligately anaerobic haloarchaeaon, which demonstrated a metabolic type that was previously unknown among the haloarchaea and the whole archaeal kingdom. *Halanaeroarchaeum sulfurireducens*, isolated from the anaerobic sediments and brines of hypersaline lakes (3.5 – 5 M) in Kulunde Steppe (Altai, Russia), is able to obtain energy by the dissimilatory reduction of elemental sulfur using acetate as the sole electron donor (Sorokin *et al.*, 2016a, 2016b). Similarly, the classification of a novel genus containing obligately anaerobic lithoheterotrophic archaea (*Halodesulfurarchaeum*), capable of utilising formate or hydrogen as electron donors and elemental sulfur, thiosulfate or dimethylsulfoxide as electron acceptors, provides a novel functional group of the newly described sulfur-respiring haloarchaea (Sorokin *et al.*, 2017). These examples demonstrate how our understanding of the microbial inhabitants in hypersaline environments is continually expanding. The simultaneously discovery and genome sequencing of the Nanohaloarchaea, a ubiquitous and highly abundant lineage within the Euryarchaeota, demonstrates how re-examination of even well-studied environments can lead to the unearthing and characterisation of previously undetected or un-cultivated groups (Narasingarao *et al.*, 2012).

Table 1.1 Concentration of the major cations (Na^+, Mg^{2+}, Ca^{2+}, K^+) and anions (Cl^-, SO_4^{2-}) in various hypersaline brines and seawater (g/l). Brine ionic composition can vary considerably between hypersaline environments. This table from McGenity & Oren (2012) serves to illustrate the potential diversity in brine ionic composition between examples from both thalassohaline and athalassohaline environments.

	Na^+	Mg^{2+}	Ca^{2+}	K^+	Cl^-	SO_4^{2-}	Salinity	Notes*	Ref†
Seawater	10.8	1.3	0.4	0.4	19.4	2.7	35		1
Seawater at onset of gypsum precipitation	49.5	6.8	1.7	2.0	91.5	12.5	164		1
Seawater at onset of halite precipitation	98.4	14.5	0.4	4.9	187.0	19.3	324		1
Seawater at onset of potash precipitation	61.4	39.3	0.2	12.8	189.0	51.2	354		1
Great Salt Lake (North Arm), USA	105.0	11.1	0.3	6.7	181.0	27.0	333	North Arm, 1977	1
Dead Sea, Israel-Jordan	39.7	42.4	17.2	7.6	219.0	0.4	327	Lower water mass, 1975	1
Don Juan Pond, Antarctica	11.5	1.2	114.0	0.2	212.0	0.01	339	$CaCl_2$-rich brine, 1962	1
Lake Magadi, Kenya	161.0	0	0	2.3	111.8	16.8	315	CO_3^{2-}/HCO_3^- = 23.4; pH = 11	2
Bannock deep-sea brine lake, Mediterranean	97.4	15.8	0.7	5.0	190.0	13.2	322		3
Urania deep-sea brine lake, Mediterranean	80.6	7.7	1.3	4.8	132.2	10.3	237	HS^- concentrations up to 16 mM	3
Discovery deep-sea brine lake, Mediterranean	1.6	121.4	0.1	0.8	336.5	9.2	470	$MgCl_2$-rich brine	3

* Dates of original publications are indicated where changes in salinity have occurred subsequently. The salinity of the Dead Sea, for example, increased to 347 g/l in 2007, with an increase in Mg^{2+} and a decrease in Na^+ (Bodaker *et al.*, 2010).

† References: 1, Javor (1989) and references therein; 2, Grant (2004); 3, van der Wielen *et al.* (2005).

1.4 Polyextremophilic Halophiles

High ionic strength, elevated temperatures and UV radiation are characteristic features of hypersaline environments. Consequently, many of the Haloarchaea that thrive in these environments can be termed “poly-extremophiles”, as they have developed efficient mechanisms to withstand a wide variety of environmental stressors. *Hbt. salinarum NRC-1* was the first species of the Haloarchaea to be genome sequenced and has often been used as a model to investigate the stress response of Haloarchaea to various extreme conditions (Ng *et al.*, 2000).

UV radiation from sunlight results in photochemical reactions that damage DNA and various components of the cell. Haloarchaea show remarkable resistance to UV radiation (demonstrated by 37% survival of *Hbt. salinarum NRC-1* at 280 J/m^2), which is facilitated by efficient DNA repair mechanisms and physiological adaptations that provide photoprotection (Baliga *et al.*, 2004; Jones & Baxter, 2017). Haloarchaea are equipped with a variety of DNA repair systems than enable them to respond to different forms of DNA damage (e.g. single/double-stranded breaks and dimerization), the most widely used are direct photoreactivation, nucleotide excision repair, base excision repair and homologous recombination. For greater detail on the listed DNA repair mechanisms see (Jones & Baxter, 2017). As noted, haloarchaeal cells possess many photoprotective features that serve to mitigate the harmful effects of UV radiation. Pigmentation by carotenoids such as bacterioruberin, high concentrations of intracellular KCl and a high Mn:Fe ratios protect cells from DNA damage by stabilising macromolecules and scavenging/detoxifying reactive oxygen species (ROS) that form in response to ionizing radiation and desiccation (Shahmohammadi *et al.*, 1998; Kish *et al.*, 2009; Robinson *et al.*, 2011). Similarly, polyploidy, which is a widespread feature of haloarchaeal cells, is an advantageous feature that limits the harm caused by double-stranded breaks, and permits repair through homologous recombination (Soppa, 2013). Lastly, in hypersaline environments the entombment of cells in halite crystals has been shown to provide Haloarchaea with physical protection against UV radiation and desiccation, affording them with an opportunity for continued survival upon dissolution and release (Norton & Grant, 1988; Fendrihan *et al.*, 2009; Bodaker *et al.*, 2010).

Hypersaline soda lake brines are often highly alkaline (pH 9-11) environments, rich in NaCl, $NaHCO_3$ and Na_2CO_3 and scarce in Mg^{2+} and Ca^{2+}(McGenity & Oren, 2012) . Haloalkaliphilic archaea, such as the genome-sequenced *Natronomonas pharaonis,* are one of the main inhabitants found in salt-saturated alkaline lakes (Falb *et al.*, 2005). Haloarchaeal and bacterial inhabitants of such environments have developed adaptations

that enable them to maintain pH homeostasis and intracellular osmotic pressure (Sorokin *et al.*, 2014). Many haloalkaliphiles make use of Na^+/H^+ antiporters to generate energy by forming an electrochemical gradient of H^+ that exerts a proton motive force (Speelmans *et al.*, 1995). The extrusion of sodium ions in exchange for protons creates a gradient in which the inside of the cell remains acidic compared to the external alkaline brine (van de Vossenberg *et al.*, 1999). The halophilic alkalithermophile *Natranaerobius thermophilus* is able to grow optimally at multiple extremes of salinity, temperature and pH (3.5 M Na^+, pH 9.5 and at 53°C) and utilises a large repertoire of similar $Na^+(K^+)/ H^+$ antiporters in order to adapt to the multiple extremes of their environment (Mesbah *et al.*, 2009). To maintain intracellular conditions and the structural integrity of the cell in alkaline conditions, Haloalkaliphilic archaeal cell envelopes have unique cell walls that contain glutaminylglycan polymers, as well as reinforced lipid structures containing C_{20}-C_{20}, C_{20}-C_{25}, and C_{25}-C_{25} diethers core lipids (De Rosa *et al.*, 1983; Falb *et al.*, 2005).

Finally, most Haloarchaea are mesophilic, growing optimally between 28°C and 35°C, and often show growth up to 45-50°C (Bowers & Wiegel, 2011). Nevertheless, haloarchaeal species operate over a wide range of temperatures; *Natrinema thermaphila,* for instance, is the most thermophilic representative (T_{opt} ~55˚C and T_{max} ≤ 66˚C) whereas an psychochrotolerant ecotype of *Halorubrum lacusprofundi* (optimal growth at 33°C) was found among the dominant archaeal genera of Deep Lake (Antartica), which has a temperature that ranges from -18°C to 12°C (Bowers & Wiegel, 2011; Williams *et al.*, 2014; Kim *et al.*, 2018).

1.5 Microbial Entombment in Halite

Historically salt was added to fish, meat and animal hides as a method of preservation. Often a distinctive reddening on salted fish was observed as the cause of spoilage and was the source of considerable economic loss to the fishing industry (Anderson, 1953). Harrison & Kennedy (1929) cultivated red-pigmented organisms from salted cod and traced their origin to the salt or brine used for curing. This led to the assumption that food spoilage was a consequence of curing food and hides with contaminated salt. Despite there being a clear relationship between the addition of salt and the occurrence of red-halophilic bacteria (now known to likely have been haloarchaea), the exact nature of the relationship was poorly understood.

Halite and other evaporative minerals are formed by precipitation in saline waters. When seawater undergoes evaporation, major minerals precipitate in order of their solubility: first is calcium carbonate (calcite and aragonite), followed by gypsum and halite, which are then

followed by variations of certain K-Mg minerals (potash) (Javor, 1989). Brine inclusions are abundant in halite (up to 10^{10} inclusions per cm^3) and are usually of micrometre scale (Jaakkola *et al.*, 2016). Lab experiments by Norton & Grant (1988) demonstrated the entombment of haloarchaea within salt-saturated brine inclusions of growing halite crystals. In their experiment, crystals were grown under controlled conditions from solutions containing pure cultures of 40 strains of haloarchaea, and from hypersaline water samples containing mixed microbiota. The ability to survive in association with crystalline salt was demonstrated as a widely-distributed property and a characteristic feature of the Halobacteria class with all tested strains retaining viability inside halite for at least six months. It was proposed that entombment in halite is a habitat-specific mechanism that enables Halobacteria to survive temporary habitat loss (desiccation or a chaotropic Mg-rich bittern brine) by providing a stable protective microenvironment (Norton & Grant, 1988).

Inside halite brine inclusions, organisms are shielded from the harshness of UV light, desiccation and the chaotropic effects of Mg-rich bittern brines (Fendrihan *et al.*, 2009; Bodaker *et al.*, 2010), and so, it is reasonable to assume that certain organisms, if not many, favour temporary entombment in exceptionally arid conditions. Studies investigating haloarchaeal entombment have often observed relationships between halophilic microbes and the size, shape and the rate in which crystals form. It was noted by Norton & Grant (1988) that crystallisation began earlier, and that brine inclusions of lab-grown crystals containing Halobacteria were considerably larger and greater in number than those in crystals formed from a sterilised control solution. One explanation for this derives from the interaction of Na^+ and Cl^- ions with the surface layer (S-layer) of haloarchaea. Lopez-Cortes *et al.* (1994) reported an increase in the number and size of crystals from solutions containing haloarchaea and identified an association between the S-layer and increased dendritic crystal formation. Consequently, they proposed that S-layers act as a nucleus that induces salt formation. Regulation of internal salt concentrations, through accumulation of K^+ and extrusion of Na^+ ions (salting-in), is also thought to aid halite precipitation by increasing the local concentration of Na^+ and Cl^- ions (Castanier *et al.*, 1999). Furthermore, in saltern pools, crystallisation is increased by the presence of red-pigmented halophiles. Haloarchaeal pigments, such as bacterioruberin and β-carotene, decrease the reflectance of sunlight and thus cause faster heating and evaporation of water from brine (Lopez-Cortes *et al.*, 1994).

Studies linking specific features and strategies to crystal formation give credence to the concept of preferential entombment. Comparisons of haloarchaeal communities found in brine and halite samples from nearby locations in the Saline Valley (California) show slight compositional differences. Out of 26 clusters of archaeal sequences identified; nineteen were found in both brine and crystals whilst two were unique to brine and five were

exclusively in crystals (Gramain, 2009). Analysis of clusters present in both brine and crystals demonstrated a number of significant differences in the size of clusters and therefore implied preference to one of the two conditions (Gramain, 2009). Similarly, Baati *et al.* (2010b) compared archaeal and bacterial community structures in halite collected from a Tunisian saltern to those of a previously studied brine from the same source. Like Gramain (2009), Baati *et al.* (2010b) noted a few differences between communities in halite and those in brine, largely in the form of proportional differences in abundance, as well as the presence of certain genera in only one of the two conditions (Baati *et al.*, 2010b).

Amplicon sequencing analysis (16S rRNA gene) performed on nine different food-grade salts from solar saltern environments around the world showed significant differences in the relative abundance of haloarchaeal genera that varied between the location of origin (Henriet *et al.*, 2014). It was noted that whilst *Haloquadratum* (alongside *Halorubrum* and *Haloarcula)* is usually among the dominant genera found in solar saltern waters, it generally appeared as a minor component of communities inside food-grade salts (Henriet *et al.*, 2014; Gibtan *et al.*, 2017). In comparison, *Halorubrum, Haloarcula* or *Halobacterium* were each shown to dominate in at least one of the nine tested salt samples (Oh *et al.*, 2010; Henriet *et al.*, 2014; Gibtan *et al.*, 2017). Interestingly, a similar study by Clark *et al.* (2017) demonstrated that *Haloquadratum* was significantly more relatively abundant in halite from the Mediterranean than any other biogeographic region, and that *Halolamina* and *Halobacterium* were the most abundant and widely distributed genera found in halite derived from all regions (Mediterranean, Western Europe and East Africa).

The dominance of *Halobacterium* inside salt suggests a preference for entombment in halite, however, it is not clear whether all organisms in a mixed microbial community are trapped in halite or whether entrapment is selective and occurs preferentially in those species with features that induce crystal formation. Further research is needed to elucidate the selective process that occurs in the brine-to-crystal transition as well as in the immediate periods following entombment in halite brine inclusions (the focus of this study). Whilst experiments have shown entombment of members from all three domains of life, haloarchaea are seen to dominate and maintain viability for greater periods of time than any others (Adamski *et al.*, 2006; Baati *et al.*, 2010b; Schubert *et al.*, 2010a; Gramain *et al.,* 2011).

1.6 Isolation and Detection of Haloarchaea from Ancient Evaporites

Salt deposits (rock salt) result from the evaporitic concentration of dissolved salt water from marine or non-marine origins. Ancient subterranean salt deposits are common throughout the world and are the remnants of ancient hypersaline waters that once supported dense populations of halophilic microorganisms (Grant *et al.*, 1998). The remarkable isolation of viable organisms from ancient halite deposits has positioned microorganisms at the centre of the debate over long-term survival (Grant *et al.*, 1998).

Reiser & Tasch (1960) were first to isolate bacteria from brine inclusions of Permian salt deposits (formed 225-290 MYA). Originally thought to be a sterile environment, Reiser & Tasch (1960) described the isolation of gram-positive diplococci. Dombrowski (1963) reported similar findings, yielding *Bacillus circulans* from enrichment media containing Permian salts. Norton *et al.* (1993) isolated haloarchaea from two British salt mines. Halite from Winsford mine originated in the Triassic period (195-225 MYA) and yielded seven haloarchaeal strains; four of which were representatives from the genus *Haloarcula*, and three from the genus *Halorubrum*. Norton *et al.* (1993) proposed that Halobacteria found in the mines may be the descendants of ancient populations that were originally trapped when the salts first formed. This was supported by the subsequent discovery of *Halococcus salifodinae,* isolated from Permian rock salt from Austria (Denner *et al.*, 1994). Additional cases in which *Hcc. salifodinae* has been isolated from geographically distant salt deposits of similar ages have since provided backing for the hypothesis that these halococci represent a relict population from hypersaline Permo-Triassic seas that were buried when the habitat became restricted and seas evaporated (Stan-Lotter *et al.*, 1999). Nevertheless, this was still not conclusive as samples were from brines or crystals that had not been surface-sterilised in the most rigorous way (Gramain et al., 2011).

Many studies have since successfully isolated live organisms from ancient halite and have identified novel haloarchaeal species from deposits of various geological ages (Norton *et al.*, 1993; Stan-Lotter *et al.*, 1999; Vreeland *et al.*, 2000, 2007; Mormile *et al.*, 2003). For instance; the isolation and identification of *Halococcus dombrowskii* (Stan-Lotter *et al.*, 2002) and *Halobacterium noricense* (Gruber *et al.*, 2004) from Permian deposits of Austrian salt mines; the isolation and subsequent genome sequencing of *Halobacterium hubeiense* from a rock salt core of the Jianghan Basin (Hubei province, China), thought to have formed during the early Cretaceous period (100-145 MYA); and most recently the identification of *Haloparvum sedimenti,* a novel member of the genus *Haloferacaceae,* isolated from rock salt of the Jiangcheng Salt Mine (Yunnan province, China) (Zhou *et al.*, 2016). The development of efficient DNA sequencing technologies in recent times has facilitated the widespread use

of the 16S rRNA gene as a biomarker for detection and characterisation of prokaryotic communities. The retrieval of 16S rRNA gene sequences has been an especially useful method in the study of microbial life in ancient deposits and has enabled detection of organisms from halite crystals of significant age (up to 425 MYA) (Radax *et al.*, 2001; Fish *et al.*, 2002; Vreeland *et al.*, 2007; Park *et al.*, 2009; Schubert *et al.*, 2010b; Gramain *et al.*, 2011). Phylogenetic analysis of 16S rRNA sequences have highlighted the close relation of ancient strains with those found in contemporary hypersaline environments (Stan-Lotter *et al.*, 1999, 2002; McGenity *et al.*, 2000; Gramain *et al.*, 2011). Community analysis has shown Haloarchaea to dominate in both ancient halite and present-day hypersaline surface environments. In a recent review on microbial life in ancient environments, Jaakkola *et al.* (2016b) list many instances in which haloarchaea and bacteria have been recorded from surface-sterilised ancient halite (See Table 1.2).

The isolation and origin of microbes from ancient evaporites have not been without debate. Early studies were criticised for the insufficient authentication of findings, and the lack of procedures capable of completely excluding contamination as a source of false-positive results (Fish *et al.*, 2002; Hebsgaard *et al.*, 2005). A summary of criteria needed for the authentication of ancient DNA can be found in Hebsgaard *et al.* (2005). To ensure that isolated cells or DNA are of ancient origin, it is important that halite age is accurately estimated (using radiometric methods) and samples are sourced from primary crystal formations. Primary crystals are syndepositional and contain numerous small brine inclusions arranged in a regular pattern that makes them distinct from secondary crystals that form from recrystallization. Gases and brine ionic composition of primary halite crystals can be analysed to ascertain geological age (Satterfield *et al.*, 2005; Jaakkola *et al.*, 2016). Access to primary halite often requires blasting away or drilling through secondary crystals, consequently, rigorous surface sterilisation procedures are required to eliminate external DNA contaminants. Recent methods specifically for the isolation of microbes from ancient halite have been developed by Gramain *et al.* (2011) and Sankaranarayanan *et al.* (2011). Alternatively to bulk extraction methods, Mormile *et al.* (2003) demonstrated the microscopic identification and in-situ retrieval of *Halobacterium salinarum* directly from halite brine inclusions.

Gramain *et al.* (2011) isolated *Halobacterium noricense* from halite cores of the Solar Grande evaporitic basin (Chile). Lab experiments comparing recovery rates of haloarchaeal isolates following entombment demonstrated the rapid recovery of *Hbt. noricense* able to return to growth as rapidly after 27 months as at day 0. Analysis of the global distribution of *Hbt. noricense* showed it to be most commonly found in ancient halite and a small selection of surface environments. Strikingly 16S rRNA gene sequences of isolates from deposits of

vastly different age (more than 400 MYA) often showed >99% identity. It was concluded that some *Halobacterium* species are specialists and exceptionally well adapted to long-term survival in halite (Gramain *et al.*, 2011). Wider acceptance of ancient entombed organisms has shifted the focus to the adaptations and mechanisms that have enabled them to survive for geological periods of time. As discussed previously, haloarchaea as a group possess many features that afford them protection from harsh conditions and enable them to counteract DNA damage. Polyploidy is an important feature of entombed haloarchaea enabling reduced mutations rates (enables repair of DSBs) and phosphate storage, allowing cells to grow, in a nutrient limited environment (Jaakkola *et al.*, 2014, 2016; Zerulla & Soppa, 2014).

Table 1.2: A recent summary of Haloarchaeal and Bacterial genera isolated or detected from ancient halite of various geological ages. Table is as shown in Jaakkola *et al.* (2016)**.**

Genus	Domain[a]	Location	Age[b]	Refs
Isolates				
Haloarcula	A	Winsford mine, UK	195–225 Mya	[24]
Halobacterium	A	Altaussee, Austria Bad Ischl, Austria Death Valley, USA Salar Grande, Chile Sergipe Basin, Brazil Qianjiang depression, China Winsford mine, UK Yunying mine, China	225–280 Mya 225–280 Mya 97 kya 2 Mya 112–121 Mya 123 Mya 195–225 Mya 40 Mya	[2,3,5,10,22–24,88]
Halococcus	A	Bad Ischl, Austria Berchtesgaden, Germany	225–280 Mya 225–280 Mya	[49,50,88,89]
Halolamina	A	Yunying mine, China	40 Mya	[23]
Halorubrum	A	Death Valley, USA	22–34 kya	[35]
Haloterrigena	A	Death Valley, USA	22–34 kya	[35]
Natronobacterium	A	Sergipe Basin, Brazil	112–121 Mya	[90]
Natronomonas	A	Death Valley, USA	22–34 kya	[35]
Oceanobacillus	B	Yunying mine, China	34–49 Mya	[33]
Virgibacillus	B	Salado formation, USA	250 Mya	[2]
Unidentified	A	Boulby mine, UK	225–270 Mya	[24]
Ribosomal 16S Sequences				
Acinetobacter	B	Khorat plateau, Thailand	65–96 Mya	[8]
Burkholderia	B	Khorat plateau, Thailand Wieliczka mine, Poland Wyandotte, USA	65–96 Mya 11–16 Mya 415–425 Mya	[8]
Haloarcula	A	Remolinos, Spain Death Valley, USA	23 Mya 22–34 kya	[7,9]
Halobacterium	A	Alpine region, Austria/Germany Death Valley, USA Michigan Basin, USA Salar Grande, Chile Sergipe Basin, Brazil Wieliczka mine, Poland	225–280 Mya 22–34 kya 419 Mya 2 Mya 112–121 Mya 11–15.8 Mya	[5–9]
Halobiforma	A	Death Valley, USA	22–34 kya	[9]
Halomicrobium	A	Death Valley, USA	22–34 kya	[9]
Halonotius	A	Death Valley, USA	22–34 kya	[9]
Halorhabdus	A	Death Valley, USA	22–34 kya	[9]
Halorubrum	A	Remolinos, Spain Death Valley, USA	23 Mya 22–34 kya	[7,9]
Halosimplex	A	Death Valley, USA	22–34 kya	[9]
Natronomonas	A	Death Valley, USA	22–34 kya	[9]
Pseudomonas	B	Khorat plateau, Thailand	65–96 Mya	[8]
Stenotrophomonas	B	Wieliczka mine, Poland	11–16 Mya	[8]
Unidentified	A	Alpine region, Austria/Germany Death Valley, USA Michigan Basin, USA Sergipe Basin, Brazil	225–280 Mya 22–34 kya 419 Mya 112–121 Mya	[6,7,9]

[a]A, Archaea; B, Bacteria.
[b]kya, thousand years ago, or thousand years of age; Mya, million years ago, or million years of age.

1.7 Physiological Changes in Response to Entombment

Halite-entombed organisms undergo physiological changes that enable them to survive starvation, high ion concentrations, degradation of cellular components, deleterious mutations and low oxygen conditions (Jaakkola *et al.*, 2016). It is noted by McGenity *et al.*(2000) that, early on, brine inclusions are packed with cells and thus a plentiful source of usable substrates are available in the form of biomass. Over periods of geological time however, this diminishes and therefore survival strategies must be employed to reduce energy expenditure (See McGenity *et al.* (2007) for more detail).

The miniaturization of prokaryotic cells is widely reported in soil and sea water as an important phase of starvation-survival in which organisms respond to nutrient-poor conditions (Morita, 1997 in Schubert *et al.*, 2009). Similar morphological changes have been observed in haloarchaea in laboratory experiments and in ancient halite (Norton & Grant, 1988; Schubert *et al.*, 2009b; Winters *et al.*, 2015). Winters *et al.* (2015) showed that starved populations of *Hbt. salinarum* and *Haloterrigena* strain DV582A-1 temporarily increased in abundance (likely due to fragmentations) and changed cell morphology from rods to small cocci within just 56 days of nutrient deprivation. Such miniaturisation is advantageous to life in halite as it serves to increase the surface-to-volume ratio of the cell enabling better absorption of nutrients and requires less energy to perform cellular maintenance (Winters *et al.*, 2015).

Haloarchaea and the unicellular alga *Dunaliella salina* are commonly found to co-exist (Oren & Gurevich, 1995). Glycerol, produced as an osmotic compatible solute by *D. salina*, has long been recognised as a potential energy source in hypersaline environments (Schubert *et al.*, 2009a). Schubert *et al.* (2010a) cultured haloarchaea from a salt core (100 KYA) taken from Death Valley and reported the presence of dead *D.salina* cells inside brine inclusions of primary halite crystals. It was hypothesised that glycerol, accumulated by *D. salina* cells, may provide an energy source for prokaryotic survival and enable the repair of DNA damage over geological times (Schubert *et al.*, 2010a). In carbon-limited environments, *D. salina* undergoes cycles of programmed cell death to complement the nutritional needs of co-occurring heterotrophic cells such as *Hbt. salinarum*. In response *Hbt. salinarum* re-mineralizes the carbon, and thus provides nutrients for *D. salina,* thereby allowing the cycle to continue and perpetuate (Orellana, et al., 2013). Previous research shows haloarchaea able to grow on media containing glycerol as the sole carbon source, and that the breakdown of glycerol by haloarchaea often produces pyruvate, acetate and D-lactate that are further metabolised aerobically by many of the same organisms (Oren & Gurevich, 1994). Dihydroxyacetone produced in glycerol metabolism by the halophilic bacteria

Salinibacter ruber is used by *Haloquadratum walsbyi* and other haloarchaea (Elevi Bardavid & Oren, 2008), thus highlighting the benefit of mutualistic relationships in hypersaline environments. Gramain *et al.* (2011) demonstrated the relationship of *S. ruber* and *Hqd. walsbyi* in halite entombment experiments, and showed that when co-entombed, survival and recovery times were significantly improved.

Haloarchaea in modern hypersaline environments are metabolically diverse (see Section 1.3). Such flexibility is thought to enable members of the haloarchaea to survive entombment for millions of years. Early on in the stages of entombment a plentiful source of usable substrates are available in the form of biomass (McGenity *et al.*, 2000). Over time, finite sources of nutrients and oxygen are depleted and shifts to alternative forms of metabolism are required. Many haloarchaea are facultative anaerobes able to switch to alternative modes of energy generation and are able to use of alternative terminal electron acceptors (such as nitrate, DMSO, TMAO, or fumarate) or fermentation for growth (Oren *et al.*, 1995; Oren, 2006). Interestingly, early comparison of the protein expression in *Hbt. salinarum* following entombment suggest an upregulation of systems involved in the accumulation of fumarate (Gramain, 2009). It has been hypothesised that, in response to entombment, *Hbt. salinarum* shifts metabolism towards fumarate production in order to use fumarate as a terminal electron acceptor (TEA). However, it is noted by Gramain (2009), that to date there is no evidence of microbes producing their own TEA. Alongside its potential use as a TEA, fumarate accumulation may influence crystal formation and dictate flagellar motility in entombed cells (Gramain, 2009).

Recent research has furthered our understanding on haloarchaeal metabolic plasticity and recognised new modes of energy generation. *Halorubrum* strain BV1, first isolated from the Bonneville Salt Flats (Utah, USA), has been identified as the first member of the Euryarchaeaota capable of oxidising carbon monoxide (CO) as an energy source in high salinity media. Such findings establish CO as a plausible substrate for the energy generation of extra-terrestrial microbial life on Mars where CO occurs at relatively high concentrations in the atmosphere (>800 ppm). Furthermore, the discovery of *Halanaeroarchaeum sulfurireducens*, an obligately anaerobic sulfur-reducing haloarchaeaon, and the classification of a novel and ubiquitous group of obligately anaerobic lithoheterotrophic haloarchaea (*Halodesulfurarchaeum*) capable of utilising formate or hydrogen as electron donors provide compelling evidence against the traditional view of haloarchaea as just aerobic chemoorganotrophs (Sorokin *et al.*, 2016a, 2017). Such diversity and plasticity in haloarchaeal metabolism is likely a key part to their success in surviving halite entombment for extended periods of time.

1.8 Aims and Objectives

The aim of this project was to identify whether microorganisms from salt-saturated brines are preferentially entombed inside halite brine inclusions by analysing saturated brine and halite crystals from Trapani salt pans in Italy. In order to address this central aim I have two objectives:

1) to compare *in-situ* community composition of brine and halite samples taken from Trapani Salterns (Sicily);

2) to identify changes in community composition in lab-made halite (from solar saltern waters) derived from Trapani brines over 21 weeks.

2 Materials and Methods

2.1 Sampling

For laboratory experiments, brine samples were collected from Trapani Salterns, Trapani, Sicily (37°58'49.9"N 12°29'42.0"E; Figure 2.1). Brines were collected in 1-litre Duran bottles from three saltern ponds (1, 2 and 3; Figure 2.2), and the salinity of each was determined using a hand-held refractometer (BS Eclipse 45-41). For *in-situ* community analysis, brine (10 ml) from three locations of Pond 1 (a, b and c), approximately 5 m apart, was pushed through a 0.22 µm Sterivex filter (Millipore) using a 50-ml syringe (Figure 2.1 and 2.2). Filters were injected with 3 ml of RNAlater (Qiagen) and placed in 50 ml Falcon tubes. Halite crystals were collected in Falcon tubes from the brine-crystal interface at locations 1A, 1B and 1C. Filters and crystals were stored and transported on dry ice until returned to the lab where they were stored at -20°C. Water activity of the three brines was measured at room temperature using an AW SPRINT 5000 (Novasina). Reverse osmosis water was used as a standard (1.000 a_w). The ionic composition of the three brines was analysed by LC-MS (Dionex ICS-3000) following the same procedure as stated in Aslam *et al.* (2016). Prior to each run, brine samples were diluted 1000-fold to a volume of 20 ml in 30-ml universal tubes.

2.2 Succession Experiment

From each of the 1-litre brine samples 40 ml was transferred into 50 ml Falcon tubes in triplicate, and 20 ml from each sample was transferred into Petri dishes (100 mm × 15 mm) in triplicate and left to evaporate in the ambient conditions of the lab. When halite crystals formed they were transferred into 50 ml Falcon tubes using a spatula. Cells were collected from each brine before crystal formation (T_0), and from brines and crystals after 1 week (T_1), 3 weeks (T_2), 8 weeks (T_3) and 21 weeks (T_4). Cells from 3 ml of brine 1 and 3, and 4.5 ml of brine 2 were collected by centrifugation at 11300 × *g* for 10 min (Minispin, Eppendorf). Halite entombed cells were collected in 50 ml Falcon tubes by dissolving 5 g of halite crystals in 20 ml of 10% NaCl, 1% $MgSO_4.7H_2O$, and then centrifuging at 10000 × *g* for 40 min at 4°C (Biofuge Stratos, Sorvall). After centrifugation the supernatant was removed, leaving approximately 5 ml of liquid. Cells were re-suspended and transferred into 1.5 ml micro-centrifuge tubes for centrifugation at 11300 × *g* for 5 min, and the cell pellet was frozen for later use.

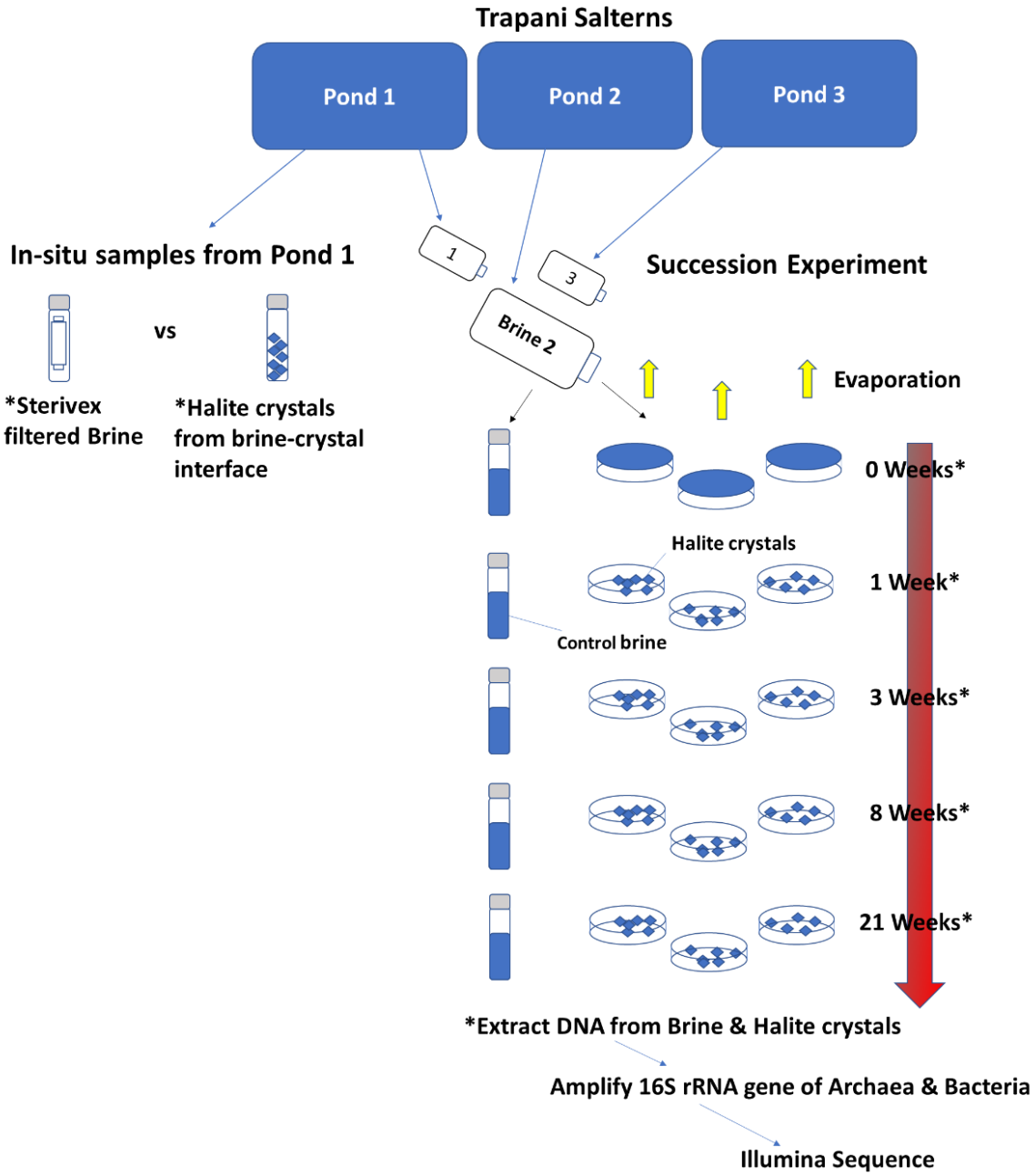

Figure 2.1: A schematic diagram illustrating the sampling and experimental design described in this thesis (Section 2).

2.3 DNA Extraction, 16S rRNA Gene Amplification and Gel Electrophoresis

MilliQ water (200 µl) was added to the cell pellet and transferred into 2-ml bead-beating tubes containing 0.5 g of 0.1 mm zirconia/silica beads (BioSpec). DNA extraction was carried out according to the method in Griffiths *et al.* (2000) (Appendix). Extracted DNA samples were stored at -20°C. Initial amplification of archaeal and bacterial 16S rRNA genes was carried out using the archaeal primer pair 344F and 915Ru and bacterial primer pair 341F and 534R (Table 2.1). Archaeal 16S rRNA genes were amplified by PCR (Applied Biosystems) for 35 cycles (94°C for 15 s, 60°C for 15 s and 72°C for 15 s, with an initial denaturation step at 94°C for 3 min and a final elongation step of 72°C for 10 min). Bacterial 16S rRNA genes were amplified by PCR for 30 cycles (95°C for 15 s, 60°C for 15 s, 72°C for 15 s, with an initial denaturation step at 95°C for 1 min and a final elongation step of 72°C for 10 min). All initial PCRs were composed of 12.5 µl AppTaq Redmix (2X) (Appleton Woods), 1 µl of each primer (10 µM), 1 µl of DNA extract and 9.5 µl of PCR water (25 µl total reaction volume). DNA and PCR products (5 µl) were loaded onto 1% agarose gels immersed in a 1X Tris-acetate (TAE) solution and run alongside 5 µl of GeneRuler Ladder Mix (#SMO333) (Thermo Scientific) for 35-50 min at 105 V. All agarose gels were stained in ethidium bromide (10 mg/ml) before visualising under the UV-light of a transilluminator (Alpha Innotech Multi Image I).

2.4 Extraction of DNA from Sterivex Filters and *In-situ* Halite Crystals

RNAlater (Qiagen) was pushed out of the filters using a 60 ml syringe. Filter casings were opened using sterile pliers and the internal filters were removed using forceps. Each filter was cut into four pieces of equal size using a scalpel and placed into 1.5 ml micro-centrifuge tubes. One quarter of each filter was placed into a new micro-centrifuge tube containing 200 µl of autoclaved MilliQ water and vortexed briefly. The cell suspension / lysed cells (200 µl) and the filter were transferred to bead-beating tubes for DNA extraction. Cells from *in-situ* halite crystals were collected using the same method as those from lab-grown crystals (Section 2.3).

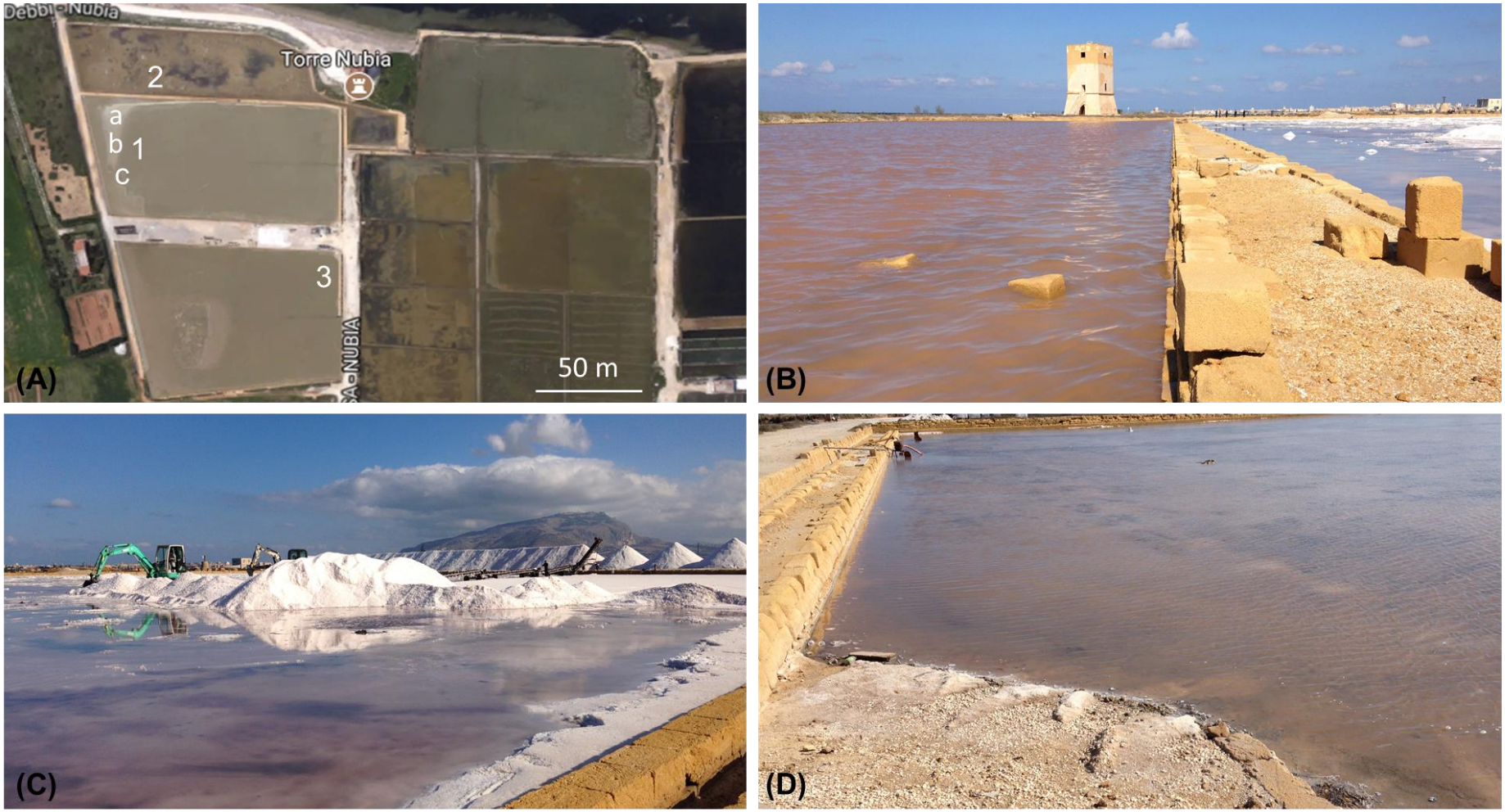

Figure 2.2: Photographs of the sampling site at Trapani Salterns (Trapani, Sicily). Panel A displays a labelled map (Google) indicating the approximate sampling locations: numbers 1, 2 and 3 show the locations of ponds 1, 2 and 3, from which 1 L of brine was collected, and letters a, b and c show the locations in which *in-situ* samples were collected from Pond 1. Panels B, C and D show the three sampled saltern ponds – 2, 1 and 3, respectively.

2.5 16S rRNA Gene Amplicon Sequencing Library Preparation

2.5.1 Amplicon PCR

Sequencing-library preparation was carried out according to the protocol provided by Illumina (2015). The 16S rRNA genes from all samples were amplified using primer pairs to introduce 5' overhang nucleotide adaptor sequences. Bacterial 16S rRNA genes were amplified by PCR for 25-30 cycles (95°C for 30 s, 55°C for 30 s, 72°C for 30 s, with an initial denaturation step at 95°C for 3 min and a final elongation step of 72°C for 5 min) using the forward and reverse primers from Klindworth *et al.* (2013) (Table 2.1). Archaeal 16S rRNA genes were amplified by PCR for 30-35 cycles (94°C for 15 s, 60°C for 15 s and 72°C for 15 s, with an initial denaturation step at 94°C for 3 min and a final elongation step of 72°C for 10 min) using the amplicon primer pair 344F and 915R (Table 1). All amplicon PCRs were composed of 12.5 µl AppTaq Redmix (2X) (Appleton Woods), 1 µl of each primer, 1 µl of DNA extract and 9.5 µl of PCR water (25 µl total reaction volume). All PCR products (5 µl) were visualised on a 1% agarose gel (as described in Section 2.3). The remaining PCR products (20 µl) were loaded onto two 96-well PCR plates.

2.5.2 Purification of PCR Products

PCR products were purified following the protocol provided by Illumina (Section 2.5.1). SPRI beads (20 µl of AxyPrep™ Mag PCR Clean-up) were pipetted into each sample well of the 96-well plate (Star Lab) and mixed with the amplified PCR products (20 µl). PCR plates were incubated at room temperature (5 min) to facilitate binding of amplicon products to the beads, before they were placed on a magnetic plate stand (IMAG™ Handheld Magnetic Separation Device) for 2 min. Whilst on the magnetic plate, the supernatant of each sample was removed, and samples were washed twice with 200 µl of ethanol (80%). After the second wash, residual ethanol was removed, and samples were air-dried for 10 min. PCR plates were removed from the magnetic plate stand and the bead-bound amplicons were re-suspended with 52.5 µl of Buffer EB (Qiagen). PCR plates were incubated for 2 min at room temperature before they were transferred to the magnetic plate stand. Samples were left on the magnetic plate stand at room temperature for 2 min to enable separation of the magnetic SPRI beads from the remaining solution. Avoiding the SPRI beads, 50 µl of each sample was transferred to a new PCR plate and used as template DNA in the index PCR.

2.5.3 Index PCR

Following the purification of amplicon PCR products, a second stage PCR was carried out to introduce dual indices and Illumina sequencing adaptors. Both archaeal and bacterial sequences were further amplified by PCR for 8 cycles (95°C for 30 s, 55°C for 30 s and 72°C for 30 s, with an initial denaturation step at 95°C for 3 min and a final elongation step at 72°C for 5 min). All samples were indexed using Nextera® XT Index Kit v2 (Set A). Index PCRs were composed of 25 µl of AppTaq Redmix (2X) (Appleton Woods), 5 µl of Index primer 1 (i7), 5 µl of Index primer 2 (i5), 10 µl of PCR water and 5 µl of purified PCR product as template (total reaction volume of 50 µl).

2.5.4 Clean-up of Indexed PCR Product

Purification of Indexed-PCR products was carried out following an alternative version of the procedure outlined in Section 2.5.2. These alterations consisted of: (1) a larger volume of SPRI beads (56 µl), which were added to a 50 µl starting volume, and (2) a lesser volume of EB buffer (27.5 µl) used in the elution stage in order to concentrate the final purified sample. Finally, 25 µl of each purified sample was transferred to a new 96-well PCR plate. After purification, 5 µl from all indexed samples was run on a 1% agarose gel (as described in Section 2.3).

2.5.5 DNA Quantification, Pooling and Denaturation

Purified Indexed PCR products were quantified using the Quant-iT™ PicoGreen™ ds DNA Assay Kit (Invitrogen) according to the manufacturer's instructions. Samples were diluted (50-100 fold) and pipetted (10 µl) in triplicate on to 384-well microtitre plates (Greiner). Each sample was mixed with 10 µl of 1× PicoGreen dye solution (1:1 ratio) and quantified by use of a FLUOstar Omega Microplate Reader (BMG Labtech). Approximate amplicon size was determined by running purified Index PCR products on a 1% agarose gel (as described in Section 2.2). Samples requiring re-quantification (e.g. if there was a discrepancy between the reading from the microplate and agarose gels) were quantified individually using a NanoDrop 3300 (Thermo Scientific). The following formula was used to work out the nanomolar concentration (nM) of individual samples and pooled libraries:

$$\frac{(Concentration\ in\ ng/\mu l\ )}{(660 \times Average\ Library\ Size)} \times 10^6$$

Pooling of archaeal and bacterial libraries were conducted separately by pipetting quantities of each purified Index-PCR product that were equimolar to 1 µl of the most concentrated (nM) sample. Both archaeal and bacterial libraries were re-quantified individually, and then combined in equimolar concentrations (1.5 ml micro-centrifuge tube). The final pooled amplicon library was re-quantified and diluted with EB buffer (Qiagen) to a 4 nM concentration.

The final pooled amplicon library (5 µl) was pipetted into a 1.5 ml micro-centrifuge tube and mixed with 5 µl of 0.2 N NaOH. Following a brief vortex and centrifuge at 280 × *g* for 1 min, the amplicon library was incubated at room temperature for 5 min to allow the DNA to denature and form single strands. The denatured amplicon library was diluted to 6 pM in two steps: first to 20 pM by combining the library (10 µl) with 990 µl of pre-chilled HT1 (Hybridization Buffer), and then, in a separate micro-centrifuge tube, by combining 180 µl of the 20 pM amplicon library with 420 µl of HT1. Separately, a PhiX control library (5 µl consisting of 2 µl of PhiX library (Illumina) and 3 µl of EB buffer) was prepared, denatured and diluted to 6 pM following the same protocol. The two libraries were combined to form a final reaction volume of 600 µl, which consisted of 480 µl of the denatured 6 pM amplicon library and 120 µl of the denatured 6 pM PhiX control library.

Finally, the combined amplicon/PhiX library was incubated in a water bath at 96°C for 2 min (to facilitate heat-denaturation), mixed by inversion and placed in an ice-water bath for 5 min before being pipetted into the Miseq Reagent cartridge and initiating the start of the Illumina Miseq sequencing run.

2.6 Sequence Analysis

As the MiSeq run contained samples from multiple experiments, the initial bioinformatic analyses of the resulting sequence read files were led by Dr. Boyd McKew. Due to the size of the archaeal amplicon, only the forward archaeal reads were used in subsequent analyses. Bacterial paired reads were quality trimmed using Sickle (Joshi et al. 2011) and error corrected using the BayesHammer algorithm (Nikolenko et al. 2013) within SPADes (Nurk et al. 2013). Bacterial sequences were then pair-end aligned using PEAR (Zhang et al. 2014) within PANDASeq (Masella et al. 2012). Both the archaeal single reads and paired-end bacterial sequences were dereplicated and sorted by their abundance before OTU centroids were picked using VSEARCH (Rognes et al. 2016) at a 97% similarity threshold. UCHIME (Edgar et al. 2011) was used to identify both de-novo and reference-based chimera sequences. Taxonomy assignment was performed with the RDP classifier (Wang et al. 2007). An OTU table was constructed using Microsoft Excel. In Excel, the following were

removed: all OTUs identified with sequences containing de-novo chimeras; all archaeal OTUs with a sequence length shorter than 200 base pairs and all bacterial OTUs with a sequence length shorter than 400 base pairs; all samples yielding fewer than 1000 reads, or suspected of contamination; and any singleton OTUs.

Individual centroid OTUs of interest were identified based on sequence identity using BLAST (16S ribosomal RNA (Bacteria and Archaea) and Nucleotide collection (nt)). Multiple sequence alignments were performed in MEGA7 (Kumar *et al.*, 2016) using the Muscle algorithm (basic settings: UPGMA, gap opening penalty -400, gap extend 0). Alignments were trimmed to 340 bp for archaea and 468 bp for bacteria. Phylogenetic trees (Neighbour-Joining, Jukes-Cantor) were also constructed in MEGA and subject to the bootstrap test (500 repeats).

2.7 Quantitative Real-time PCR Amplification of Archaeal and Bacterial 16S rRNA Gene Sequences

The abundances of archaeal and bacterial 16S rRNA gene sequences present in each DNA extract were determined using quantitative real-time PCR (qPCR). Archaeal and bacterial 16S rRNA gene amplification was measured using the CFX384 Touch™ Real-Time PCR Detection System (Bio-Rad). All runs were programmed using the accompanying software Bio-Rad CFX Manager v3.1.

Standards for archaeal and bacterial reactions were generated by amplifying DNA from sample T0-B2B. Template DNA from T0-B2B was amplified for 32 cycles using archaeal primers 344F and 915R, and for 27 cycles using bacterial primers 341F and 915R (Settings described in Section 2.3). PCR products were purified using a GenElute™ PCR Clean-up Kit (Sigma-Aldrich) according to the manufacturer's instructions. Purified standards were quantified using Quant-iT™ PicoGreen™ ds DNA Assay Kit (as described in Section 2.5.5) and 16S rRNA gene sequence copy numbers were calculated using the formula:

$$\frac{(Avogadro\ constant\ \times\ Concentration\ of\ DNA\ (ng/\mu l\ )}{(Size\ of\ product\ (bp)\ \times\ 660)}$$

All PCRs were performed in triplicate and consisted of 5 µl of SensiFAST™ SYBR® No-ROX Mix (2X) (Bioline), 0.2 µl of domain-specific forward primers (10 µM) and reverse primers (10 µM) as indicated in Table 2.1, 3.6 µl of PCR water and 1 µl of template DNA (total reaction volume of 10 µl). Each run included a series of 10-fold diluted standards (10^{-3} through to 10^{-7}) to generate a standard curve, as well as a no-template control. Archaeal 16S rRNA genes were amplified for 39 cycles (consisting of 95°C for 10 s and 60°C for 30 s, and included an

initial denaturation step at 95°C for 3 min) using the primer pair 344F and 915R (Table 2.1). Bacterial 16S rRNA genes were similarly amplified for 39 cycles (consisting of 95°C for 10 s and 55°C for 30 s, and included an initial denaturation step at 95°C for 3 min) using the primer pair 341F and 534R (Table 2.1). To assess the binding specificity of respective primer sets, all reactions were programmed to include a melt curve. After 39 cycles, samples were heated to 95°C for 10 s, cooled to 65°C for 5 s and then heated up to 95°C in 0.5°C increments.

The mean 16S rRNA gene sequence copies per cm^3 were calculated from three experimental replicates at each time point (T0-T4). Experimental replicates in turn were calculated from the starting quantity of three technical replicates. To account for differences between the physical states and densities of fluid brines and solid halite crystals, the 16S rRNA gene copy numbers derived from each sample were normalised to equal 1 cm^3. The density of saturated NaCl solution is 1.202 g/cm^3 whereas the density of halite is 2.165 g/cm^3. As 1 ml is equivalent to 1 cm^3, the 16S rRNA gene copy number from 1 ml of saturated brine was divided by 1.202 g/cm^3. Gene copy numbers from 1 g of halite were multiplied by 2.165 g/cm^3.

2.8 Data Analysis

Community analyses were carried out together with Dave R. Clarke (leading) and were performed on rarefied communities (1500 sequences per sample) using the vegan package (https://CRAN.R-project.org/package=vegan) in R. Community dissimilarity was quantified using the Sorensen index, and evenness quantified as Pielou's evenness. Non-metric Multidimensional Scaling plots (NMDS) were generated based on the Sorensen index. PERMANOVAs were run using 1000 permutations. After accounting for differences in pond source (1, 2 or 3) and sample type (brine or halite crystal), the significance of time was assessed using marginal p-values. Differences in evenness and richness between time points were modeled using mixed effects models. For richness, negative binomial models were used with brine as a random intercept. For evenness, Gaussian mixed models were used with logit-transformed evenness values, and brine as a random intercept.

The relative abundances of sequences were calculated using MS Excel 2016. Pairwise comparisons between communities of brine and halite samples and between time points were performed at two hierarchical levels (Genus and OTU) using the statistical package STAMP (Parks *et al.*, 2014) employing the criteria: Two-sided Welch's t-test, $P<0.05$, Sequence filter: Difference between proportions <0.2 or difference between ratios <1.5.

STAMP was used to generate extended error bar plots with corrected p-values. Data were sorted according to their effect size. Differences in genera or OTU abundances across time points were compared using a one-way ANOVA followed by Tukey's HSD (Honest Significant Difference) in GraphPad (Prism 6).

Table 2.1: Details of primers used throughout this thesis.

Primer Name	Sequence (5' - 3')	Detection (D), Sequencing (S) or Quantification (Q)	Annealing temperature (°C)	Reference
Bac 341F	**CCTACGGGAGGCAGCAG**	D, Q	55	Muyzer *et al.* (1993)
Bac 534R	**ATTACCGCGGCTGCTGG**	D, Q	55	Muyzer *et al.* (1993)
Arch 344F	**ACGGGGYGCAGCAGGCGCGA**	D, Q	59	Raskin *et al.* (1994)
Arch 915Ru	**GTGCTCCCCCGCCAATTCCT**	D, Q	59-61	Stahl and Amann. (1991) in Raskin *et al.* (1994)
Arch 344F*	TCGTCGGCAGCGTCAGATGTGTATAAGAGACAG**ACGGGGYGCAGCAGGCGCGA**	S	59	Raskin *et al.* (1994)
Arch 915R*	GTCTCGTGGGCTCGGAGATGTGTATAAGAGACAG**GTGCTCCCCCGCCAATTCCT**	S	59-61	Stahl and Amann. (1991) in Raskin et al. (1994)
Bac 341F *	TCGTCGGCAGCGTCAGATGTGTATAAGAGACAG**CCTACGGGNGGCWGCAG**	S	55	Klindworth *et al.* (2013)
Bac 785R *	GTCTCGTGGGCTCGGAGATGTGTATAAGAGACAG**GACTACHVGGGTATCTAATCC**	S	55	Klindworth *et al.* (2013)

* Primers sequences including 5' overhang adaptor (red) required for 16S rRNA gene library preparation

The degenerate bases **Y** (either C or T), **W** (A or T), **H** (A, C or T), **V** (A, C or G) and **N** (A, C, G or T) indicate positions at which there are more than one nucleotide base possibilities.

3 Results

3.1 Brine Composition

Table 3.1 shows the water activity and ionic composition of the three brines. Brine 1 (from Pond 1) was from a crystalliser pond that was being harvested on the day of sampling and had the lowest water activity of 0.716 a_w of the three samples. This was followed by brine 3 (0.734 a_w), which was also from the brine of a recently harvested crystalliser pond (Pond 3) next to Pond 1. Brine 2 (from Pond 2) had the highest water activity of the three samples at 0.755 a_w and was derived from an evaporation pond approaching saturation also near to Pond 1 (Figure 2.1). The Mg^{2+} and SO_4^{2-} concentrations were (highest to lowest) Brine 1 > Brine 3 > Brine 2, while the Na^+ concentration showed the opposite trend.

Table 3.1: Major ion concentrations (g/L) and water activity (a_w) of brines derived from three hypersaline saltern ponds

Ponds from which the brines derived (g/L)			
Ion	**1**	**2**	**3**
Na^+	82.5	116.7	100.9
Mg^{2+}	42.3	16.8	24.2
Ca^{2+}	0.2	0.1	0.2
K^+	11.8	5.9	6.8
Li^+	0.002	0.001	0.002
Cl^-	198.9	200.4	193.5
SO_4^{2-}	59.1	19.8	32.4
Water activity (a_w)	0.716	0.755	0.734

3.2 Comparing the Abundance of Archaea and Bacteria Following Entombment in Halite crystals

3.2.1 Halite Entombment and Succession

Archaeal and bacterial 16S rRNA gene copies from halite-crystal DNA extractions were quantified using qPCR to assess changes in abundance over the 21-week period of halite entombment (Figure 3.1). Comparisons between the mean (n = 3) archaeal and bacterial numbers in parent brines before crystallisation (T0) showed that archaea were considerably more abundant than bacteria (1.4×10^8 to 1.6×10^9 archaeal cells/cm^3 compared with 7.6×10^4 to 3.5×10^5 bacterial cells/cm^3). Comparisons in abundance between parent brines and halite samples show that cells from both domains were entombed inside halite in numbers similar to those present in the parent brines (Figure 3.1).

No significant differences in archaeal abundance were found across time points (from brine to 21-weeks entombed) for communities originating from Pond 1 (ANOVA, $F_{4,10} = 1.888$, $P = 0.1891$) nor Pond 2 ($F_{4,10} = 0.9749$, $P = 0.4631$). However, abundances were more variable across time points in samples from Pond 3; archaea were significantly more abundant in the parent brine (T0) than in T1 and T2 halite ($F_{4,10} = 10.87$, P<0.01; Tukey's HSD, $P < 0.05$ for all T0 comparisons). Moreover, archaea were significantly more abundant in T4 samples than in T1 and T2 ($P < 0.05$) (Figure 3.1A). Alternatively, comparisons of bacterial 16S rRNA gene copy numbers showed differences in abundances across time points in Ponds 1 ($F_{4,10} = 4.015$, $P < 0.05$) and Pond 2 ($F_{4,10} = 6.993$, $P < 0.01$) but not in Pond 3 ($F_{4,10} = 3.147$, $P = 0.0644$). In Pond 1, bacteria were significantly more abundant in T4 samples than in the parent brine (T0) ($P < 0.05$), however no other significant differences were observed between any other time points. In Pond 2, bacteria were significantly more abundant in T3 samples than in samples from any other time point ($P < 0.05$ for all comparisons).

Comparisons in abundance between parent brines showed higher numbers of archaeal 16S rRNA copies in Pond 3 than in Pond 1 (ANOVA, $F_{2,6} = 20.66$, $P < 0.01$; Tukey's HSD, $P < 0.01$) and Pond 2 ($P <0.01$). There were no significant differences in bacterial numbers between the three brines ($F_{2,6} = 1.019$ $P = 0.4159$).

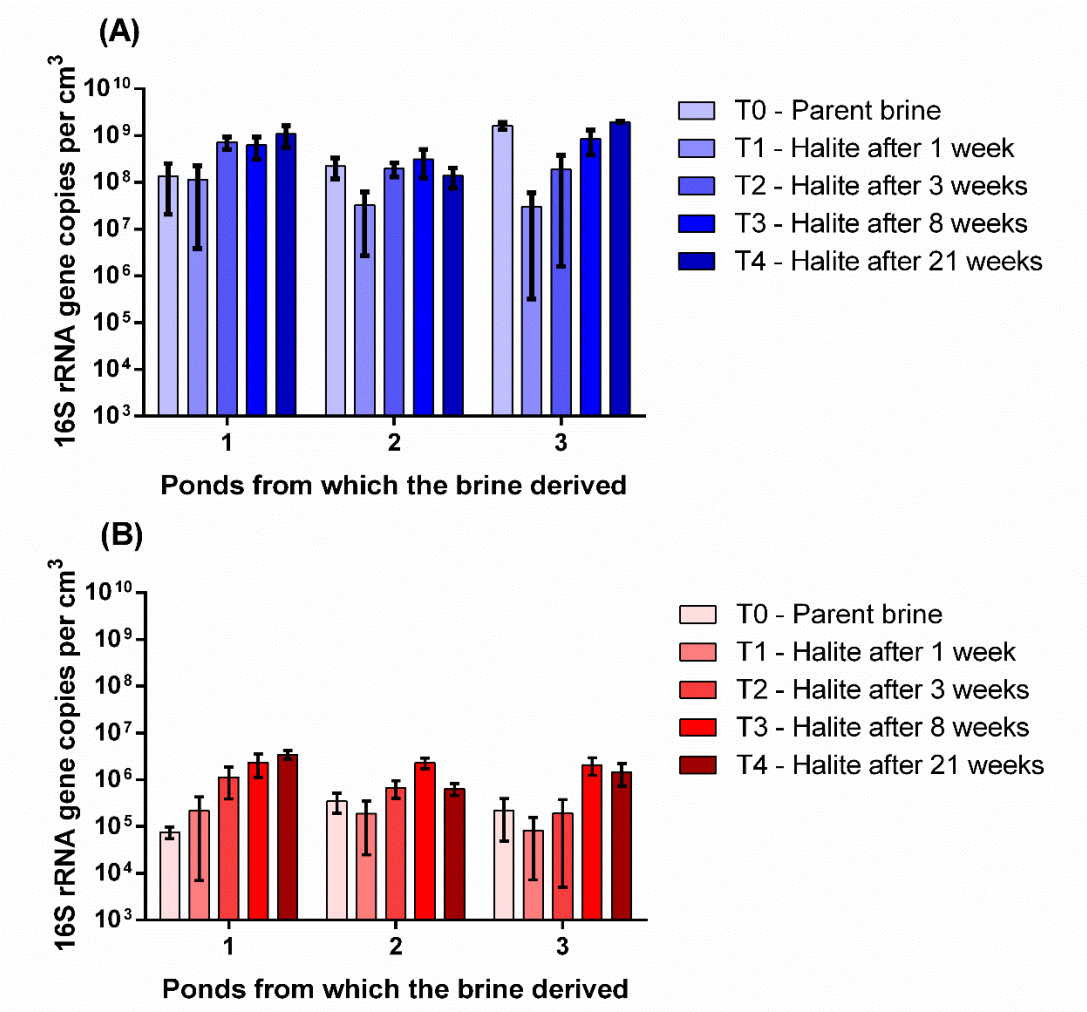

Figure 3.1: The mean number of 16S rRNA gene copies per cm^3 quantified from DNA extracts taken at each set point of the 21-week period. Each bar represents the mean 16S rRNA gene copies of three experimental replicates (i.e. brines transferred to Petri dishes to allow halite crystals to form), which in turn derived from the mean of three technical replicates, i.e. replicates of the same sample on the qPCR run. Error bars represent the standard error of the experimental replicate mean values. **Archaeal (A)** 16S rRNA copy numbers were quantified using archaeal primers 344F and 915R (R^2 = 0.999, E = 110.4%). **Bacterial (B)** 16S rRNA copy numbers were quantified using bacterial primers 341F and 534R (R^2 = 0.990, E = 78.9%). To account for differences between the physical states and densities of fluid brines and solid halite crystals, the 16S rRNA gene copy numbers derived from each sample were normalised to equal 1 cm^3. The density of saturated NaCl solution is 1.202 g/cm^3 whereas the density of Halite is 2.165 g/cm^3. As 1 ml is equivalent to 1 cm^3, the 16S rRNA gene copy number from 1 ml of saturated brine was divided by 1.202 g/cm^3. Gene copy numbers from 1 g of halite were multiplied by 2.165 g/cm^3. Time points at which DNA was extracted from halite were: 1 week (T1), 3 weeks (T2), 8 weeks (T3) and 21 weeks (T4).

Comparisons using the mean archaeal 16S rRNA copies across all three ponds showed that with the exception of T1 compared with T4 halite, which showed that archaea were significantly more abundant in T4 samples (Tukey's HSD, $P = 0.0294$), no other significant differences were observed between pairs of time points (Figure 3.2). In contrast, bacterial abundances were much more variable ($F_{4,10} = 17.46$, $P < 0.01$). While no significant differences were observed in comparisons between T0, T1 and T2 samples ($P > 0.5$ for all comparisons) nor in comparisons between T3 and T4 samples ($P = 0.752$), bacteria were significantly more abundant in T3 and T4 samples than any others ($P < 0.05$ for all comparisons pairing either T1, T2, and T3 with T3 or T4).

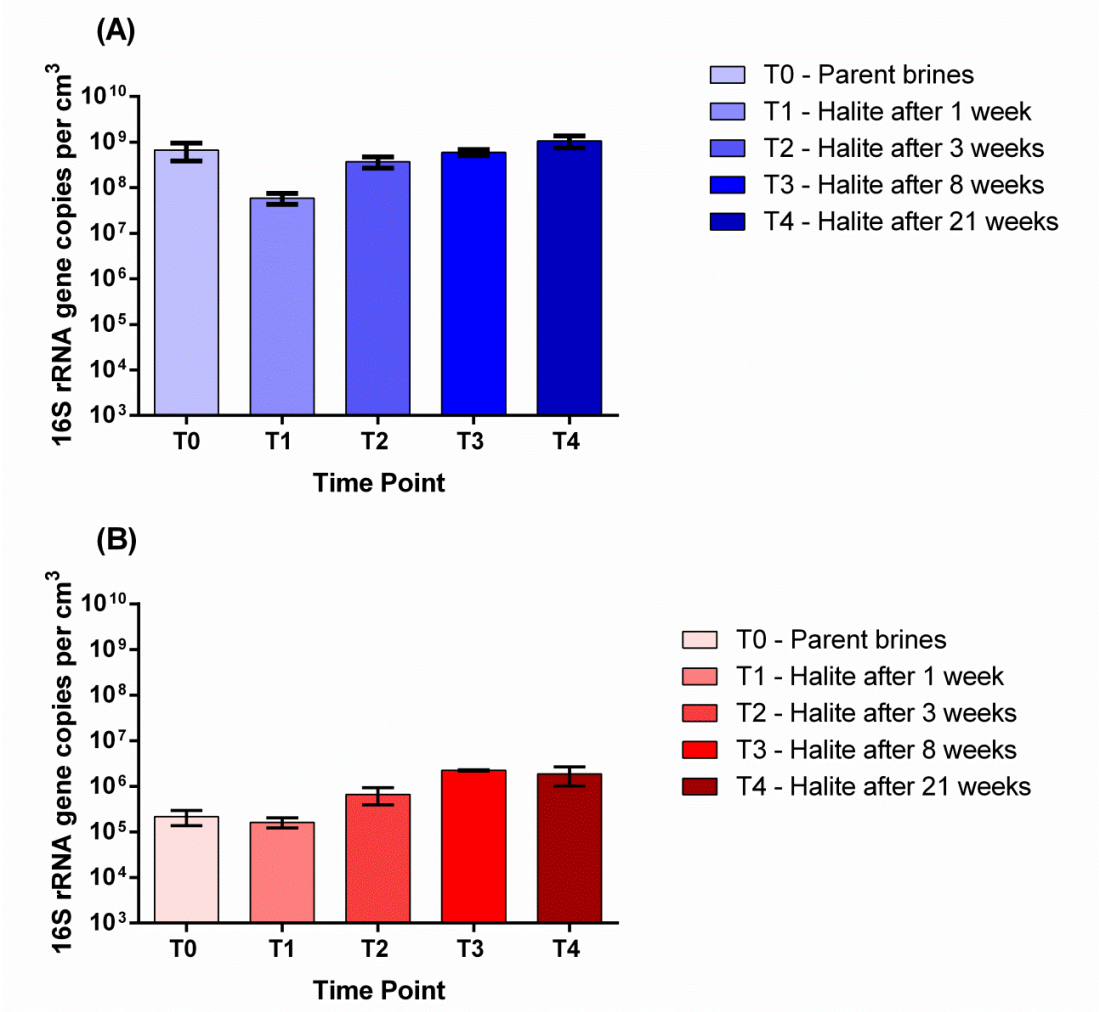

Figure 3.2: The mean number of 16S rRNA gene copies per cm^3 quantified from DNA extracts taken across all ponds at each set point of the 21-week period. Each bar represents the mean number of 16S rRNA gene copies across all ponds ($n = 3$). Mean copy numbers were calculated for both **Archaea (A)** and **Bacteria (B)** using the mean values of three sample replicates per brine, which derived from the mean of three technical replicates. Error bars represent the standard error of the sample mean values. Further details associated with the qPCR run conditions and the normalisation of data from two different sample types are available in Figure 3.1.

3.2.2 *In-situ* Brine and Halite crystals

The 16S rRNA gene copies from *in-situ* brine and halite DNA extractions were quantified using qPCR to compare the differences in abundances between the two sample types. Figure AI.1 indicates that there were more archaea in halite than in brine, however, the volume of brine filtered for each replicate was an estimated amount (approx. 10 ml). There is no data for *in-situ* bacterial abundance.

3.3 Quality Control of MiSeq Analysis

Out of 87 samples, seven failed to yield archaeal amplicons, whereas only three samples failed to yield bacterial amplicons (Electronic Appendix I). Sequences from successfully amplified samples were clustered into operational taxonomic units (OTU) at the 97% similarity level. OTUs were removed if they: identified as *de-novo* chimeras, were <200 bp (archaea) or <400 bp (bacteria). Moreover, samples which were presumed to be contaminated (due to their unusual community structures/members), negative controls and those with fewer than 1000 reads were also removed from analyses (detailed in EAI.1 and EAI.2). Finally, singleton OTUs across the remaining samples were removed. A total of 2,288,565 archaeal sequences from 80 samples were reported before OTU and sample removal (EAI.1). After the removal of OTUs and individual samples based on the above criteria a total of 1,715,018 archaeal sequences remained from 75 samples. A total of 1,732,463 bacterial sequences from 84 samples were reported before OTU and sample removal (EAI.2). After the removal of OTUs and individual samples based on the above criteria a total of 593,746 remained from 80 samples. Further details of the number of sequences removed from each sample are included in Electronic Appendix I (EAI.3 and EAI.4), along with the final archaeal and bacterial OTU tables used for analyses (EAI.5 and EAI.6).

3.4 Comparisons of Brine and Halite-entombed Archaeal Communities

3.4.1 Non-Metric Multidimensional Scaling (NMDS) of Archaeal Communities in Brine and Halite Crystals

NMDS analysis using Sorensen's index (Figure 3.3) shows little separation between archaeal communities from different time points (stress = 0.12). In both sample types (brine and halite), the communities in samples from Pond 2 (squares in Figure 3.3) were distinct from communities in Ponds 1 and 3 at all time points. The Pond 1 *in-situ* community was very similar to that of Pond 1 brine (i.e. the brine samples that were left in Falcon tubes and collected at each time point over the 21-week period).

PERMANOVA analyses showed a small but significant difference in community composition between brine and halite communities ($F_{1,\ 73} = 2.28$, $R^2 = 0.03$, $P = 0.031$). This difference was also observed when *in-situ* samples were removed from the analysis ($F_{1,\ 68} = 2.38$, $R^2 = 0.03$, $P = 0.027$). Time had a significant effect on the composition of brine communities ($F_{5,\ 31} = 2.12$, $R^2 = 0.25$, $P = 0.006$), but did not have a significant effect on the composition in halite communities ($F_{4,\ 33} = 1.04$, $R^2 = 0.11$, $P = 0.39$). Lastly, the source pond had a small but significant effect on both brine ($F_{1,\ 35} = 2.87$, $R^2 = 0.08$, $P = 0.018$) and halite ($F_{1,\ 36} = 2.76$, $R^2 = 0.07$, $P = 0.012$) community composition.

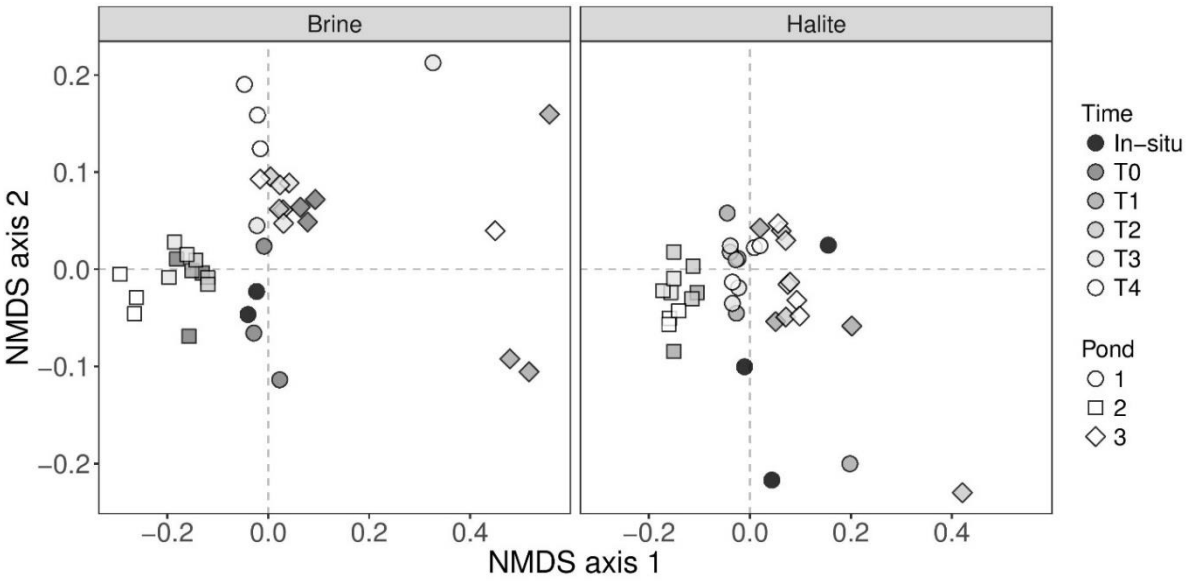

Figure. 3.3: NMDS analysis of archaeal brine and halite samples from *in-situ* and lab succession experiments using Sorensen's index. Brine (left) and halite (right) communities are shown separately for clarity but were analysed together. The brine and halite source of each sample is indicated by circles (Pond 1), squares (Pond 2), diamonds (Pond 3). The *in-situ* communities from Pond 1 are represented by black circles. Samples from different time points are represented by shading (dark grey to white). Time points at which DNA was extracted from brine and halite were: 0 weeks (T0), 1 week (T1), 3 weeks (T2), 8 weeks (T3) and 21 weeks (T4) (See Figure 2.1). Figure was produced by Dave R. Clark

3.4.2 Comparing the Effect of Time, Pond Origin and Sample-type on OTU Richness of Archaeal Communities

Generalised linear mixed-model analyses showed that, when comparing with T0 archaeal communities from all sample-types and Ponds (but excluding *in-situ* communities), the T1 communities showed a significant decrease in richness (coef = -0.24, *z*-value = -2.25, $P < 0.05$), largely attributed to changes in Pond 3. However, no significant differences were observed in comparisons between T0 and communities at any other time point ($|z\text{-value}| < 0.23$, $P = 0.81$ for all other time points) (Figure 3.5A).

When considering communities from brine and halite individually, a similar pattern was observed in brine communities (all Ponds), with a significant decrease in OTU richness in T1 communities relative to T0 communities (coef = -0.66, $z = -3.67$, $P < 0.001$), however no significant differences were observed between T0 and communities from any other time point ($|z| < 0.64$, $P > 0.52$ for all other time points) (Figure 3.4A). In halite (all Ponds), relative to T0 communities (there were no T0 points for halite communities) there were no significant

differences in OTU richness between any time points ($P > 0.40$ for all time points) (Figure 3.4A).

When considering differences in OTU richness between Ponds (both sample types), relative to communities from Pond 1, communities from derived from Pond 2 showed significantly higher OTU richness (coef = 0.32, $z = 4.25$, $P < 0.0001$), whereas communities derived from Pond 3 were significantly lower in OTU richness (coef = -0.33, $z = -4.22$, $P < 0.0001$) (Figure 3.4B). The same pattern was observed when sample types were separated. Both brine (coef = 0.33, $z = 2.66$, $P < 0.01$) and halite (coef = 0.35, $z = 5.42$, $P < 0.001$) communities from Pond 2 had a significantly higher OTU richness than those from Pond 1 and, likewise, both brine (coef = -0.33, $z = -2.56$, $P < 0.05$) and halite (coef = -0.30, $z = -4.29$, $P < 0.001$) communities from Pond 3 were significantly less rich than Pond 1. Lastly, when comparing between sample types (from all Ponds), there was no significant difference in OTU richness between brine and halite communities (coef = -0.03, z-value = -0.43, $P = 0.67$) (Figure 3.4C).

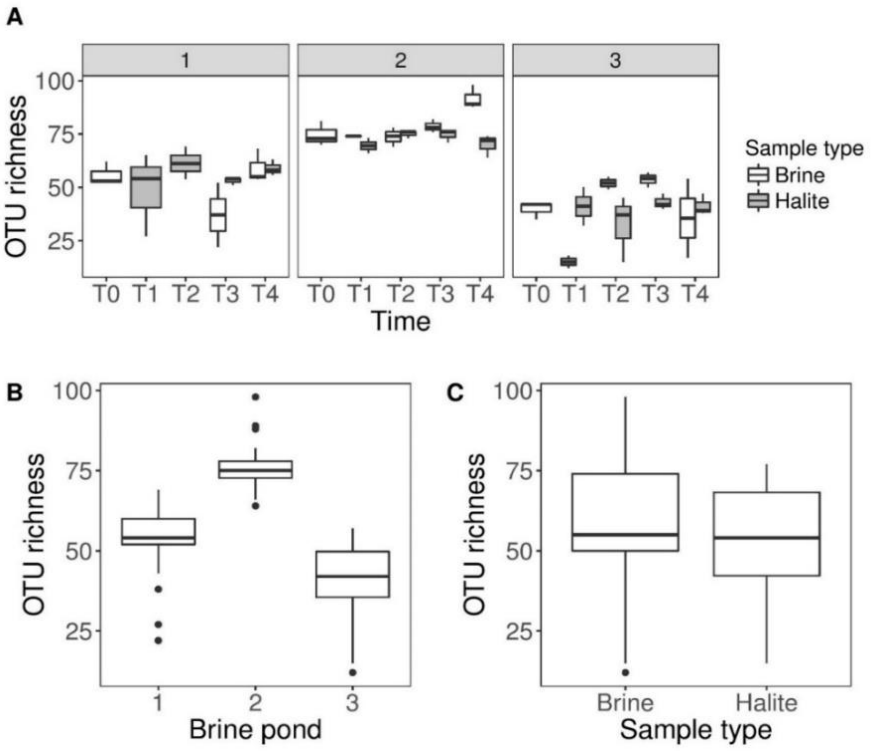

Figure 3.4: Comparisons of OTU richness in archaeal communities. Panel A displays the changes in OTU richness over time for archaeal communities derived from three Ponds (indicated in the grey boxes). Wider boxes represent time points at which only one sample-type (white for brine, grey for halite) was available for analyses because <2 replicates were available for the comparator sample. **Panel B** shows the differences in archaeal OTU richness (both sample-types) between Ponds, and **Panel C** compares sample types (all Ponds).

3.4.3 Comparing the Effect of Time, Pond Origin and Sample-type on OTU Evenness of Archaeal Communities

Generalised linear mixed-models analyses were also used to perform matching comparisons of OTU evenness between archaeal communities (Figure 3.5). When comparing with T0 archaeal communities from all sample-types and Ponds (but excluding *in-situ* communities), T1 (coef = 0.27, $t = 3.12$, $P < 0.01$) and T4 (coef = 0.18, $t = 2.21$, $P < 0.05$) communities were significantly more even. Interestingly, T2 and T3 communities were more even, as observable in Figure 3.5A, yet the difference with T0 was not significant ($|t| < 1.33$, $P > 0.18$ for all other timepoints).

When considering communities from brine and halite individually, a similar pattern was observed in brine communities (all Ponds), likewise, when comparing with T0 communities, the T1 (coef = 0.54, $t = 5.17$, $P < 0.0001$) and T4 communities (coef = 0.31, $t = 3.86$, $P < 0.001$) were significantly more even, whereas communities at T2 and T3 showed no significant difference in evenness to those at T0 ($|t| < 1.72$, $P > 0.09$ for all other timepoints) (Figure 3.5A). In halite (all Ponds), T1 and T2 communities were significantly more even (T1; coef = 0.13, $t = 2.06$, $P < 0.05$, T2; coef = 0.13, $t = 2.09$, $P < 0.05$) than communities in the T0 parent brine, however there were no significant differences in OTU evenness between T0 and T3 or T4 ($P > 0.16$ in both cases) (Figure 3.5A).

When considering differences in OTU evenness between Ponds (both sample types), relative to communities from Pond 1, communities derived from both Ponds 2 (coef = -0.26, $t = -4.27$, $P < 0.0001$) and 3 (coef = -0.34, $t = -5.60$, $P < 0.0001$) were significantly less even (Figure 3.5B). Likewise, when sample types were separated, brine communities from Ponds 2 (coef = -0.36, $t = -3.84$, $P < 0.001$) and 3 (coef = -0.36, $t = -3.93$, $P < 0.001$) were significantly less even than communities from Pond 1. However, halite communities from Pond 3 were significantly less even than communities in Pond 1 (coef = -0.22, $t = -2.59$, $P < 0.05$) and there were no significant differences in OTU evenness between Ponds 1 and 2 ($P = 0.55$). Lastly, when comparing between sample types (from all Ponds), there was no significant differences in OTU evenness between brine and halite communities (coef = -0.07, $t = -1.43$, $P = 0.15$) (Figure 3.5C).

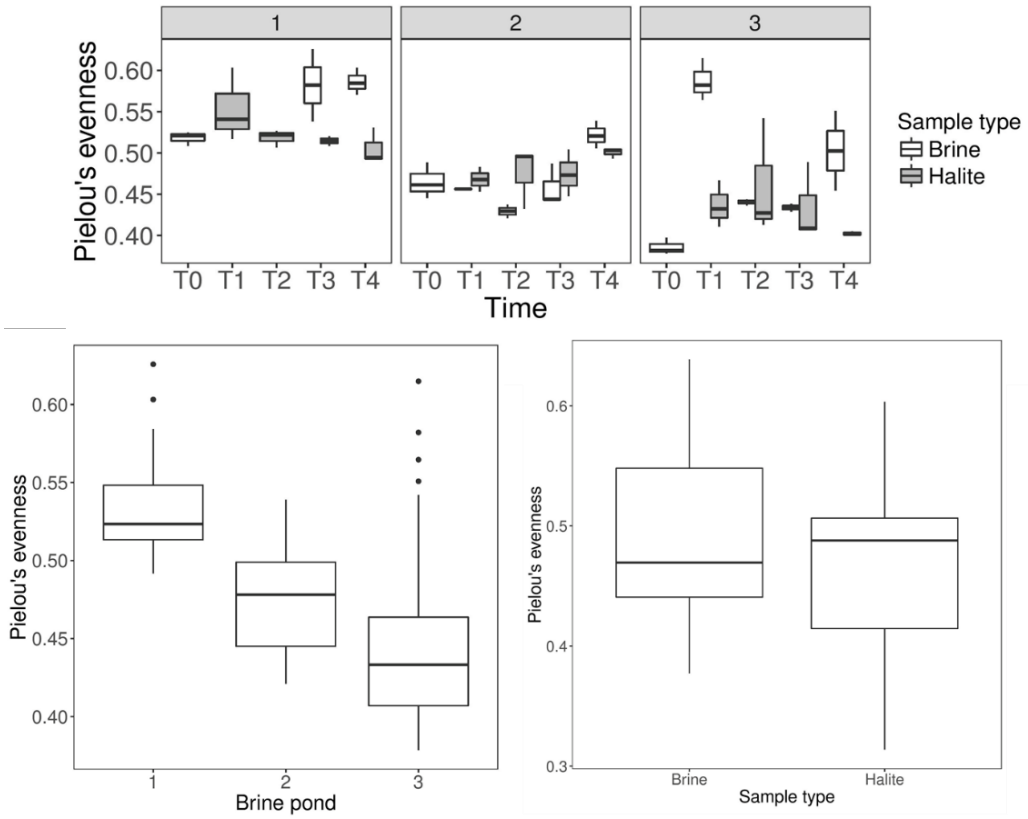

Figure 3.5: Comparisons of OTU evenness in archaeal communities. Panel A displays the changes in OTU evenness over time for archaeal communities derived from three Ponds (indicated in the grey boxes). Wider boxes represent time points at which only one sample-type (white for brine, grey for halite) was available for analyses because <2 replicates were available for the comparator sample. **Panel B** shows the differences in archaeal OTU evenness (both sample-types) between Ponds, and **Panel C** compares sample types (all Ponds).

3.4.4 Comparing the Archaeal Community Composition of *In-situ* Brine and Halite from Pond 1

Despite amplifying archaeal 16S rRNA gene sequences from all *in-situ* halite crystal samples, only brine samples from locations 1A and 1C were available for comparison as no archaeal sequences were detected in any repeated brine DNA extractions from location 1B (Figure 3.6). The mean relative abundance of archaeal genera across the replicate samples is shown in Figure 3.6. Comparisons of community composition in the *in-situ* brine and halite samples showed some obvious differences in the proportions of haloarchaeal genera. *Halorubrum* and *Haloquadratum* dominated archaeal communities (together they formed 69.5% of the brine community and 82.7% of the halite community). However, *Halorubrum* was significantly more abundant in halite than brine, whereas *Haloquadratum* was significantly more abundant in brine than halite as shown by STAMP analysis (Figure 3.7). All other genera of considerable relative abundance (≥1% in brines) were relatively less abundant inside halite (Figure 3.6). These included *Halobellus* (7.6 to 4.9%), *Halorientalis* (8.1 to 2.3%), *Haloplanus* (5.1 to 4.7%), *Halomicrobium* (3.2 to 0.5%), *Natribaculum* (1.7 to 1.3%) and *Candidatus* Nanosalina (1.7 to 0.2%). However, of these genera, only *Candidatus* Nanosalina showed a significant difference in relative abundance between brine and halite (Figure 3.7).

Pairwise comparisons of archaeal OTU abundances in brine and halite (Figure 3.8) showed that the genus *Halorubrum* was dominated by two main OTUs; Trp-Arc-1 was significantly more abundant in halite, whereas Trp-Arc-3 was significantly more abundant in the brine. In comparison, the genus *Haloquadratum* was dominated by Trp-Arc-2, which was significantly more abundant in brine. Moreover, an additional three low abundance OTUs were also significantly more abundant in brine than halite. Interestingly, Trp-Arc-1 alone constitutes up to 69.3% of the total archaeal community inside halite. A BLAST search (16S rRNA database) showed that Trp-Arc-1, Trp-Arc-2 and Trp-Arc-3 shared high sequence similarities with *Halorubrum arcis strain* AJ201 (97%), *Haloquadratum walsbyi* strain JCM 12705 (99%) and *Halorubrum orientale* strain CECT 7145 (99%), respectively (Figure AI.2).

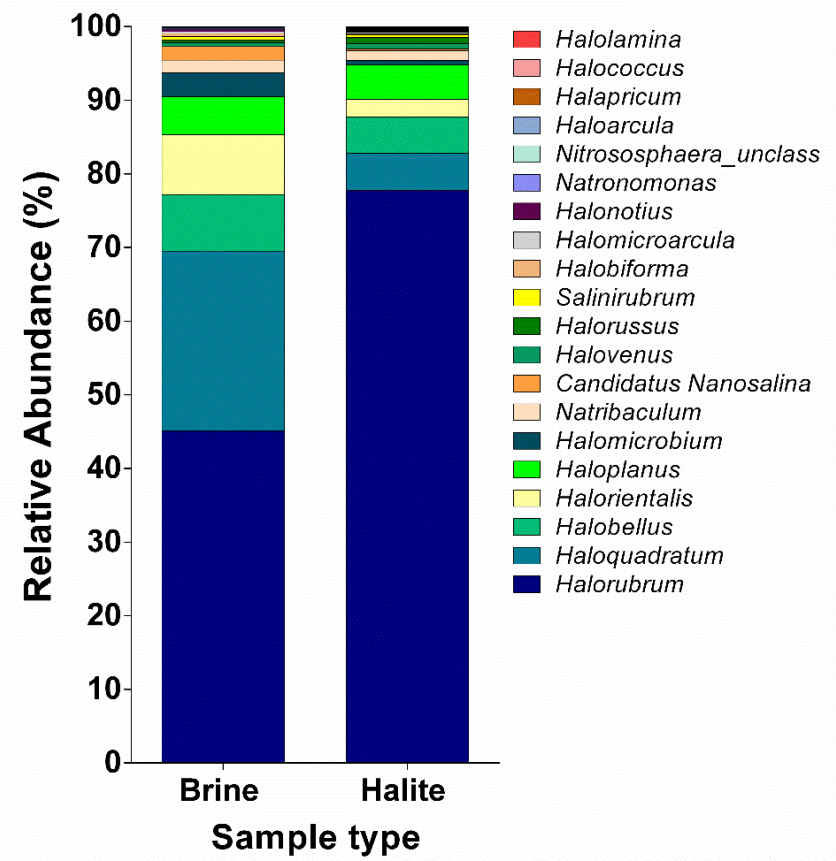

Figure 3.6: The mean relative abundances of archaeal genera identified from *in-situ* brine and halite samples from Pond 1. Brine (*n* = 2) and halite (*n* = 3) samples were collected from Pond 1. PCR amplification of DNA extracts from sample location 1b yielded no archaeal sequences from brine. The figure legend displays the top 20 (of 40) most abundant genera in ascending order. The relative abundance (%) for each genus was calculated by summing the abundances of all OTUs with taxonomy assigned to that specific genus. Taxonomy was assigned to each OTU by the RDP classifier based on the top hit, and therefore it should be noted that these assignments are indicative only and in some cases may not represent the true taxonomy of OTUs that were equidistant to multiple known strains.

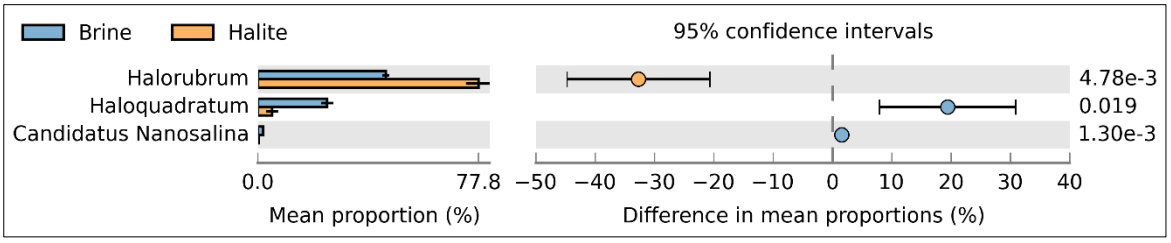

Figure 3.7: Differences in the relative abundance of archaeal genera between *in-situ* brine and halite samples from Pond 1. Brine (*n* = 2) and halite (*n* = 3) samples were from Pond 1. Analysis was performed using STAMP (Parks *et al*., 2014), using default parameters (Welch's T-test, Two-sided), except that parameters for filtering out were: *P* value < 0.05; and difference between proportions < 0.2 or difference between ratios <1.5. Data were sorted according to effect size and show corrected p-values.

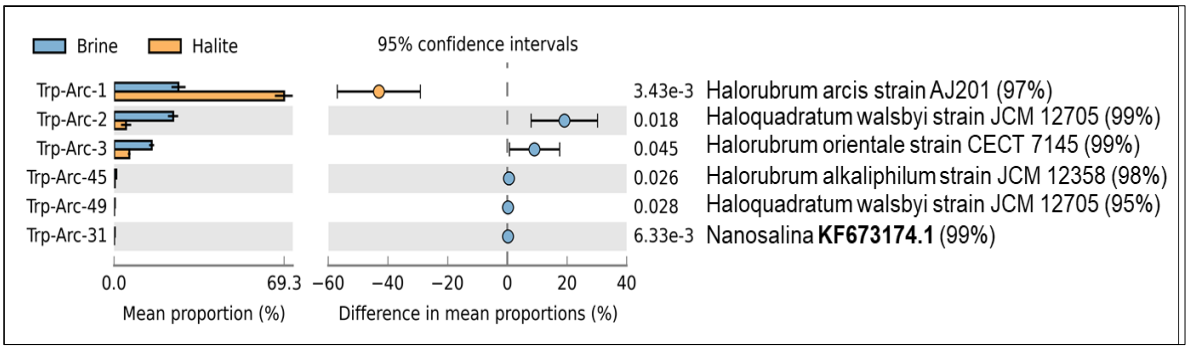

Figure 3.8: Differences in the relative abundance of archaeal OTUs between *in-situ* brine and halite samples from Pond 1. Brine (*n* = 2) and halite (*n* = 3) samples were collected from pond 1. Analysis was performed using STAMP (Parks *et al*., 2014) as described in Figure 3.7. A BLAST search (16S rRNA and nr/nt) was used to identify strains with high sequence similarity (right). Trp-Arc-31, presumed to be a member of the *Candidatus* Nanosalina, failed to show sequence similarity with any characterised strain and is annotated with the accession number (bold) of its closest uncultivated match.

3.4.5 Comparing the Archaeal Communities found in Parent Brines (T0) from Ponds 1, 2 and 3

Similarly, to the *in-situ* communities from Pond 1, all three brines from Ponds 1, 2 and 3 were inhabited by large populations of the two genera *Halorubrum* and *Haloquadratum* (Figure 3.9, EAII.4). Figure 3.9 shows that *Halorubrum* was most abundant in Pond 3 whereas *Haloquadratum* was most abundant in Pond 2 (the Pond with the highest A_w). Moreover, pairwise comparisons of the abundance of archaeal genera between T0 brines showed that *Haloplanus, Halorientalis, Halomicrobium, Natribaculum, Salinirubrum* and *Halorussus* were significantly more abundant in Pond 1 than in Ponds 2 and 3, whereas *Candidatus* Nanosalina, *Halovenus, Halobiforma* and *Natranomonas* were more abundant in Pond 2 than in Ponds 1 and 3 (Figure 3.10). Interestingly, out of all archaeal genera reported in T0 brine samples (all Ponds), no single genus was more abundant in Pond 3 than in Ponds 1 or 2. Overall, the archaeal community in Pond 3 was considerably less diverse at the genus level than ponds 1 and 2. Only 27 of 48 identified genera were identified in T0 samples from Pond 3, whereas 38 genera were identified in Pond 1 and 41 in Pond 2 (EAII.4). Moreover, Figures 3.4 and 3.5 show that overall samples from Pond 3 were lower in both OTU richness and OTU evenness.

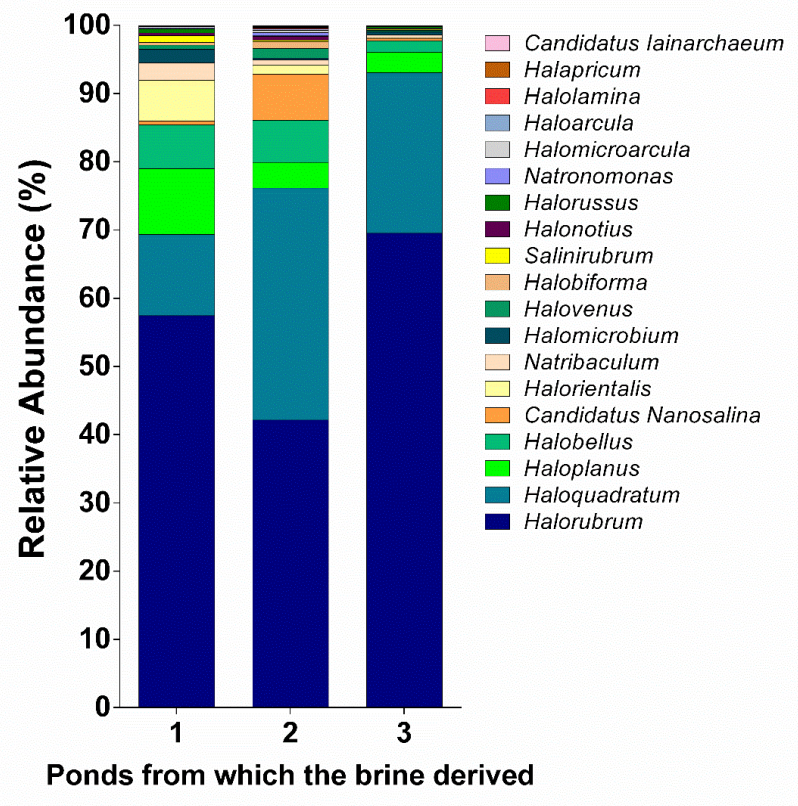

Figure 3.9: The relative abundance of archaeal genera in T0 brine (parent) samples derived from three ponds. Each bar displays the average relative abundances of archaeal genera derived three experimental repeats. The legend shows the top 20 (of 45) most abundant archaeal genera in brines across all ponds. The relative abundance (%) values for each genus were calculated by summing the abundances of all OTUs with taxonomy assigned to that specific genus. Taxonomy was assigned to each OTU by the RDP classifier based on the top hit, and therefore it is worth noting that these assignments are indicative only and in some cases may not represent the true taxonomy of OTUs that were equidistant to multiple known strains.

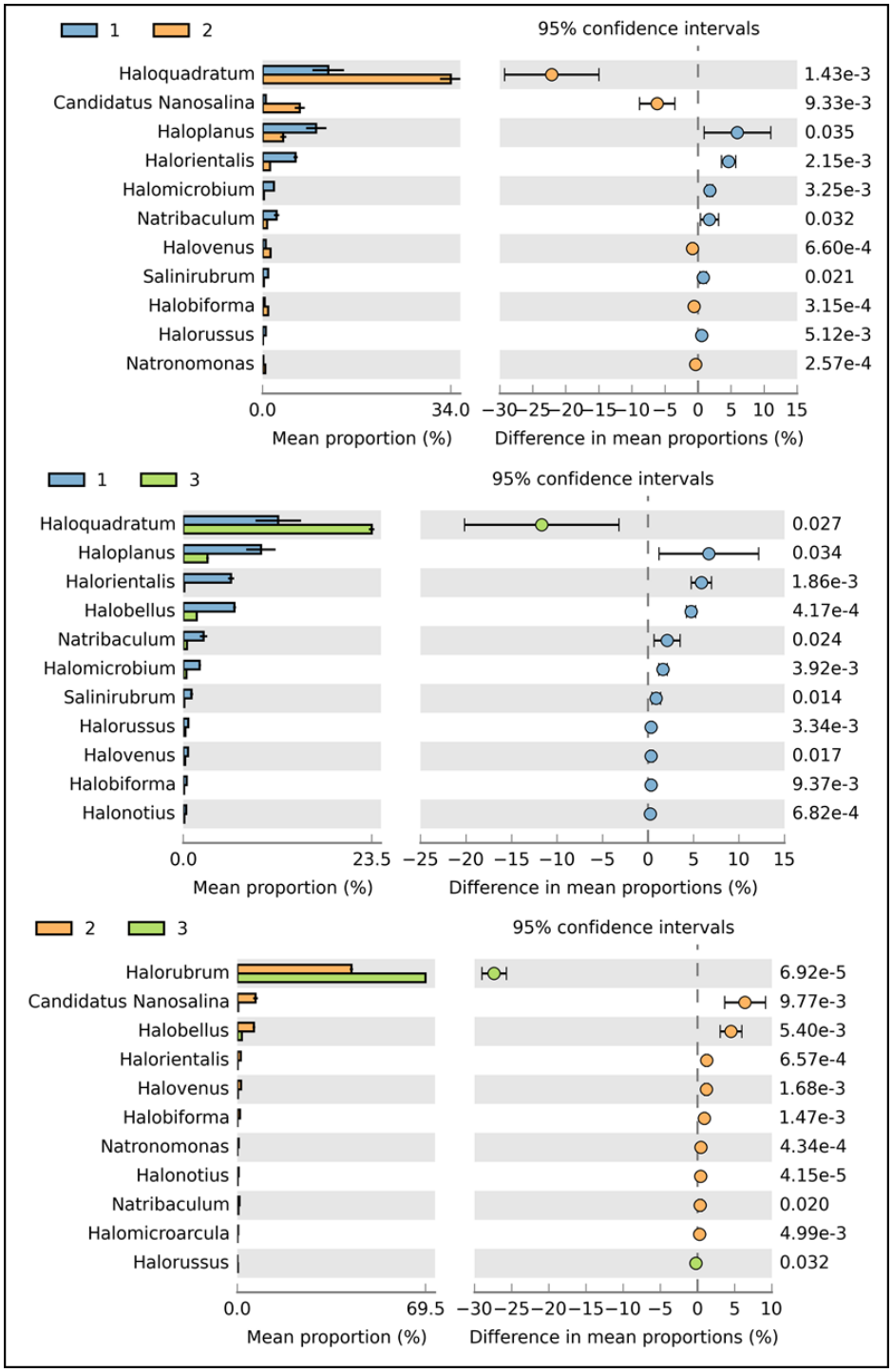

Figure 3.10: Differences in the relative abundance of archaeal genera between parent brine samples. Pairwise comparisons of the relative abundance of archaeal genera were performed between the parent brine (*n* = 3) community of ponds 1, 2 and 3. Analysis was performed using STAMP (Parks *et al*., 2014) as described in Figure 3.7.

There were many significant differences in the relative abundance of archaeal OTUs between T0 brine communities (Appendix I, EAII.1), most of which align with those observed at the genus level in Figure 3.9. Interestingly, while all three communities were dominated by the genus *Halorubrum,* some intra-genus differences were observed; in Pond 2, Trp-Arc-3

(99% similarity with *Halorubrum orientale*) was the most abundant phylotype and formed the dominant *Halorubrum* population as opposed to Trp-Arc-1 (97% similarity with *Halorubrum arcis*), which dominated in Ponds 1 and 3 (EAII.1, Figure 3.11).

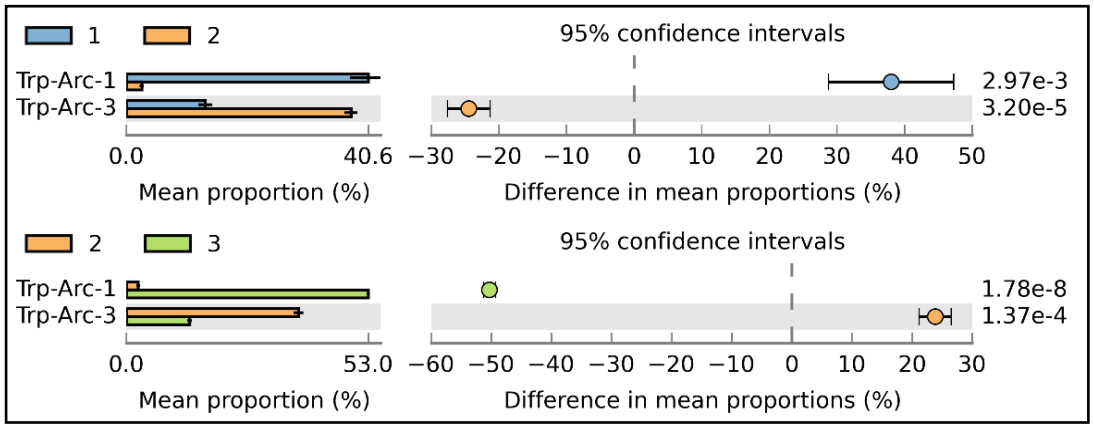

Figure 3.11: Differences in the predominant *Halorubrum* phylotype between parent brines. Pairwise comparisons of the relative abundance of Trp-Arc-1 (97% similarity with *Halorubrum arcis* AJ201*)* and Trp-Arc-3 (99% similarity with *Halorubrum orientale* CECT 7145) were performed between the parent brines (*n* = 3) of ponds 1, 2 and 3. No significant differences were observed in comparisons between ponds 1 and 3. Analysis was performed using STAMP (Parks *et al*., 2014) as described in Figure 3.7.

3.4.6 Changes in the Relative Abundance of Archaeal Genera over Time inside Lab-made Halite Crystals

Overall, comparison of archaeal communities between T0 brines and the halite derived from them across all time points (T1 to T4) showed relatively few differences in the relative abundances of major community constituents (i.e. those with >1% relative abundance) (Figure 3.12, EAII.2). Pairwise comparisons of the relative abundances of archaeal genera were performed to identify significant changes between parent brines and 1-week old halite (T0 vs T1) and between 1-week old and 21-week old halite (T1 vs T4), respectively (Figure 3.13). In all ponds, *Halorubrum* showed no significant change in abundance between parent brine (T0) and 1-week old halite (T1), nor after 21 weeks of entombment (T4). In Pond 1, *Haloquadratum* and *Candidatus* Nanosalina were significantly more relatively abundant in T1 halite than in the parent brine, however no significant differences were observed for any genus between T1 and T4 halite samples (Figure 3.13). In Pond 2, no significant differences were observed between the T0 brine and T1 halite, yet, *Candidatus* Nanosalina was significantly less relatively abundant in T4 halite than T1 halite, whereas *Natribaculum and Halorientalis* were significantly more abundant in T4 halite than T1 halite. Lastly, in Pond 3, *Halobellus, Candidatus* Nanosalina and *Halovenus* were significantly more abundant in T1

halite than in T0 brine, however, in comparisons between T1 halite and T4 halite, only *Candidatus* Nanosalina was significantly less abundant in T4 halite. As *Candidatus* Nanosalina decreased in relative abundance over a 20-week period of entombment in halite from derived from Ponds 2 and 3, it is worth noting that there was also a non-significant decrease also in Pond 1 from T1 to T4.

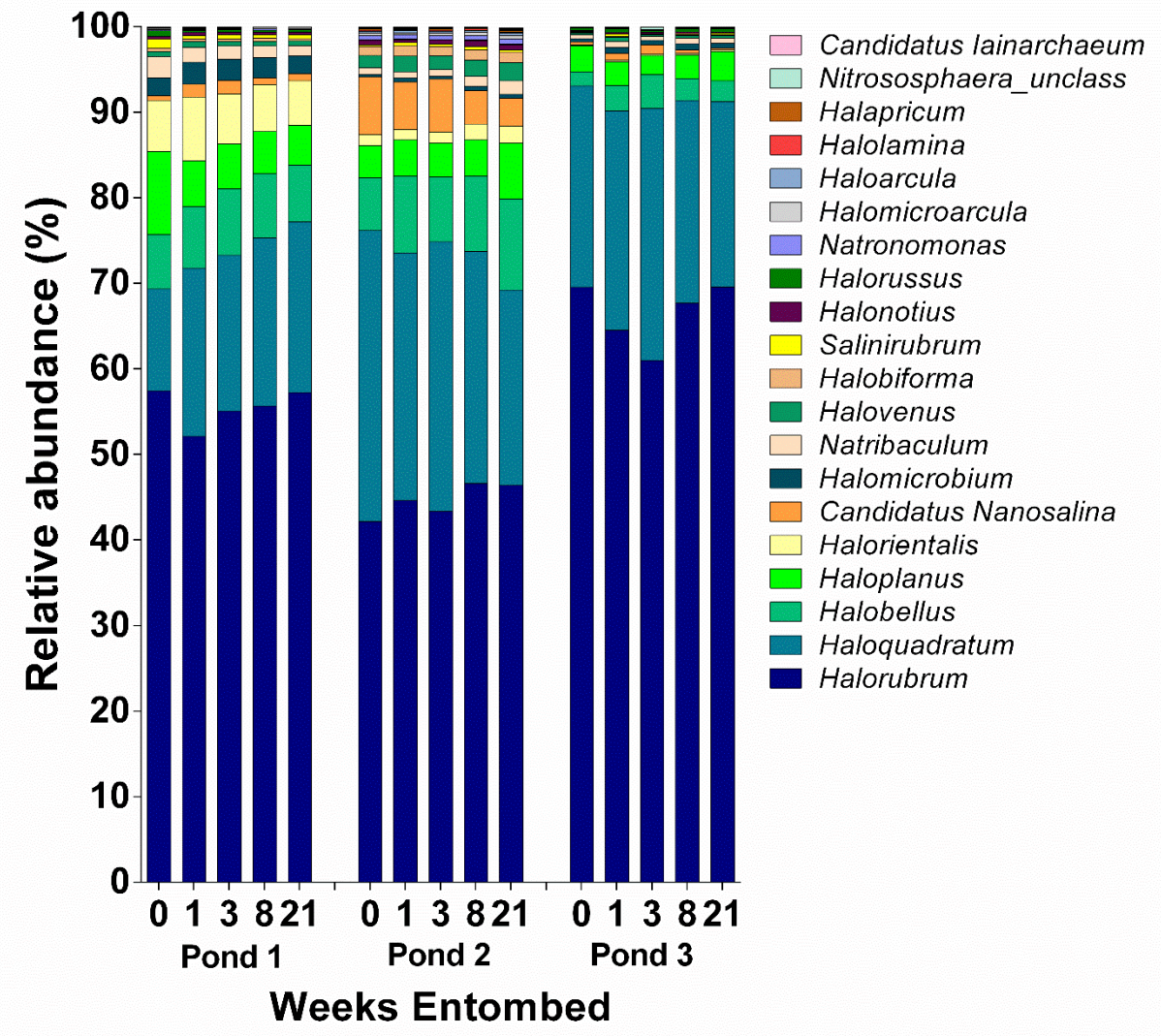

Figure. 3.12: The changes in the relative abundance of archaeal genera entombed in halite crystals over a 21-week period. Brine samples were collected from three saltern ponds. DNA was extracted from parent brines (T0) and from halite after 1 week (T1), 3 weeks (T2), 8 weeks (T3) and 21 weeks (T4). Figure legend represents the top 20 (of 48) most abundant archaeal genera across all time points and Ponds. Each bar displays the average relative abundances of archaeal genera derived from three experimental repeats. The relative abundance (%) values for each genus were calculated by summing the abundances of all OTUs with taxonomy assigned to that specific genus. Taxonomy was assigned to each OTU by the RDP classifier based on the top hit, and therefore it is worth noting that these assignments are indicative only and in some cases may not represent the true taxonomy of OTUs that were equidistant to multiple known strains.

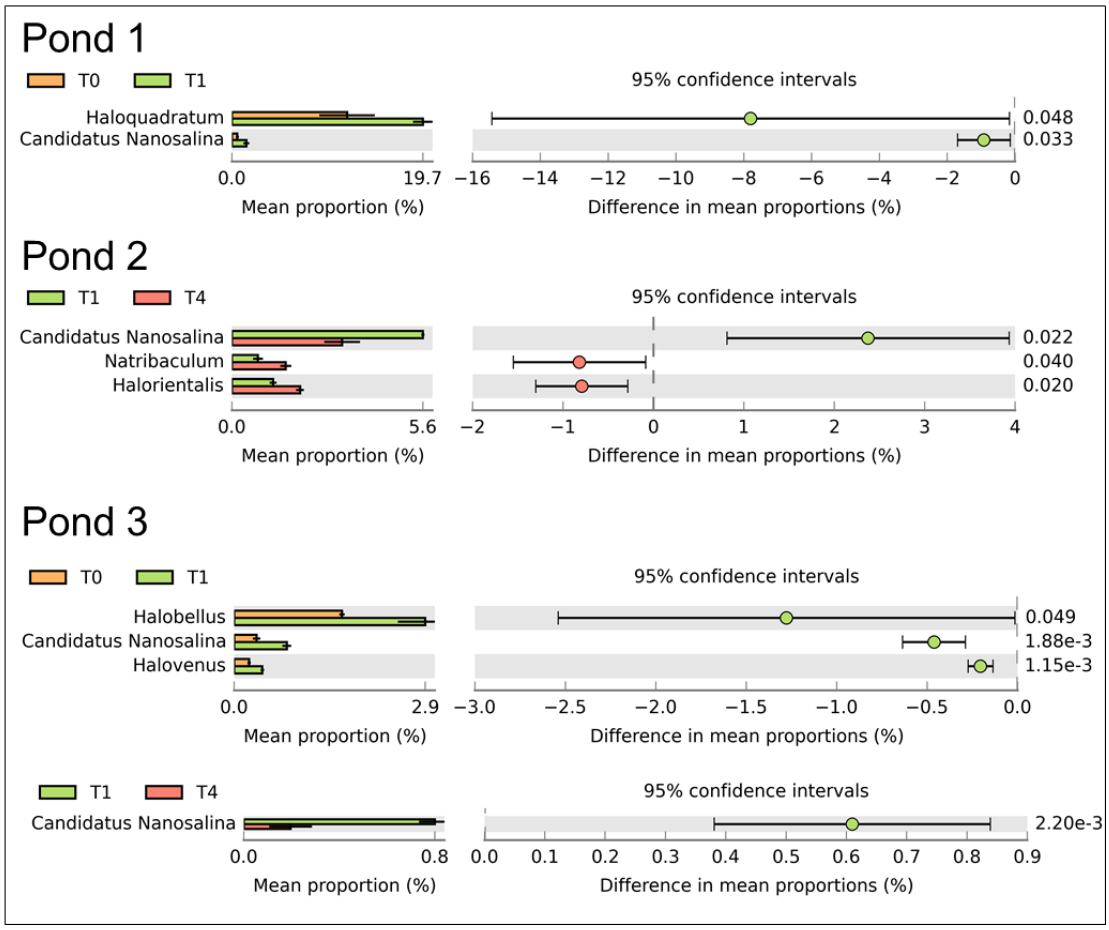

Figure 3.13: Pairwise comparisons of archaeal communities at the genus level during entombment in halite: comparisons were made between communities in parent brines (T0) and in 1-week old halite crystals (T1), and between communities in 1-week and 21-week old halite crystals (T4). No significant differences were observed between T1 and T4 communities of Pond 1 nor between T0 and T1 of Pond 2 communities. Analysis was performed using STAMP (Parks *et al*., 2014) as described in Figure 3.7.

3.4.7 Changes in the Relative Abundance of Individual Archaeal OTUs over Time inside Lab-made Halite Crystals

Pairwise comparisons of the relative abundance of archaeal OTUs showed some significant differences between time points (Figure 3.14). Most notably in Pond 2 where six OTUs were differentially abundant between T1 and T4 halite. Three OTUs related to *Candidatus* Nanosalina were poor survivors inside halite and were found to be significantly less abundant in T4 halite than at T1. In comparison, an additional three OTUs seemed to preferentially survive inside halite and were significantly more abundant at T4 than at T1. A BLAST search of these three OTUs showed that Trp-Arc-11 was equally related to multiple different strains among *Halosimplex* and *Halorientalis*, whereas both Trp-Arc-14 and Trp-Arc-45 shared high sequence similarity (99%) with *Halorubrum sodomense* strain JCM 8880.

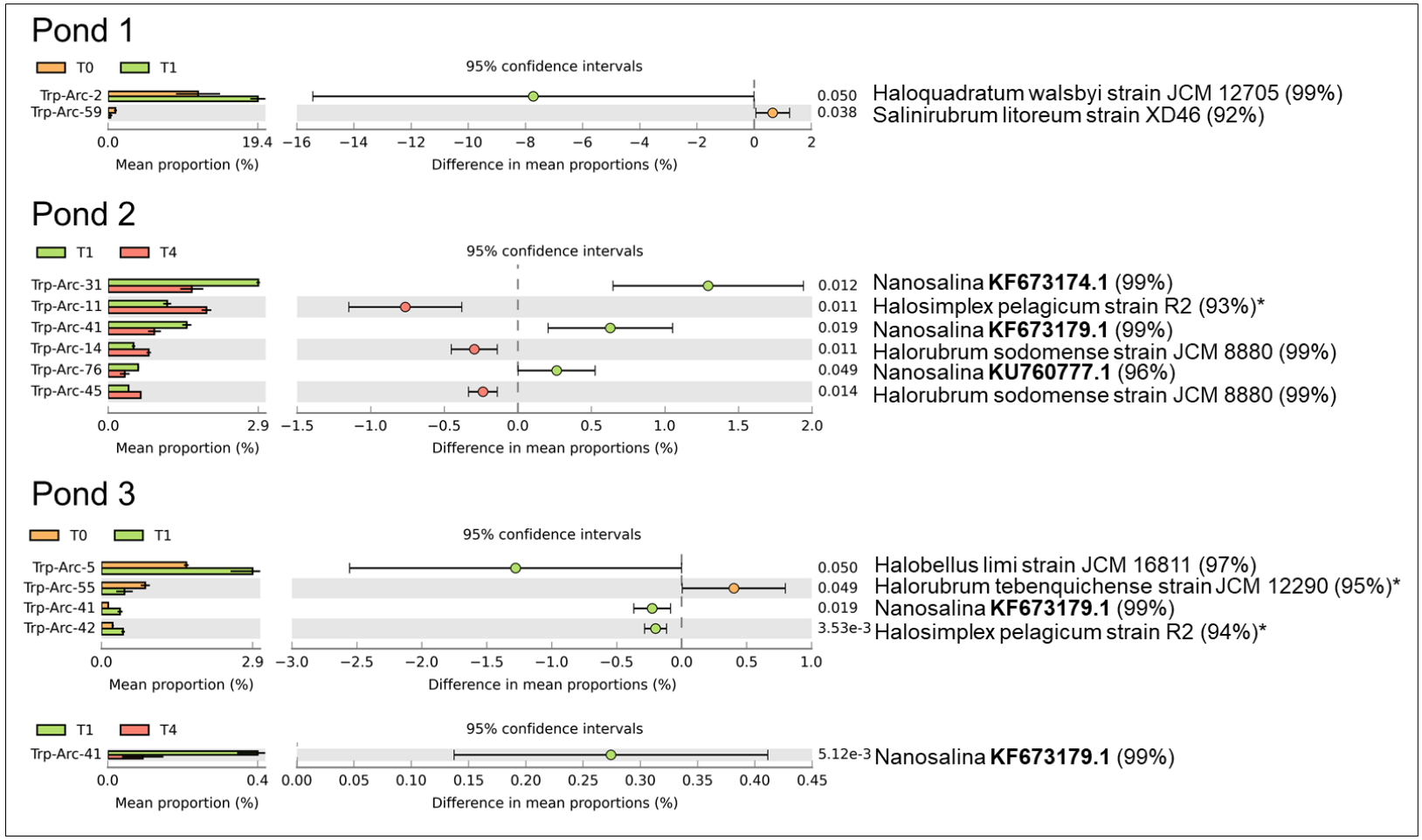

Figure 3.14: Pairwise comparisons of archaeal communities at the OTU level during entombment in halite: Comparisons were made between communities in parent brines (T0) and in 1-week old halite crystals (T1), and between communities in 1-week and 21-week old halite crystals (T4). No significant differences were observed between T1 and T4 communities of Pond 1 nor between T0 and T1 of Pond 2 communities. A BLAST (16S rRNA and nr/nt) search was used to identify strains with highest sequence similarity (right). Those labelled with an asterisk indicate that the query sequence was equidistant to two or more archaeal strains. OTUs labelled “Uncultured archaeon” failed to show sequence similarity with any cultivated strain and are presumed to be members of *Candidatus* Nanosalina - all are accompanied with an accession number (bold) for their most related sequence within the nr/nt database. Analysis was performed using STAMP (Parks *et al*., 2014) as described in Figure 3.7.

3.4.8 Collective Changes in Archaeal Communities over Time inside Lab-made Halite Crystals (All ponds)

Considering the average relative abundances across the three ponds, there were few changes in the overall archaeal community between time points post-entombment (Figure 3.15). In general, *Halorubrum* (approx. 53-57%) and *Haloquadratum* (approx. 21-24%) had the highest relative abundance across all time points, followed by *Halobellus* (4-7%), *Haloplanus* (4-5%), *Halorientalis* (2.5%), *Candidatus Nanosalina* (1.4-2.5%), *Natribaculum* (1-1.2%) and *Halomicrobium* (0.8-1.2%). The remaining community was formed of 41 minor genera (<1%) which similarly showed few differences in relative abundance between time points. Interestingly, no significant differences were observed in comparisons between archaeal communities, at neither the genus nor OTU level, in parent brines (T0) and 1-week old halite, nor between communities in 1-week old and 21-week old halite.

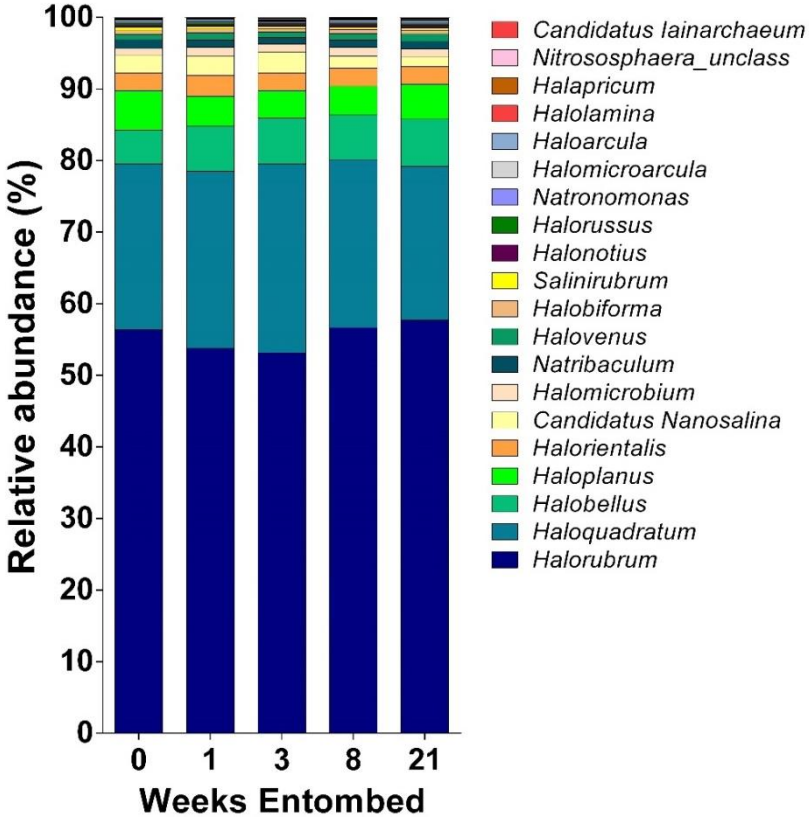

Figure 3.15: The changes in the relative abundance of the collective archaeal community (average across all ponds) entombed in halite crystals over a 21-week period. Brine samples were collected from three saltern ponds. DNA was extracted from parent brines (T0) and from halite after 1 week (T1), 3 weeks (T2), 8 weeks (T3) and 21 weeks (T4). Each bar displays the average relative abundances of archaeal genera across the three ponds. Figure legend represents the top 20 most abundant archaeal genera across all succession time points (all Ponds). Taxonomy was assigned to each OTU by the RDP classifier based on the top hit, and therefore it is worth noting that these assignments are indicative only and in some cases may not represent the true taxonomy of OTUs that were equidistant to multiple known strains.

3.5 Comparisons of Brine and Halite-entombed Bacterial Communities

3.5.1 Non-Metric Multidimensional Scaling (NMDS) of Bacterial Communities in Brine and Halite Crystals

NMDS analysis using Sorensen's index showed similar results to those seen with archaeal samples. Little separation was seen between bacterial communities from different time points (stress = 0.14). In both sample types (brine and halite) the communities from Pond 2 (squares in Figure 3.16) were distinct from communities in Ponds 1 and 3.

PERMANOVA analyses similarly showed a small but significant difference in bacterial community composition between brine and halite communities ($F_{1, 79} = 4.32$, $R^2 = 0.05$, $P < 0.01$). Likewise, this difference was also observed when *in-situ* samples were removed from the analysis ($F_{1, 73} = 3.23$, $R^2 = 0.04$, $P < 0.05$). Time had a significant effect on the composition of brine communities ($F_{5, 35} = 2.86$, $R^2 = 0.29$, $P = 0.01$), and, in contrast to the archaea, also had a significant effect on the composition in halite communities ($F_{4, 34} = 2.10$, $R^2 = 0.20$, $P = 0.05$). Lastly, brine communities did not significantly differ by source Pond ($F_{1, 39} = 1.50$, $R^2 = 0.04$, $P = 0.18$), whereas halite communities showed a small but significant difference in bacterial community composition between Ponds ($F_{1, 37} = 2.62$, $R^2 = 0.07$, $P < 0.05$).

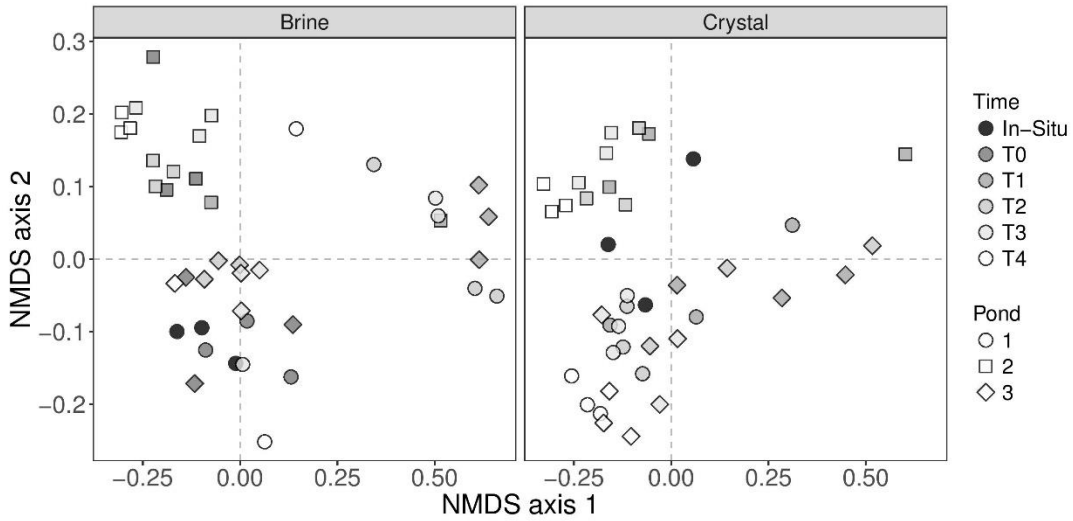

Figure. 3.16: NMDS analysis of bacterial brine and halite samples from *in-situ* and lab succession experiments using Sorensen's index. Brine (left) and halite (right) communities are shown separately for clarity but were analysed together. The brine and halite source of each sample is indicated by circles (Pond 1), squares (Pond 2), diamonds (Pond 3). The *in-situ* communities from Pond 1 are represented by black circles. Samples from different time points are represented by shading (dark grey to white). Time points at which DNA was extracted from brine and halite were: 0 weeks (T0), 1 week (T1), 3 weeks (T2), 8 weeks (T3) and 21 weeks (T4) (See Figure 2.1). Figure was produced by Dave R. Clark

3.5.2 Comparing the Effect of Time, Pond Origin and Sample-type on the OTU Richness of Bacterial Communities

Generalised linear mixed-model analyses showed that, when comparing bacterial communities from all sample-types and Ponds (but excluding *in-situ* communities), there were no significant differences in OTU richness between T0 communities and those at any other time point (|*z-value*| < 1.91, $P > 0.06$ for all time points) (Figure 3.17A).

When considering communities from brine and halite individually, T1 (coef = -0.35, $z = -2.93$, $P < 0.01$) and T2 (coef = -0.28, $z = -2.95$, $P < 0.01$) brine communities were significantly less OTU rich than T0 brine communities, however no significant differences were observed between T0 brine communities and those at T3 or T4 ($|z| < 1.35$, $P > 0.18$ for both time points) (Figure 3.17A). In halite (all Ponds), relative to T0 brine, communities did not significantly differ in OTU richness at any of the time points ($P > 0.47$ for all comparisons).

When considering differences in OTU richness between Ponds (both sample types), relative to communities from Pond 1, there were no significant differences in OTU richness in communities from Ponds 2 or 3 ($|z| < 1.2$, $P > 0.23$). Likewise, when sample types were separated, relative to Pond 1, there were no significant differences in OTU richness between Ponds for both brine ($|z| < 1.91$, $P > 0.06$ for all Ponds) and halite communities ($|z| < 0.91$, $P > 0.36$ for all Ponds) (Figure 3.17B). Lastly, when comparing between sample types (from all Ponds), halite communities were significantly more OTU rich than those from brines (coef = 0.15, z-value = 2.99, $P < 0.01$) (Figure 3.17C).

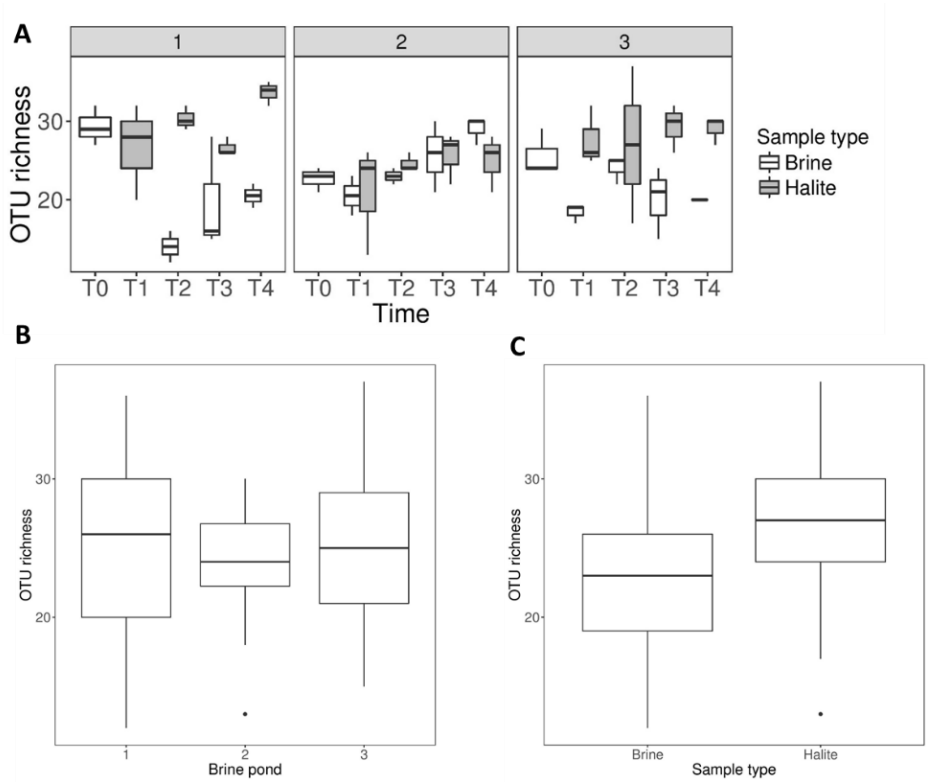

Figure 3.17: Comparisons of OTU richness in bacterial communities. Panel A displays the changes in OTU richness over time for bacterial communities derived from three Ponds (indicated in the grey boxes). Wider boxes represent time points at which only one sample-type (white for brine, grey for halite) was available for analyses because <2 replicates were available for the comparator sample. **Panel B** shows the differences in bacterial OTU richness (both sample-types) between Ponds, and **Panel C** compares between sample types (all Ponds).

3.5.3 Comparing the Effect of Time, Pond Origin and Sample-type on the OTU Evenness of Bacterial Communities

Generalised linear mixed-models analyses were also used to perform matching comparisons of OTU evenness between bacterial communities (Figure 3.18). When considering bacterial communities from all sample-types and Ponds (but excluding *in-situ* communities), there were no significant differences in OTU evenness between T0 communities and those at any other time point ($|t| < 1.37$, $P > 0.17$ for all time points) (Figure 3.18A).

When considering communities from brine and halite individually, a similar pattern was observed in brine communities (all Ponds), with no significant differences in OTU evenness between T0 brine communities and those from brine at any other time points ($|t| < 1.76$, $P > 0.07$). In halite, T4 communities were significantly less even than those from T0 brine (coef = -0.23, $t = -2.23$, $P < 0.05$), however there were no significant differences between T0 brine communities and those in halite from any of the other time points ($P > 0.08$).

When considering differences in OTU evenness between Ponds (both sample types), relative to communities from Pond 1, there were no significant differences in OTU evenness in communities from Ponds 2 or 3 ($|t| < 1.03$, $P > 0.30$). When sample types were compared individually, there were similarly no significant differences in OTU evenness observed between brine communities from different Ponds ($|t| < 0.40$, $P > 0.69$ for all Ponds).Whereas in halite, communities from Pond 2 were significantly less even (coef = -0.40, $t = -4.51$, $P < 0.0001$) than those from Pond 1, and no significant differences were observed when comparing halite communities from Ponds 1 and 3 ($t = -1.16$, $P = 0.26$) (Figure 3.18B). Lastly, when comparing OTU evenness between sample types (from all Ponds), there was no significant differences between brine and halite communities ($t = 0.14$, $P = 0.89$).

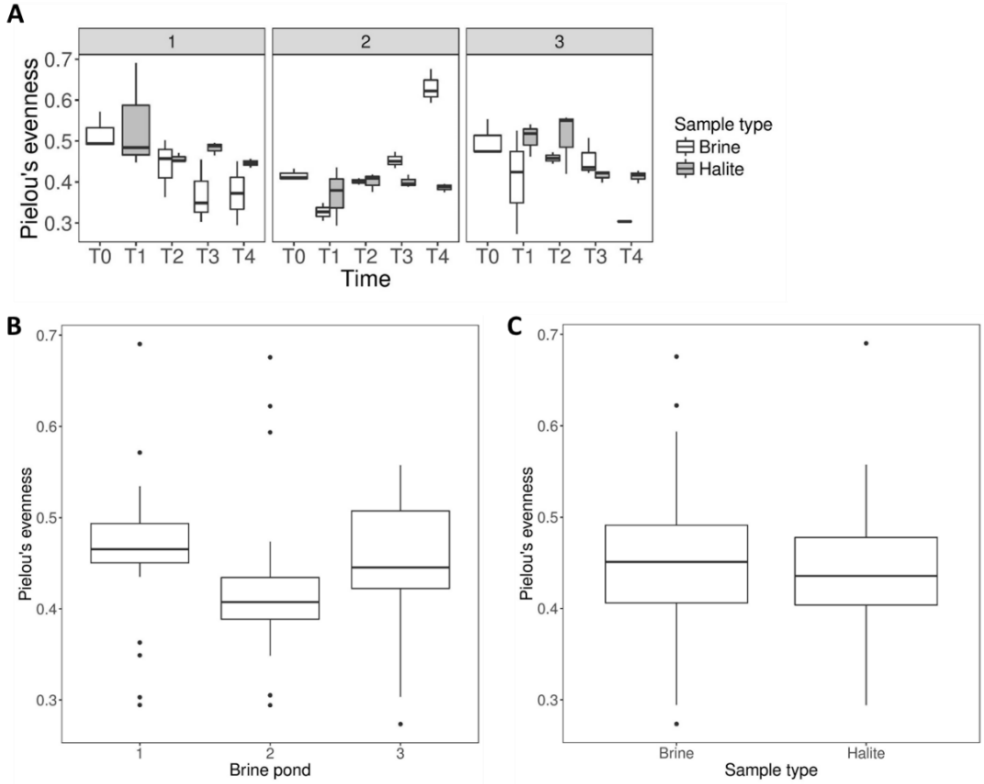

Figure 3.18: Comparisons of OTU evenness in bacterial communities. Panel A displays the changes in OTU evenness over time for bacterial communities derived from three Ponds (indicated in the grey boxes). Wider boxes represent time points at which only one sample-type (white for brine, grey for halite) was available for analyses because <2 replicates were available for the comparator sample. **Panel B** shows the differences in bacterial OTU evenness (both sample-types) between Ponds, and **Panel C** compares sample types (all Ponds).

3.5.4 Comparing the Bacterial Community Composition of *In-situ* Brine and Crystal Samples from Pond 1

The bacterial community composition in the *in-situ* brine and halite samples were similar (Figure 3.19) as was found in archaeal communities. In both conditions, *Salinibacter* and *Salisaeta/Longibacter* dominated the bacterial communities, together forming 88.4% of the brine community and 91.5% of crystal communities. Interestingly, a BLAST search (16S rRNA and nr/nt databases) of abundant phylotypes showed that the dominant *Salisaeta/Longibacter* phylotype, Trp-Bac-1, was equidistant with both *Longibacter salinarum* strain WDS2C18 and *Salisaeta longa* strain S4-4 (95%). Pairwise comparisons of bacterial genera showed that *Salisaeta/Longibacter* was significantly more abundant in brine than halite. Surprisingly, comparisons performed at the genus level did not report a significant difference between the abundance of *Salinibacter* in either condition (Figure 3.20). However, Trp-Bac-3 (99% similarity with *Salinibacter ruber M1*), which formed one of the two dominant *Salinibacter* phylotypes alongside Trp-Bac-2, was significantly more abundant in halite than in brine (Figure 3.21).

Other bacterial genera of considerable relative abundance (≥1% in brines), *Pelomonas* (3.5 to 3.2%)*, Rhodovibrio* (2.1 to 1.7%), did not differ significantly in relative abundance between brine and halite (Figure 3.19, EAIII.2). However, a single OTU (Trp-Bac-14, with <90% similarity with any other bacterial strain), and two low-abundance groups of cyanobacteria (GpVII and GpXIII) (<1%) were significantly more abundant in brine (Figure 3.20).

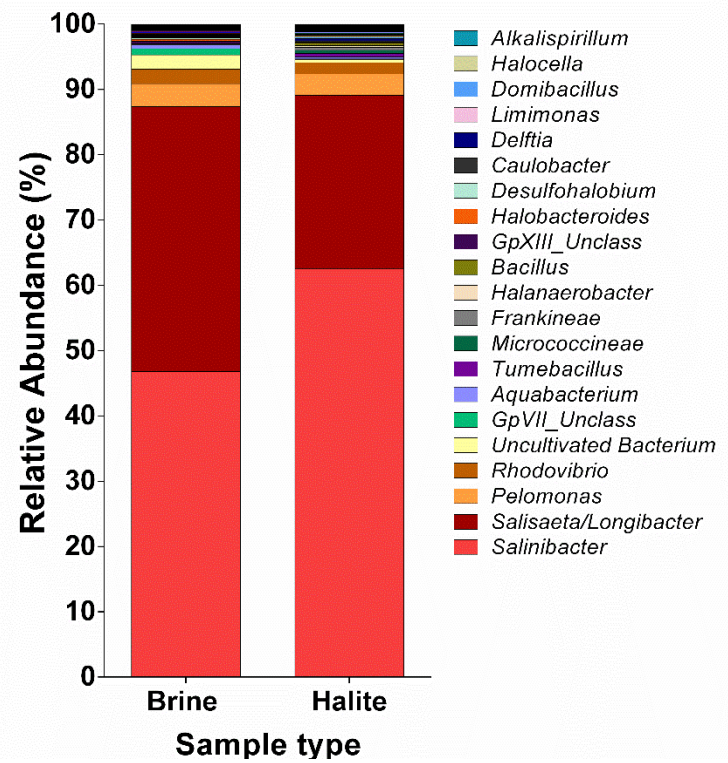

Figure 3.19: The mean relative abundances of bacterial genera identified from *in-situ* brine and halite samples from Pond 1. Brine (*n* = 3) and halite (*n* = 3) samples were collected from Pond 1. The figure legend displays the top 20 (of 115) most abundant genera in ascending order. The relative abundance (%) values for each genus were calculated by summing the abundances of all OTUs with taxonomy assigned to that specific genus. GpVII_Unclass and GpXIII_Unclass refer to unclassified genus-level groups belonging to the Cyanobacteria. Taxonomy was assigned to each OTU by the RDP classifier based on the top hit, and therefore it is worth noting that these assignments are indicative only and in some cases may not represent the true taxonomy of OTUs that were equidistant to multiple known strains.

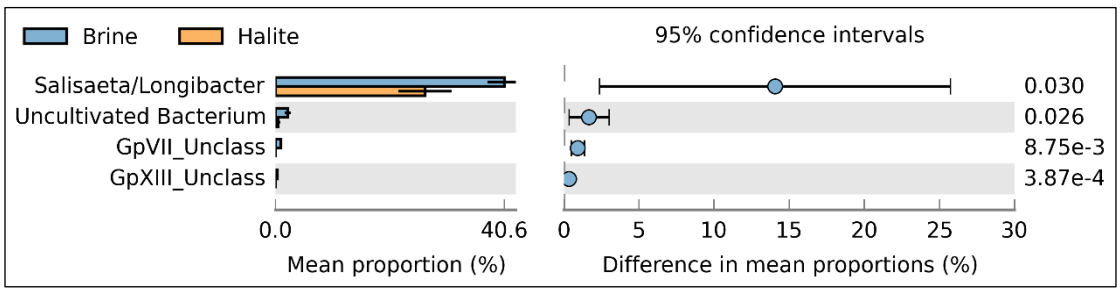

Figure 3.20: Differences in the relative abundance of bacterial genera between *in-situ* brine and halite samples from Pond 1. Brine (*n* = 3) and halite (*n* = 3) samples were collected from Pond 1. GpVII_Unclass and GpXIII_Unclass refer to unclassified genus-level groups belonging to the Cyanobacteria. Analysis was performed using STAMP (Parks *et al*., 2014) as described in Figure 3.7.

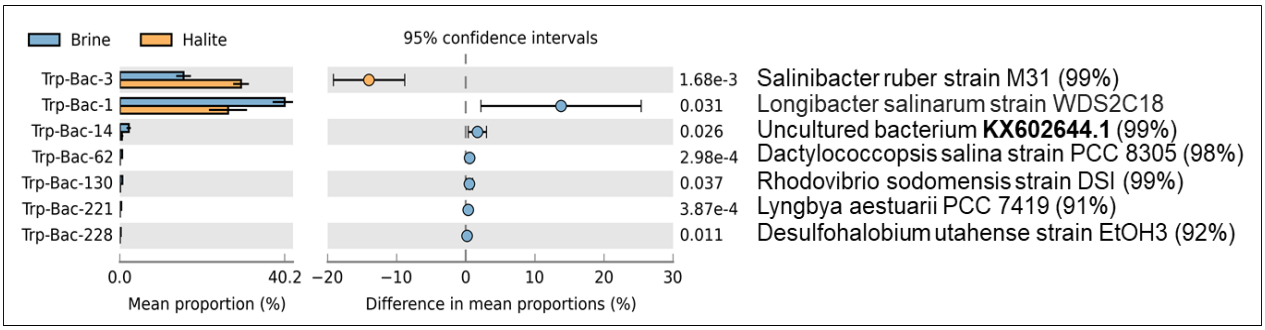

Figure 3.21: Differences in the relative abundance of bacterial OTUs between *in-situ* brine and halite samples from Pond 1. Brine (*n* = 3) and halite (*n* = 3) samples were collected from pond 1. Analysis was performed using STAMP (Parks *et al*., 2014) as described in Figure 3.7. A BLAST (16S rRNA and nr/nt) search was used to identify strains with high sequence similarity (right). Trp-Bac-14 showed low sequence similarity (≤85%) with all characterised strains and therefore is annotated with the accession number (bold) of its closest uncultivated match.

3.5.5 Comparing the Bacterial Communities found In Parent Brines (T0) from Ponds 1, 2 and 3

Similarly to the *in-situ* communities from Pond 1, all three brines from Ponds 1, 2 and 3 were dominated by the two genera *Salinibacter* and *Salisaeta/Longibacter* (Figure 3.22, EAIII.4). Pairwise comparisons of the abundance of bacterial genera between T0 brines showed that both *Salisaeta/Longibacter* and an uncultivated group were significantly more abundant in Pond 2 than in Ponds 1 and 3, whereas only GpVII Cyanobacteria were significantly more abundant in Ponds 1 and 3 than in Pond 2 (Figure 3.23). *Pelomonas, Aquabacterium, Rhodovibrio* and *Caulobacter* all formed relatively large proportions of the community in brines from Ponds 1 and 3 but did not show a significant difference when compared with the abundances of those in Pond 2. Overall, the bacterial community in Pond 2 was considerably less diverse at the genus level than Ponds 1 and 2; *Salisaeta/Longibacter* and *Salinibacter* combined constituted 96% of the total community. Only 47 of 97 identified genera were identified in T0 samples from Pond 2, whereas 63 genera were identified in Pond 1 and 62 in Pond 3 (EAIII.4). Moreover, figures 3.17 and 3.18 show that samples from Pond 3 were lower in both OTU richness and OTU evenness.

Compared with the archaea, there were fewer differences in the relative abundance of bacterial OTUs between T0 brine communities (Figure 3.24). While most aligned with those observed at the genus level in Figure 3.23, some small (OTUs each form <1% of total community) but significant intra-genus differences were observed. For example, Trp-Bac-387 (94% similarity with both *Longibacter salinarum* WDS2C18 and *Salisaeta longa* S4-4) was significantly more abundant in Pond 1 than in Ponds 2 and 3, moreover comparisons between Ponds 2 and 3 showed that Trp-Bac-35 (94% similarity with *Salinibacter luteus* DGO) was significantly more abundant in Pond 2, whereas Trp-Bac-69 (96% similarity with *Salinibacter ruber* M31) was

significantly more abundant in Pond 3. Finally, a BLAST search of Trp-Bac-14 showed low sequence similarity (≤85%) with any known bacterial strain (Figure A.3)

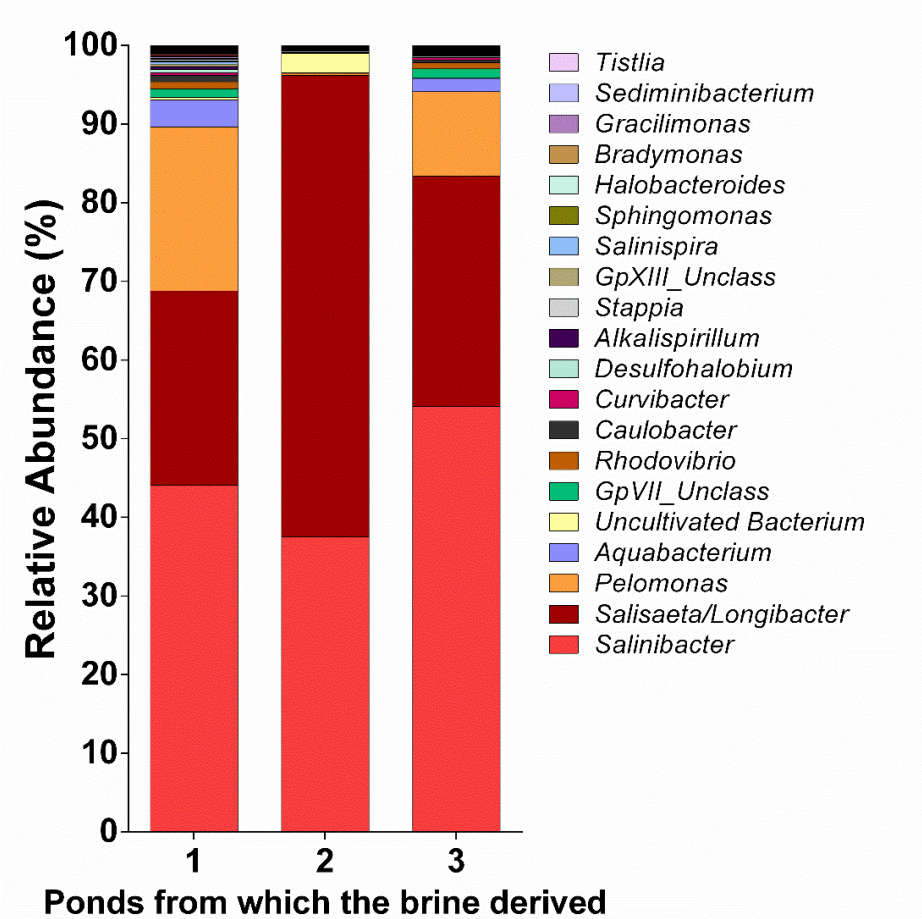

Figure 3.22: Relative abundance of bacterial genera in T0 brine (parent) samples derived from three ponds. Each bar displays the average relative abundances of bacterial genera across the three ponds. Figure legend represents the top 20 most abundant bacterial genera in brine across all ponds. The relative abundance (%) values for each genus were calculated by summing the abundances of all OTUs with taxonomy assigned to that specific genus. GpVII_Unclass and GpXIII_Unclass refer to unclassified genus-level groups belonging to the Cyanobacteria. Taxonomy was assigned to each OTU by the RDP classifier based on the top hit, and therefore it is worth noting that these assignments are indicative only and in some cases may not represent the true taxonomy of OTUs that were equidistant to multiple known strains.

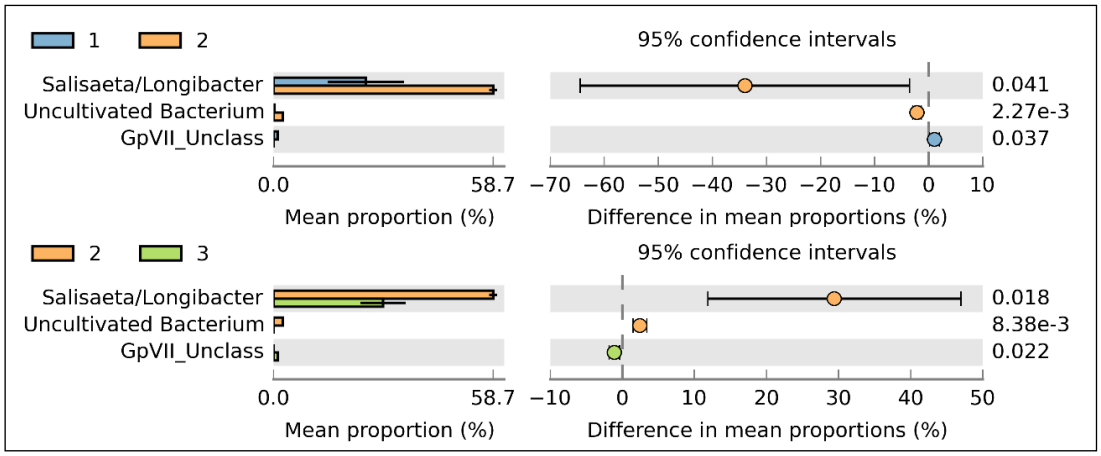

Figure 3.23: Differences in the relative abundance of bacterial genera between parent brine samples. Pairwise comparisons of the relative abundance of bacterial genera were performed between the parent brine (*n* = 3) community of ponds 1, 2 and 3. No significant differences in bacterial relative abundances were observed in comparisons between Pond 1 and 3. GpVII_Unclass refers to an unclassified genus-level group belonging to the Cyanobacteria. Analysis was performed using STAMP (Parks *et al*., 2014) as described in Figure 3.7.

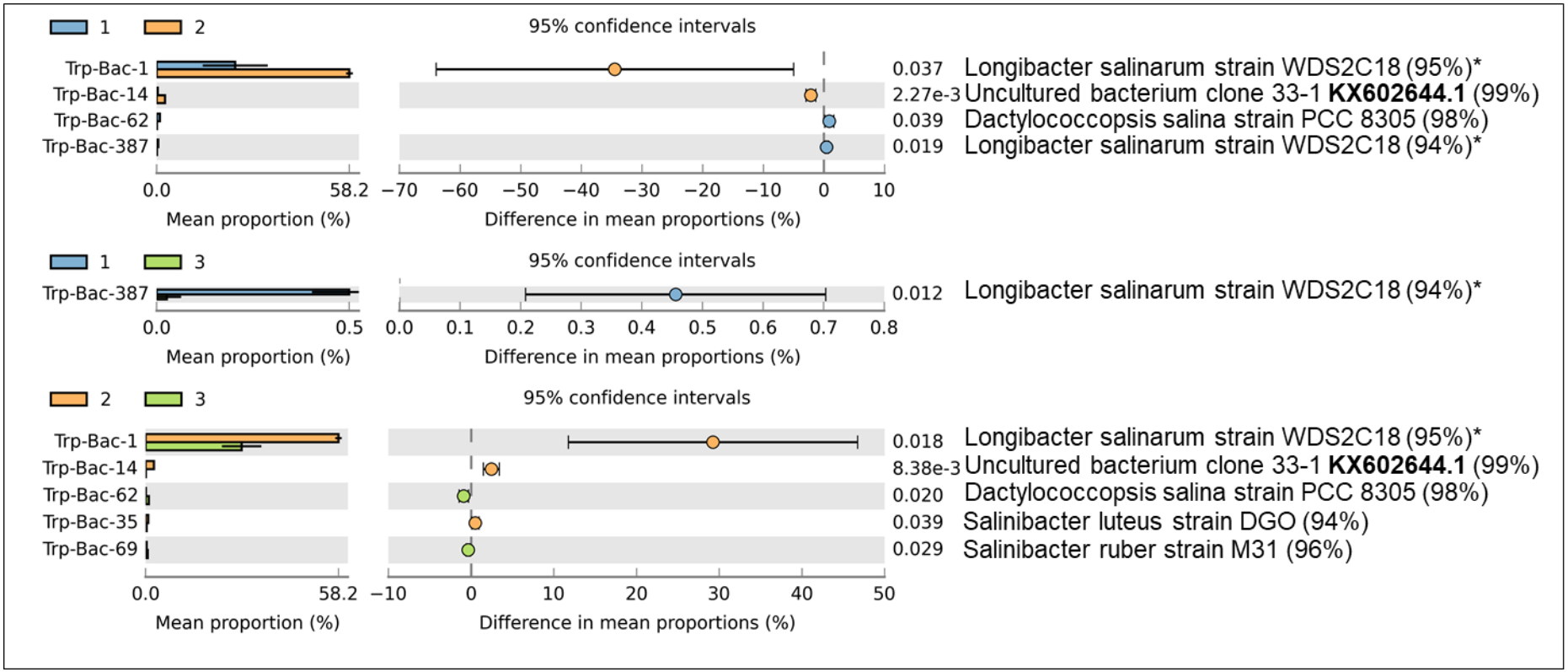

Figure 3.24: Differences in the relative abundance of bacterial OTUs between parent brine samples: Pairwise comparisons of the relative abundance of bacterial genera were performed between the parent brine (*n* = 3) community of ponds 1, 2 and 3. Analysis was performed using STAMP (Parks *et al*., 2014) as described in Figure 3.7. A BLAST (16S rRNA and nr/nt) search was used to identify strains with highest sequence similarity (right). Those labelled with an asterisk indicate that the query sequence was equidistant to two or more bacterial strains; those with high sequence similarity to *Longibacter salinarum* strain WDS2C18 also showed equal sequence similarity with *Salinibacter longa* strain S4-4, and vice-versa. Trp-Bac-14, showed low sequence similarity (≤85%) with all characterised strains and therefore is annotated with the accession number (bold) of its closest uncultivated match

3.5.6 Changes in the Relative Abundance of Bacterial Genera over Time Inside Lab-made Halite Crystals

In comparison to the archaea, there were greater differences in the relative abundance of major bacterial community constituents (>1% of total community) across time points (Figure 3.25, EAIII.2). With the exception of the T1 (1-week) and T2 (3-week) halite community of Pond 3, bacterial communities in brine and halite from all ponds were dominated by *Salinibacter* and *Longibacter/Salisaeta*. Moreover, *Pelomonas* and *Aquabacterium* formed considerable proportions of parent brine and early halite-entombed communities (up to T2). However, at time points later than T2 they were among the minor community constituents (<1% of total community). At successive time points following on from T2, *Salinibacter* and *Salisaeta/Longibacter* together formed >90% of halite communities from all ponds.

Pairwise comparisons at the genus level were performed between parent brines and 1-week old halite (T0 vs T1), and between 1-week and 21-week old halite (T1 vs T4) (Figure 3.26). Interestingly, there were no significant differences at the genus level between the parent brine and 1-week old halite community (T0 vs T1) derived from any of the three ponds. Similarly, there were no significant differences between communities in 1-week old and 21-week old halite from ponds 2 and 3. In Pond 1, only *Halobacteroides* showed a small but significant increase in abundance between T1 and T4. No other genera were differentially abundant between the two time-points (Figure 3.26).

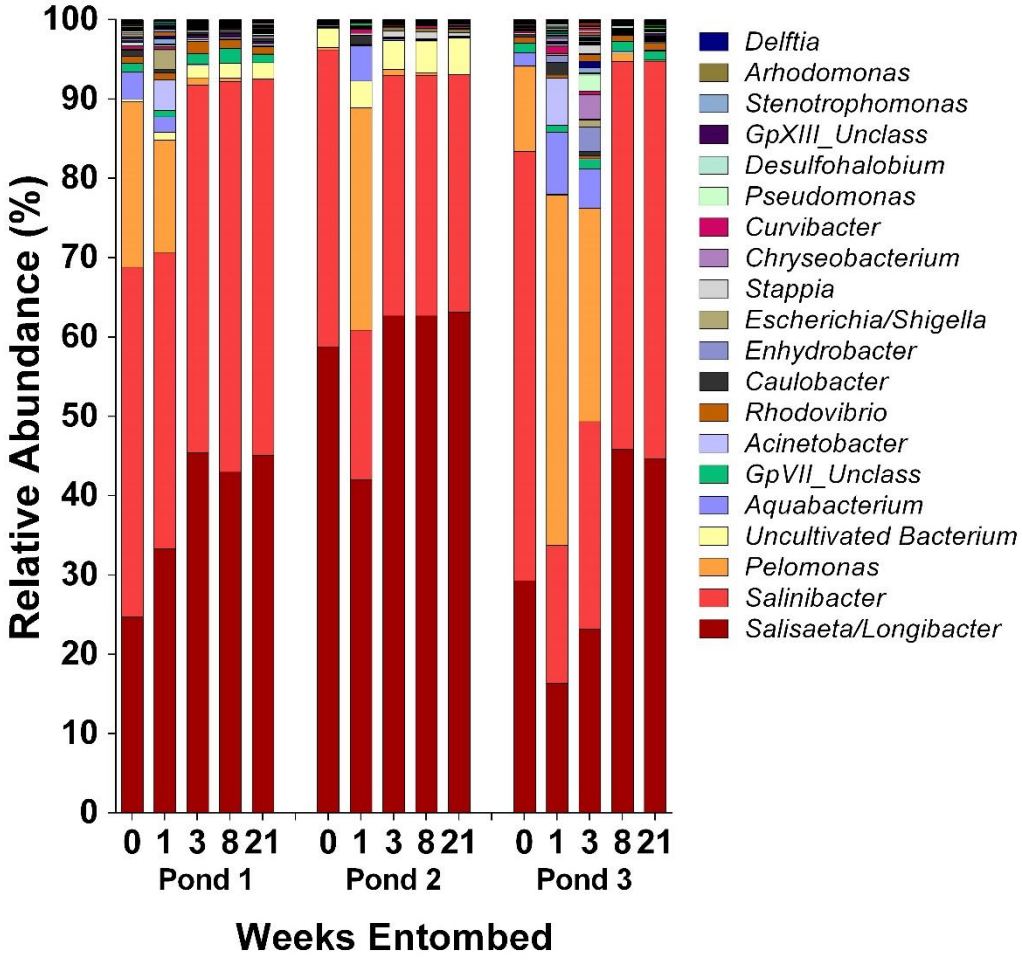

Figure. 3.25: The changes in the relative abundance of bacterial genera entombed in halite crystals over a 21-week period. Brine samples were collected from three saltern ponds. DNA was extracted from parent brines (T0) and from halite after 1 week (T1), 3 weeks (T2), 8 weeks (T3) and 21 weeks (T4). Figure legend represents the top 20 (of 176) most abundant bacterial genera across all time points and Ponds. Each bar displays the average relative abundances of bacterial genera derived from three experimental repeats. The relative abundance (%) values for each genus were calculated by summing the abundances of all OTUs with taxonomy assigned to that specific genus. GpVII_Unclass and GpXIII_Unclass refer to unclassified genus-level groups belonging to the Cyanobacteria. Taxonomy was assigned to each OTU by the RDP classifier based on the top hit, and therefore it is worth noting that these assignments are indicative only and in some cases may not represent the true taxonomy of OTUs that were equidistant to multiple known strains.

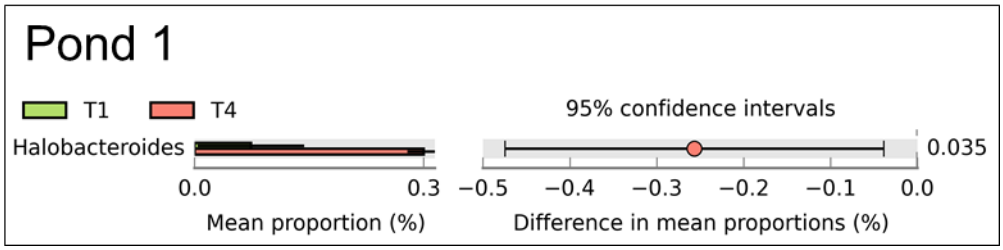

Figure 3.26: Pairwise comparisons of bacterial communities at the genus level during entombment in halite: comparisons were made between communities in parent brines (T0) and in 1-week old halite crystals (T1), and between communities in 1-week and 21-week old halite crystals (T4). No significant differences were observed between the T0 and T1 communities of Pond 1 nor in comparisons between communities from ponds 2 and 3. Analysis was performed using STAMP (Parks *et al*., 2014) as described in Figure 3.7.

3.5.7 Changes in the Relative Abundance of Individual Bacterial OTUs over Time inside Lab-made Halite Crystals

Pairwise comparisons of the relative abundance of bacterial OTUs showed some significant differences between time points (Figure 3.27). In Pond 1, Trp-Bac-387 (94% similarity with *Longibacter salinarum* and multiple other bacterial strains) showed a small but significant decrease in abundance when comparing between the parent brine (T0) and 1-week old halite community (T1). However, no significant differences were observed between the bacterial community in 1-week old and 21-week old (T4) halite. Interestingly, no significant differences were observed in comparisons made between T0 and T1 communities nor between T1 and T4 communities derived from Pond 2. In Pond 3, four OTUs with high sequence identity to members of the genus *Salinibacter* were significantly more abundant in the parent brine than in T1 halite. Out of the four differentially abundant OTUs, Trp-Bac-3 (99% similarity with *Salinibacter ruber* M31) showed the greatest decrease in abundance between the two time-points (T0 vs T1). Finally, in comparisons between T1 and T4 halite communities, five OTUs showed a small but significant increase in abundance between the two time-points. Surprisingly this included Trp-Bac-16 (96% similarity with *Salinibacter ruber* M31) which was observed to be significantly more abundant in the parent brine than in T1 halite. Also more abundant were Trp-Bac-69 (also 96% similarity with *Salinibacter ruber* 31), Trp-Bac-65 (96% similarity with *Rhodovibrio sodomensis*), Trp-Bac-176 (97% similarity with the cyanobacteria *Dactylococcopsis salina* strain PCC 8305) and finally Trp-Bac-118 (92% similarity with *Longibacter salinarum*).

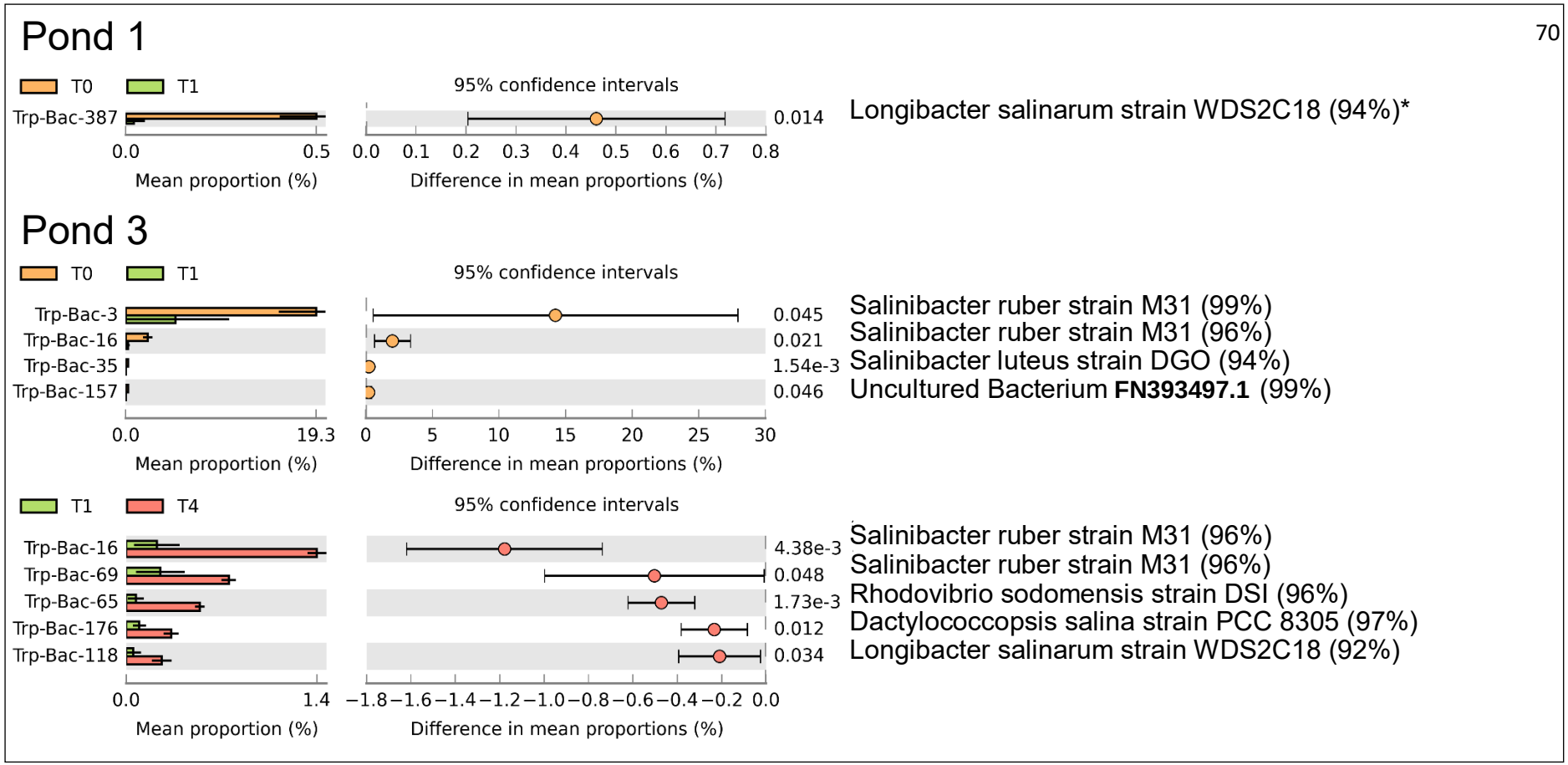

Figure 3.27: Pairwise comparisons of bacterial communities at the OTU level during entombment in halite: Comparisons were made between communities in parent brines (T0) and in 1-week old halite crystals (T1), and between communities in 1-week and 21-week old halite crystals (T4). No significant differences were observed between T1 and T4 communities of Pond 1 nor between comparisons made between communities derived from Pond 2. A BLAST (16S rRNA and nr/nt) search was used to identify strains with highest sequence similarity (right). Those labelled with an asterisk indicate that the query sequence was equidistant to two or more bacterial strains; those with high sequence similarity to *Longibacter salinarum* strain WDS2C18 showed equal sequence similarity with *Salinibacter longa* strain S4-4, and vice-versa. Analysis was performed using STAMP (Parks *et al*., 2014) as described in Figure 3.7. Trp-Bac-157 showed low sequence identity (88%) with its top hit and therefore is annotated with the accession number (bold) of its closest uncultivated match.

3.5.8 Collective Changes in Bacterial Communities over Time inside Lab-made Halite Crystals (All ponds)

In comparison to the archaea (Figure 3.15) there were greater changes in the overall bacterial community composition (average relative abundances across the three ponds) between time points (Figure 3.28, EAIII.5). In general, *Salisaeta/Longibacter* (approx. 30.5-50.9%) and *Salinibacter* (approx. 24.5-45.2%) had the highest relative abundance across all time points, followed by varying populations of *Pelomonas* (<0.1-28.8%)*, Uncultivated Bacterium* (0.9-2.2%) and *Aquabacterium* (0.1-4.7%).The remaining community was formed of 172 minor genera (<1% of total community). Pairwise comparisons between bacterial communities at the genus level showed that *Salinibacter* was significantly more abundant in the parent brine (T0) than in T1 halite (Figure 3.29). Interestingly, *Pelomonas, Aquabacterium, Caulobacter* and *Curvibacter* were all significantly more abundant in T1 than T4 halite, yet *Salinibacter* and *Salisaeta/Longibacter* were significantly more abundant in T4 than in T1 halite.

Pairwise comparisons performed at the OTU level further support the differential abundances observed at the genus level (Figure 3.30). Four OTUs with high sequence identity with members of the *Salinibacter* were significantly more abundant in the parent brine (T0) than T1 halite community. Likewise, Trp-Bac-5 (99% similarity with *Pelomonas sacharophila* NBRC 103037), Trp-Bac-20 (98% similarity with *Aquabacterium parvum* B69), Trp-Bac-82 (99% similarity with *Caulobacter flavus* RHGG3), Trp-Bac-92 (97% similarity with *Roseateles aquatilis* CCUG) and Trp-Bac-113 (97% similarity with *Curvibacter fontanus* AQ9) were all significantly more abundant in T1 halite rather than T4 halite. In contrast, Trp-Bac-1 (95% similarity with *Longibacter salinarum* and *Salisaeta longa* S4-4), Trp-Bac-2 (95% similarity with *Salinibacter ruber* M31), Trp-Bac-16 (96% similarity with *Salinibacter ruber* M31) and Trp-Bac-35 (94% similarity with *Salinibacter luteus* DGO) were all significantly more abundant in T4 halite than T1 halite.

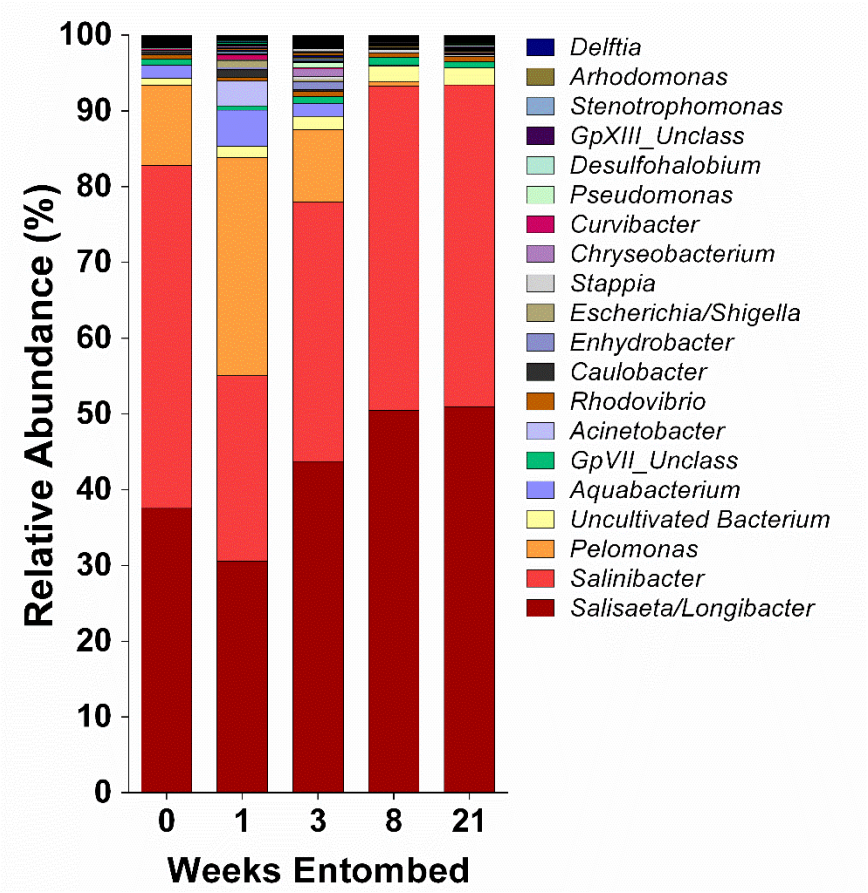

Figure 3.28: The changes in the relative abundance of the collective bacterial community (average across all ponds) entombed in halite crystals over a 21-week period. Brine samples were collected from three saltern ponds. DNA was extracted from parent brines (T0) and from halite after 1 week (T1), 3 weeks (T2), 8 weeks (T3) and 21 weeks (T4). Each bar represents the average relative abundance of each genera across the three ponds (n=3). Figure legend represents the top 20 most abundant bacterial genera across all succession time points (all Ponds). GpVII_Unclass and GpXIII_Unclass refer to unclassified genus-level groups belonging to the Cyanobacteria Taxonomy was assigned to each OTU by the RDP classifier based on the top hit, and therefore it is worth noting that these assignments are indicative only and in some cases may not represent the true taxonomy of OTUs that were equidistant to multiple known strains.

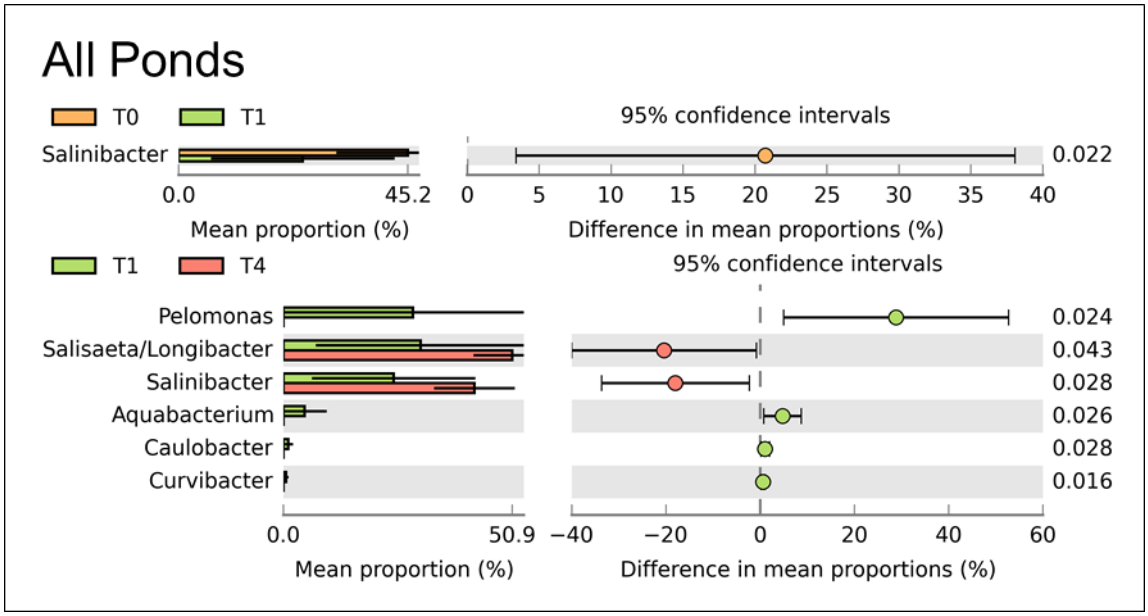

Figure 3.29: Pairwise comparisons of the collective bacterial community (All ponds) at the genus level during entombment in halite: Comparisons were made between the parent brine community (T0) and the community in 1-week old halite crystals (T1), and between the community in 1-week and 21-week old halite crystals (T4). Analysis was performed using STAMP (Parks *et al*., 2014) as described in Figure 3.7.

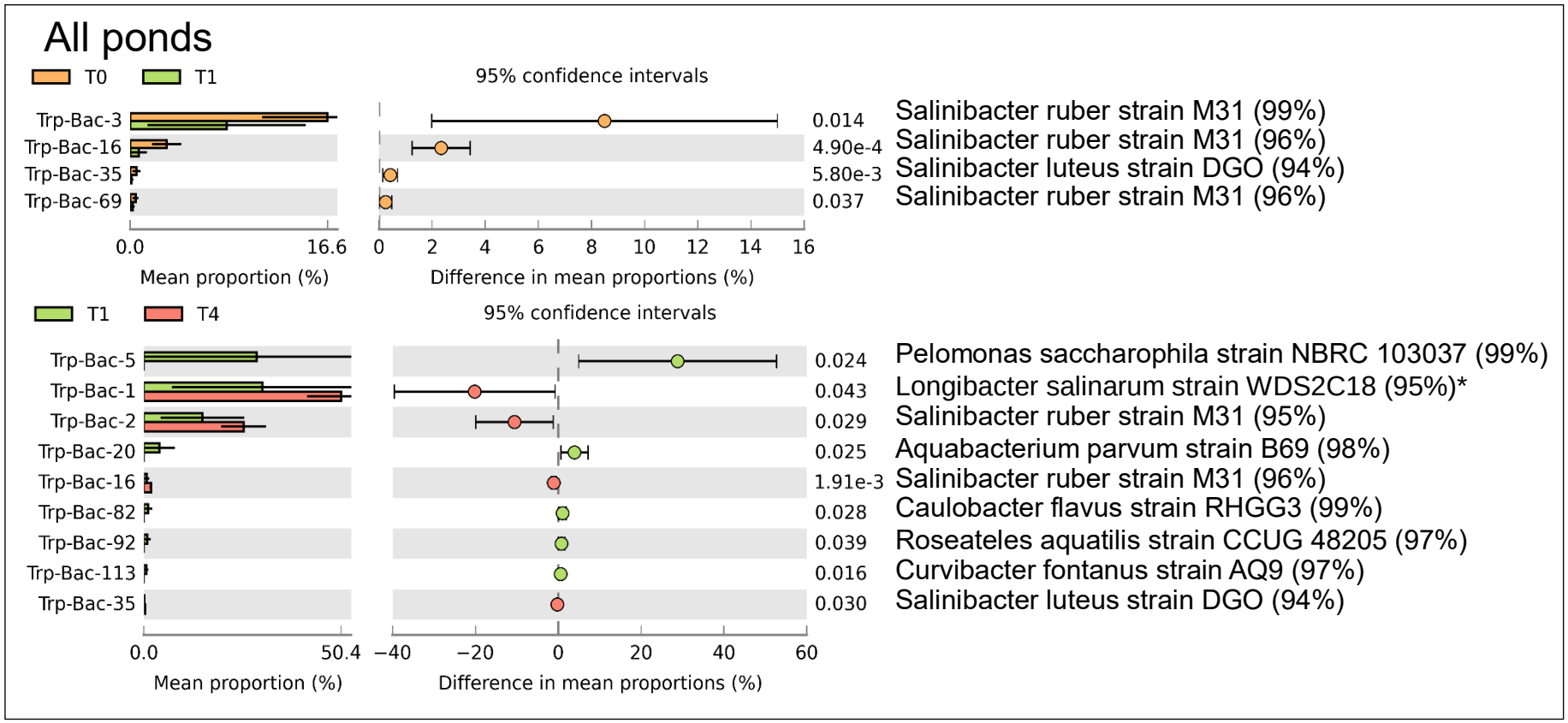

Figure 3.30: Pairwise comparisons of the collective bacterial community (All ponds) at the OTU level during halite entombment: comparisons were made between the parent brine community (T0) and the community in 1-week old halite crystals (T1), and between the community in 1-week and 21-week old halite crystals (T4). A BLAST (16S rRNA and nr/nt) search was used to identify strains with highest sequence similarity (right). Those labelled with an asterisk indicate that the query sequence was equidistant to two or more bacterial strains; those with high sequence similarity to *Longibacter salinarum* strain WDS2C18 showed equal sequence similarity with *Salinibacter longa* strain S4-4, and vice-versa. Analysis was performed using STAMP (Parks *et al*., 2014) as described in Figure 3.7.

4 Discussion

While many studies have explored the microbial diversity of hypersaline brines and halite individually (described in Section 1), less is known on how the entrapment of brine communities in halite affects community composition, nor whether individual groups show preferential growth and survival inside halite. In this study, amplicon sequencing of the 16S rRNA gene was used to perform community analyses on archaea and bacteria in brine and halite derived from hypersaline saltern waters of Trapani Salterns.

High-throughput amplicon sequencing has emerged as a valuable technique for studies on microbial diversity as it provides a relatively quick and cost-effective method for estimating the abundance and composition of OTUs within a given community (Lee *et al.*, 2012). In this study, this approach has allowed the simultaneous reading of both archaeal and bacterial 16S rRNA gene amplicons, derived from a large number of samples (sample types, brine origins and time points), within a single sequencing run. However, amplicon sequencing approaches are known to suffer from the same biases that are implicit in all PCR based studies (Poretsky *et al.*, 2014). Small biases in PCR amplification efficiency (e.g. caused by primer choice or reaction settings) and the variable number of 16S rRNA gene copies found within prokaryotic genomes can result in larger biases in read counts and in turn lead to a skewed representation of microbial community composition (Lee *et al.*, 2012).

Metagenomic approaches using whole-genome shotgun (WGS) sequencing often present a viable alternative method for characterising microbial communities from environmental samples. Instead of amplifying a single gene, WGS can be used to sample all genes in in all organisms present within a sample, including those from other kingdoms, and therefore can provide a greater level of detail into the functional potential of a microbial community as well as its taxonomic composition (Uritskiy & Diruggiero, 2019). Still, such metagenomic approaches are expensive, require more extensive data analysis than would have been possible within the time frame of this study, and come with their own limitations and challenges (Ranjan *et al.*, 2016). Moreover, Uritskiy & Diruggiero (2019) note that while improvements have been made in the assembly of metagenomic data, “the annotation of halophilic metagenomes for taxonomies and functions can be somewhat compromised because halophiles have extremely limited representation in standard-distribution taxonomic databases”. Subsequently, while public genomic databases are expanding rapidly, they do not currently compare in their usefulness to the well-described 16S rRNA gene databases for the characterisation of communities.

4.1 Differences between *In-situ* Brine and Halite Communities

4.1.1 Differences in Archaeal Community Composition Between *In-situ* Brine and Halite Samples

Phylogenetic analysis of 16S rRNA sequences from *in-situ* brine and halite revealed that, in both sample-types, archaeal communities were dominated by *Halorubrum (Hrr)* and *Haloquadratum (Hqr)* and included a handful of other major genera that formed >1% of community, such as *Halobellus, Halorientalis, Haloplanus, Halomicrobium, Natribaculum and Candidatus* Nanosalina. Surprisingly, there were few OTUs associated with the genus *Haloarcula,* which is often reported as an abundant component of haloarchaeal communities in solar salterns and within halite (Norton *et al.*, 1993; Pašić *et al.*, 2005; Oh *et al.*, 2010; Henriet *et al.*, 2014; Gibtan *et al.*, 2017). Pairwise comparisons of the relative abundances of archaeal genera showed that, *Halorubrum* was significantly more abundant in halite than brine (45.1%) and formed an even greater proportion (77.8%) of the total archaeal community. In contrast, *Haloquadratum* (24.1% in brine), and *Candidatus* Nanosalina (1.8% in brine), were significantly less abundant in halite and formed only 4.9% and 0.2% of the entombed archaeal community, respectively.

Haloquadratum forms dense populations of flat square-shaped cells and, as well as members of the *Halorubrum* and *Haloarcula*, are commonly reported as the dominant archaeal genus in solar salterns and hypersaline lakes such as the Dead Sea (Benlloch *et al.*, 2001; Pašić *et al.*, 2005; Burns *et al.*, 2007; Oh *et al.*, 2010; Fernandez *et al.*, 2014; Podell *et al.*, 2014). While *Haloquadratum* are known to thrive in near-saturated NaCl brines, recent studies suggest that *Haloquadratum* are generally poor survivors inside halite crystals. Gramain *et al.* (2011) showed that *Haloquadratum walsbyi*, relative to *Halobacterium* species, was slow to recover from extended periods of entombment in lab-made halite. Furthermore, metagenetic studies comparing the haloarchaeal community diversity of edible salts have shown that *Haloquadratum* are often absent or form only a small proportion of entombed communities in halite from varied geographic origins (Henriet *et al.*, 2014; Clark *et al.*, 2017; Gibtan *et al.*, 2017). In contrast to *Haloquadratum*, *Halorubrum* is well represented in halite. Henriet *et al.* (2014) showed that *Halorubrum* formed the major archaeal genus in two out of the nine halite samples used in metagenetic analyses and were frequently among the dominant genera (alongside *Haloarcula* and *Halobacterium*) in others. Representatives of *Halorubrum, Haloarcula, Halolamina, Halobacterium* and many other of the archaeal genera in food-grade salts have also been reported in ancient halite and are evidently well adapted for long-term survival in such

conditions (McGenity *et al.*, 2000; Park *et al.*, 2009; Schubert *et al.*, 2010b; Jaakkola *et al.*, 2016).

It is generally understood that salinity is the predominant abiotic factor influencing the composition of microbial communities in solar salterns and other hypersaline environments (Benlloch *et al.*, 2001; Casamayor *et al.*, 2002; Gomariz *et al.*, 2015). Consequently, the differences in the relative abundances of archaeal genera between brine and halite are likely indicative of strain-specific preferences in NaCl concentrations. Niche separation based on salinity enables closely related haloarchaeal species to co-exist within the same environment and could explain the differential relative abundances of the two dominant *Halorubrum* phylotypes (Trp-Arc-1 and Trp-Arc-3) between the two conditions. Trp-Arc-3 (99% identity with *Hrr. orientale*) was significantly less abundant in halite than in brine, whereas Trp-Arc-1 (99% identity with *Hrr. arcis*), the dominant phylotype in both conditions, was significantly more abundant in halite than brine. Both *Hrr. orientale* and *Hrr. arcis* exhibit optimal growth at 3.4 M NaCl, however, for *Hrr. arcis* the optimal growth window extends to 3.9 M (Castillo *et al.*, 2006; Xu *et al.*, 2007). It is important to be circumspect when predicting the exact physiological characteristics and function of an organism based on phylogeny alone (even when an OTU is 99% similar to a known species). Recent multivariate analyses have shown that *Haloquadratum*-related phylotypes, despite their low sequence divergence, can differ significantly in their environmental optima: whereas some phylotypes exhibit generalist behaviour and are found over a wide range of salinities and environmental conditions; some others have only been detected at low and medium salinities, or at specific times within the year (Gomariz *et al.*, 2015; Di Meglio *et al.*, 2016). Moreover, Clark *et al.* (2017) noted that *Haloquadratum* was significantly more relatively abundant in halite of Mediterranean origin than in halite from other geographically regions. In this study, *Haloquadratum* was almost entirely represented by Trp-Arc-2, which showed high sequence identity with an uncultured archaeal clone (AF477930) derived from a 22% salinity saltern pond reported by Benlloch *et al.* (2002) (Figure AI.2).

Since their discovery by Narasingarao *et al.* (2012), members of the Nanohaloarchaea have been found to form an abundant part of microbial communities in salt lakes and solar salterns (Ghai *et al.*, 2011; Narasingarao *et al.*, 2012; Podell *et al.*, 2014; Gomariz *et al.*, 2015; Di Meglio *et al.*, 2016). In comparison to the findings of this study, Clark *et al.* (2017) found that members of the Nanohaloarchaea were also widely distributed among food-grade salts of approximately five years in age. Genomic characteristics of Nanohalarchaea, such as *Candidatus* Nanosalina, suggest that, like most haloarchaea, they are “salt-in” strategists, however, the extent of their halophily remains unclear (Ghai *et al.*, 2011; Narasingarao *et al.*, 2012). Seasonal analyses of saltern microbial communities performed by Gomariz *et al.*

(2015) showed that Nanohaloarchaea-related phylotypes were found within a relatively narrow range of environmentally optimal conditions and that *Candidatus* Nanosalina phylotypes were comparatively less halophilic than those of *Candidatus* Nanosalinarum. This may therefore suggest that *Candidatus* Nanosalina, like Trp-Arc-2, was less abundant in halite than brine, in part, due to their comparatively lower NaCl tolerances (Gomariz *et al.*, 2015).

Yet, little is truly known regarding the physiological characteristics of the Nanohaloarchaea. While it was suggested by Narasingarao *et al.* (2012) that their small physical size may enable them to remain suspended in oxygenated surface waters and thus cater for an aerobic metabolism, recent data suggests that Nanohaloarchaea do not encode cytochrome C oxidase, and are therefore unable to use oxygen (Andrade *et al.*, 2015). According to the encoded metabolic potential of their genomes, Nanohaloarchaea have limited fermentation based metabolism and are likely dependent on metabolites from other co-existing organisms (Andrade *et al.*, 2015). Interestingly, Nanohaloarchaea possess genes for xenorhodopsin, a class of microbial rhodopsins, not found in any other members of the Euryarchaeaota, that closely resemble those found in some cyanobacteria (*Cyanothece* and *Anabaena*) (Ugalde et al., 2011). It is suggested by Ugalde et al. (2011) that xenorhopsins may play a role in photoprotection by inducing-light dependent changes in the expression of certain photoprotective pigments or alternatively proteins involved in DNA repair. However, it remains unclear what the true function of these rhodopsins may be, or whether Nanohaloarchaea are capable of phototrophic growth. Given that Nanohaloarchaea, along with other Archaea, appear to show a preference for night time conditions, it is not clear why *Candidatus* Nanosalina were less abundant in halite where both oxygen and light would have been limited (Andrade *et al.*, 2015).

Haloquadratum and *Candidatus* Nanosalina share specific physical and genomic characteristics (low G+C %) that, in ways, distinguish them from most haloarchaea. Both the distinct flattened-square morphology and small physical size each serve to increase the surface to volume ratio of the cell and likely evolved as adaptations to maximise nutrient uptake from their surrounding environments (Narasingarao *et al.*, 2012). *Haloquadratum* species are strictly aerobic, and are known for orientating their flat cells parallel to the oxygen-rich surface where they spread out like solar panels for efficient phototrophic growth (Bolhuis *et al.*, 2006). In order to maintain persistent growth in light conditions, *Haloquadratum* rely on the production of gas vesicles to optimally position their cells. Unsurprisingly, *Haloquadratum* were less abundant in halite as conditions quickly become anoxic and the tight packaging of cells would limit their potential for phototrophy. Nevertheless, studies have indeed reported the survival of *Haloquadratum* within halite up to

several years in age, and that the viability of *Haloquadratum* in halite can be enhanced by the presence of *Salinibacter ruber* (Gramain *et al.*, 2011; Clark *et al.*, 2017).

Under the assumption that the *in-situ* halite community had derived directly from that of the brine community, the differential relative abundances of archaeal genera in halite may reflect successional community change. Although comparisons between *in-situ* samples were made assuming that halite had formed from the adjacent brine at a time near to collection, it is possible that the halite, and therefore its microbial inhabitants, may be considerably older than thought. Moreover, since the mineral precipitation of sea water occurs in a predictable order (calcite, gypsum, and halite followed by potassium and magnesium rich salts), it cannot be confirmed whether the differences in community composition between brine and halite samples are a consequence of NaCl entombment, or instead due to differences in the ionic compositions of the fluid brine inclusions inside halite, relative to that of the present-day brine (at time of collection). Recent metagenetic studies have shown that both seasonal and even diel fluctuations in environmental conditions such as light, temperature, pH and ionic composition can have a significant influence on microbial community composition in hypersaline brines (Podell *et al.*, 2014; Gomariz *et al.*, 2015; Di Meglio *et al.*, 2016).

4.1.2 Differences in Bacterial Community Composition Between *In-situ* Brine and Halite Samples

Based on the data from the qPCR of experimental samples (discussed further on in 4.2), the bacteria were about 400-fold less abundant than the archaea in these systems (forming ~0.25% of community), and as such the relative changes in bacterial community composition between the two conditions are arguably less important than those of archaea. Phylogenetic analyses showed that bacterial communities in both sample types were dominated by members of the *Salinibacter (Sal.)* and *Salisaeta/Longibacter*. Combined, the two genera formed approximately 90% of the total bacterial community in both brine and in halite. Pairwise comparisons between sample types showed that, while not significantly so, *Salinibacter* were more abundant in halite than in brine, whereas *Salisaeta/Longibacter* were significantly less abundant in halite than in brine (Figure 3.19 and 3.20).

Salinibacter is ubiquitous in hypersaline environments and, as seen in this study, often forms the dominant proportion of the bacterial community in saltern crystallizer ponds (Antón *et al.*, 2008; Di Meglio *et al.*, 2016). Culture-independent studies of bacterial communities in halite have reported large proportions of sequences derived from *Salinibacter* and other members of the *Bacteroidetes* (Baati *et al.*, 2010b; Gibtan *et al.*, 2017). Like members of the Haloarchaea, *Salinibacter* appear a deep red colour due to the presence of the

photoreactive membrane-bound ion pump Xanthorhodopsin (contains salinixanthin; a light harvesting carotenoid antenna), and are salt-in strategist that accumulate high intracellular K^+ concentrations to counteract the osmotic effects of the surrounding high NaCl environment (Antón *et al.*, 2002; Balashov *et al.*, 2005; Vaisman & Oren, 2009). As a consequence of their osmoadaptation strategy, *Salinibacter* have an obligate need for salt in their environment and exhibit optimum growth at 15-25% salinity (Antón *et al.*, 2002). It is not clear whether *Salinibacter* are able to induce halite formation in the same way that Haloarchaea or the haloalkaliphilic bacterium *Salinicoccus halitifaciens* do, nevertheless, it is unsurprising that *Salinibacter,* considering their close physiological similarities to the haloarchaea, dominate bacterial communities in halite (Norton & Grant, 1988; Lopez-Cortes *et al.*, 1994; Castanier *et al.*, 1999; Ramana *et al.*, 2013).

Over years, extensive research in hypersaline environments has unearthed novel members of the *Salinibacter* and has resulted in the characterisation of novel and related genera (Munoz *et al.*, 2017; Viver *et al.*, 2018). Recent reappraisal of the phylogeny of the *Bacteroidetes,* based on 16S and 23S rRNA phylogenies and multilocus sequence analysis of 29 orthologous proteins, has proposed the formation of the *Salinibacteraceae,* a novel family group distinct from that of the *Rhodothermacaea*, and which is formed of *Salinibacter, Salisaeta* and the newly proposed *Salinivenus* (reappraisal of *Sal. iranicus* and *Sal. luteus*) (Munoz *et al.*, 2017; Viver *et al.*, 2018). In this study, the population of *Salisaeta/Longibacter* was dominated by a single abundant phylotype with close association to this new family (Trp-Bac-1). Trp-Bac-1 showed 16S rRNA sequence similarity close to both *Salisaeta longa* and *Longibacter salinarum* (95%), and thus may be indicative of a novel member of a previously uncategorised group with close affiliation to both species (Figure AI.3). With this in mind, the differential abundance of *Salisaeta/Longibacter* in halite may therefore be attributed to the fact that, relative to *Salinibacter*, both species related to Trp-Bac-1 share a preference for lower salinity conditions (5-20%, with an optimum near 10%) (Vaisman & Oren, 2009; Xia *et al.*, 2016). However, given the phylogenetic distance it is not possible to infer such physiological traits, and efforts should be made to cultivate a representative of this OTU.

Pairwise comparisons of the relative abundances of bacterial genera between sample types also highlighted the differential abundance of an uncultivated bacterial group represented by a single OTU (Trp-Bac-14). Trp-Bac-14 were significantly less abundant in *in-situ* halite than in brine. Interestingly, the closest cultured bacterium*, Fabivirga thermotolerans* strain A-4, was only very distantly related to Trp-Bac-14 (85% sequence identity). However, database searches identified closely related 16S rRNA sequences to a number of uncultured members (99% sequence identity with clone AB-578_D06) within the *Bacteroidetes* that were retrieved

from the Santa Pola salterns (CR30) by Gomariz *et al.* (2015). Given the close relation of these sequences to Trp-Bac-14, it is likely that Trp-Bac-14 represents a member of the same BC3 group of hyperhalophilic generalists, described by Gomariz *et al.* (2015), that are widely distributed globally and reportedly present across a wide-range of salinities and environmental conditions. Future cultivation efforts aimed at this group will be important to further characterise their role in hypersaline environments as well as their response to entombment in halite.

Finally, members of two low abundance cyanobacterial genera, the GpVII (*Halothece* and *Euhalothece)* and GpXIII, were also significantly less abundant in halite than in brine. Halotolerant cyanobacteria are found along the entire salinity gradient of a multi-pond solar saltern (Crits-Christoph *et al.*, 2016). Many species form dense benthic mats in intermediate salinity ponds where they are the main primary producers (Oren, 2009b). However, in crystallizer ponds and other salt-saturated environments the cyanobacterial community is often formed almost entirely of members of the *Euhalothece, Halothece* and *Dactylococopsis* (de los Ríos *et al.*, 2010; Gomariz *et al.*, 2015). The decreased abundance of cyanobacteria in halite may be explained by the fact that, for members of the extremely halotolerant cyanobacteria, entrapment in halite may be disadvantageous as, inside halite within the laboratory environment, less light is available for phototrophy. In turn, this would limit the production of compatible solutes, which are necessary for their survival at high salt concentrations (Gramain, 2009).

4.2 Does Entrapment in Halite Select Against Certain Members of a Microbial Community?

Prior studies on microbial diversity and abundance in solar salterns, as well as in other hypersaline environments, have routinely employed culture-based and microscopic approaches for the enumeration of the microbial population. Here, the present study demonstrates the use of a 16S rRNA real-time quantitative PCR approach for estimating and comparing the abundances of extremely halophilic archaeal and bacterial cells trapped inside halite. Most notably, quantification of 16S rRNA gene copy numbers derived from the succession experiment showed that both archaea and bacteria were entombed inside halite in numbers reflective of their abundance in brine (Figure 3.2).

Haloarchaea are consistently reported as the dominant inhabitants of hypersaline brines approaching saturation where they are often able to reach densities of up to 10^7 – 10^8 cells ml^{-1} (Oren, 2002; Oh *et al.*, 2010; Ghai *et al.*, 2011; Gomariz *et al.*, 2015). On the other hand, bacterial communities in such environments are generally lower in both diversity and

abundance. In keeping with prior studies, which have estimated bacterial cell densities around 10^6 cells ml^{-1}, the results of this experiment indicated that, relative to the archaea (around 10^8 – 10^9 cells cm^3), bacteria formed only a marginal proportion (~0.25%) of communities in saturated parent brines and newly-formed halite (Antón *et al.*, 2002; Benlloch *et al.*, 2002; Casamayor *et al.*, 2002; Gomariz *et al.*, 2015).

However, it is possible that the differential abundances of archaea and bacteria observed in this experiment are slightly exaggerated due to the fact that the number of cellular identical chromosomes and mean copy number of the 16S rRNA gene per chromosome can vary considerably between species (Louca et al., 2018). According to the Ribosomal RNA Database (rrnDB), the reported mean 16S rRNA gene copy numbers of members of *Haloquadratum* and *Halorubrum* are 2 and 2.5, respectively, whereas *Salinibacter* have just a single copy (Klappenbach, 2001); as of yet, no such values have been recorded in the rrnDB for members of *Salisaeta* or *Longibacter*. Polyploidy is a widespread feature among the haloarchaea and many species of bacteria, and similarly would likely have greatly contributed in the estimation of their abundances (Zerulla & Soppa, 2014). Yet, given that data for the mean genome copies and 16S rRNA gene copies is limited, it is not possible to accurately estimate to what extent such factors may have influenced the results of the qPCR. Nor is it overtly clear to what extent poor qPCR reaction efficiency may have influenced estimates of bacterial 16S rRNA gene sequences and thus it is possible that bacteria in this study were in fact more abundant than reported.

Previous laboratory studies have shown that haloarchaea and some extremely halophilic bacteria can actively promote and influence the formation of halite. The increased absorption of light by red-coloured pigments causes extreme halophiles to indirectly raise the local temperature of their habitat and in turn promote faster evaporation and precipitation of NaCl (Javor, 1989). Similarly, halite precipitation is also promoted by the action of extreme halophiles that use the salt-in strategy to maintain osmotic balance, as the cross-membrane transfer of intracellular Na^+ ions in exchange for extracellular Cl^- ions leads to increased NaCl concentrations in the neighbouring environment (Castanier *et al.*, 1999). Haloarchaeal cells and S-layers have been shown to act as templates for crystal formation and can influence the size and number of crystals formed (Norton & Grant, 1988; Lopez-Cortes *et al.*, 1994). In this study, community analyses showed that all major genus-level groups (≥1%) in the parent brine communities were also accounted for in halite. Similarly, for both archaea and bacteria, there were no significant differences in OTU richness between communities in parent brines and T1 halite (Sections 3.4.2 and 3.5.2). Comparisons of OTU evenness also showed that communities did not significantly differ between the two conditions. While archaeal communities appeared significantly less even in T1 halite, no differences were

identified between parent brine and halite communities from later time points suggesting that it is unlikely that any such significant differences truly existed. This is supported by the fact that compared to other time points, the archaeal 16S rRNA gene abundance was noticeably lower at T1 time points (Figure 3.2) indicating that DNA extractions from the T1 period may have been poor in quality. Nevertheless, the results of the T0 vs T1 comparison suggest both: that (1) all members of a mixed microbial group are equally prone to entombment; and (2) that there is no selective process imposed on a brine community that excludes specific organisms as halite precipitates.

Relative to the haloarchaea, which were about three orders of magnitude more abundant in both brine and halite, and showed few differences in community composition between the two conditions, bacterial communities (~0.25% of overall community) appeared to be considerably more variable. While there appeared to be no significant differences in OTU evenness between T0 and T1, the bacterial genus *Pelomonas* (*Pel.*) (Family *Comamonadaceae,* Class Betaproteobacteria), represented by a single OTU (Trp-Bac-5) with 99% sequence similarity to *Pel. saccharophila* (Figure A.3), appeared to be dramatically more relatively abundant inside T1 halite than in the parent brines (Figures 3.25 and 3.28). Given that few studies have reported *Pelomonas* in hypersaline brines, these results remain difficult to explain. One explanation is that the abundance of *Pelomonas,* and *Aquabacterium* (formed around 5% of community in halite), represented a case of contamination. While all procedures were performed under aseptic conditions and with sterile reagents (clearly shown through the use of negative controls), members of the *Pelomonas* have previously been studied as contaminants of pure and ultra-pure water, and therefore their presence may have arisen from insufficient sterilisation of MilliQ water added to early-succession samples at either the DNA extraction or first-stage PCR step (Kulakov *et al.*, 2002; Gomila *et al.*, 2007). However, considering the volumes of water added at each stage were constant, *Pelomonas* were not uniformly abundant in either brine or crystal samples and were shown to drastically vary in abundance between experimental replicates. Alternatively, Trp-Bac-5 could represent an exceptionally halotolerant uncultivated strain of *Pel. saccharophila*. A previous study reported *Pelomonas* as part of the bacterial community in association with halite of a Waste Isolation Pilot Plant (WIPP) repository, where they formed almost half of all bacterial sequences of a clone library derived from green/grey coloured halite (containing a kind of clay)(Swanson *et al.*, 2012). Database searches of uncultured members of *Pelomonas* with high 16S rRNA sequence identity to Trp-Bac-5 (99%) have shown sequences with diverse origins, including: fen soils, the roots of drought-resistant grass, biocrusts in dryland and mucus from *Montastraea cavernosa* coral. Thus, it could be argued that Trp-Bac-5 is somewhat of a generalist capable of surviving in a wide variety of

environmental conditions. Still, it is not obvious why such an organism would be so relatively abundant in halite as seen in this study.

4.3 Entombed Microbial Communities Show Few Changes Over 21-Weeks in Halite

Except for the comparisons between T1 and T4 halite, there were no significant differences in the mean archaeal 16S rRNA gene copies (all ponds) when comparing across time points. Bacteria, in comparison, were significantly more abundant in halite at later time points such as T3 and T4 (Figure 3.2.B). Still, when separated by their pond-origin, both archaeal and bacterial abundances (16S rRNA gene copies) in halite showed considerable variation across time points (as shown by their error bars) (Figure 3.1), and so it is not clear how accurate these measurements are. While cellular growth may continue inside halite for a short-period following entombment, it is unlikely that, in the case of the bacteria, abundance inside halite would have greatly exceeded that observed in the parent brines. These results could therefore indicate that poor quality DNA extractions/sub-optimal quantification of DNA may have been responsible for underestimating abundances from earlier time points i.e. T0 and T1. Conversely, halite is known to preserve DNA and other biological macromolecules, thus it is also possible that some of the DNA contained inside halite may have derived from dead cells, resulting in an over estimation of the remaining entombed microbial population (Fish *et al.*, 2002; Griffith *et al.*, 2008; Sankaranarayanan *et al.*, 2014). Furthermore, it is also worth considering that surface-sterilisation of halite was not possible, due to the size and number of crystals, and therefore some of the variation in abundances between experimental replicates can be explained by the varied amount of residual brine found on the surface of, and between, individual halite crystals.

Remarkably, haloarchaeal communities entombed inside halite for 21-weeks (T4) did not significantly differ in terms of OTU richness or evenness from communities in the parent brines (T0) (Sections 3.4.2 and 3.4.3). As observed in *in-situ* comparisons, archaeal communities from all ponds were dominated by *Haloquadratum* and *Halorubrum* and as well as members of *Halobellus, Haloplanus, Halorientalis* and *Candidatus* Nanosalina (Figure 3.12). In general, comparisons between archaeal communities in T4 halite with those in T1 showed few significant differences. In parallel with *in-situ* comparisons, *Candidatus* Nanosalina was the only genus significantly less abundant in T4 halite, suggesting that they are poor survivors of entombment. Conversely, comparisons at the OTU-level showed that two low abundance *Halorubrum* phylotypes (Trp-Arc-14 and Trp-Arc-45), both closely related to *Hrr. sodomense* (99%), were significantly more abundant in T4 halite from Pond 2.

Bacterial communities in lab-made halite were similarly dominated by *Salinibacter* and *Salisaeta/Longibacter* as well as large proportions of the enigmatic *Pelomonas*, uncultivated bacterium and *Aquabacterium* (Figure 3.25). In comparison to the haloarchaea, bacterial communities experienced more change over time. Although OTU richness did not differ between time points, bacterial communities were significantly less OTU even at later time points i.e. T3 and T4 (Sections 3.5.2 and 3.5.3). This is reflected by the decreased relative abundance of *Pelomonas* and *Aquabacterium* (formed <1% of total community) and increased relative abundance of *Salinibacter* and *Salisaeta/Longibacter* in T4 halite communities relative to those at T1 (Figure 3.29). Surprisingly there were no notable differences in the relative abundance of bacterial genera when analyses were separated by pond-origin. Arguably the significantly increased relative abundance of the anaerobic genus *Halobacteroides* indicated that conditions inside halite became anoxic by week 21, however such increases were only found in halite from Pond 1 and represented a very minor proportion of the overall bacterial community (~ 0.4%).

Overall, these comparisons indicate that the ability to survive in halite for short to moderate lengths of time (showed signs of growth even after 1 year, see Table AI.1) is a feature that is widespread among members of the haloarchaea and some halophilic bacteria such as *Salinibacter* and *Salisaeta/Longibacter.* In the context of solar salterns, entombment in halite protects microorganisms against harsh external conditions (such as desiccation, chaotropic ions and UV radiation) and offers a further chance of survival when more favourable conditions return and enable their release. Nevertheless, brine inclusions in halite represent a permanently salt-saturated micro-environment, in which densely packed respiring cells quickly turn the environment anoxic. For these reasons, it was hypothesised that entrapment in halite would over time act as a selective pressure on the microbial community and that communities in 21-week old halite would be observably different from those in brine. While conditions inside halite undoubtedly contributed to the decreased abundance of *Pelomonas, Aquabacterium* and *Candidatus* Nanosalina, the limited differences shown in this experiment show that the rate and scale of community change in halite was greatly overestimated.

There are many possible reasons why communities did not change significantly over the 21-week period inside halite. As noted in Section 1, haloarchaea, and extremely halophilic bacteria like *Salinibacter ruber*, are exceptionally well adapted to their environment and have many structural and physiological adaptations that enable them to withstand extremes of salinity at low energetic cost. Kurt-Kızıldoğan *et al*. (2017) demonstrated that *Halolamina* sp. YKT1, grown at both 2.7 M and 5.5 M NaCl concentrations, responded to saturated conditions by up-regulating genes related to membrane transporters and osmoprotectants, and conversely down-regulated genes related to replication, transcription and translation,

inferring that the halophilic archaeon minimises the production of nucleic acids and peptides in order to channel its energy towards maintaining the intracellular osmotic balance. Additionally, the low solubility of oxygen in saturated hypersaline brines means that microorganisms inhabiting these environments are accustomed to micro-oxic conditions and are often capable of switching to alternative forms of energy production such as arginine fermentation or anaerobic respiration (e.g. using nitrate, DMSO or TMAO) (Hechler & Pfeifer, 2009).

In spite of their shared characteristics and environment, haloarchaea are surprisingly different in their nutritional demands and metabolic pathways (Falb *et al.*, 2008). Orellana *et al.* (2013) noted that many of these biochemical pathways in different species become metabolically inter-connected such that nutrients are utilized, processed, released and re-utilised by other members of the community. Little is known about the physiological interactions that take place between cells inside halite brine inclusions. There is evidence to suggest that glycerol, produced as a compatible solute by the eukaryotic green algae *Dunaliella salina*, may provide sufficient energy for entombed microorganisms to maintain metabolic processes in halite for extended periods of time (Schubert *et al.*, 2009a). Yet the abundance of *D. salina* in solar salterns can be highly variable and can range from 10^5 cells ml^{-1} to complete absence (Oren, 2014b). Interestingly, chloroplast 16S rRNA gene sequences from *D. salina* that would have been identified by bacterial primers were not detected among samples from Trapani salterns. It is perhaps possible that *D. salina* was abundant in the brines of Trapani salterns in the preceding days before samples were collected, and that despite their reported absence, still provided a pool of glycerol to be utilised by the microbial communities analysed in this study. Alternatively, primary production in Trapani salterns may have instead been driven by compatible solute producing members of extremely halotolerant cyanobacteria (such as those mentioned in 4.1.2).

Gramain *et al.* (2011) demonstrated that *Haloquadratum walsbyi* and *Salinibacter ruber* were poor survivors inside halite as pure cultures, however, co-entombment of both species resulted in enhanced viability and faster recovery times. While it is not obviously clear how *Haloquadratum* may improve the survival capabilities of *Salinibacter* in halite, evidence suggests that *Haloquadratum* possess efficient uptake systems for dihydroxyacetone; an intermediate in the degradation of glycerol provided in abundance by *Salinibacter* (Elevi Bardavid & Oren, 2008). Considering that both glycerol and dihydroxyacetone are widely used as carbon and energy sources by heterotrophic prokaryotes, it is likely that many similar interactions and co-dependencies exist within entombed communities that act as additional factors influencing community composition and survival.

4.4 Microbial Community Composition in Halite was Strongly Influenced by the Abiotic Characteristics of the Parent Brine

The succession experiment revealed that communities of both archaea and bacteria undergo few compositional changes over time inside halite and even after 21-weeks remain closely representative of communities in the parent brine (T_0). Interestingly, recent studies have demonstrated that microbial communities in saturated brines of solar salterns and salt lakes are more dynamic than previously thought and undergo considerable changes throughout the year as a consequence of seasonal fluctuations in environmental factors such as temperature, pH, salinity and individual ion concentrations (Boujelben *et al.*, 2012; Podell *et al.*, 2014; Gomariz *et al.*, 2015; Di Meglio *et al.*, 2016). Although the samples used in this study were collected from Trapani salterns at a single point in time, the parent brines themselves were collected from three separate saltern Ponds at observably different stages in the evaporation process (Figure 3.2). As a result of the differences in their physico-chemical characteristics, archaeal and bacterial communities showed considerable compositional differences between communities from different pond-origins (Table 3.1).

Most notably, NDMS analyses show that both archaeal and bacterial communities from Pond 2 were distinct from those of Ponds 1 and 3. Interestingly, while archaeal communities in Pond 2 were significantly more OTU rich than those in Ponds 1 and 3, bacterial OTU richness did not significantly differ between ponds. Instead, bacterial communities in Pond 2 were distinct because of their significantly lower OTU evenness. This is due to the fact that both ponds 1 and 3 contained significantly greater relative abundances of *Pelomonas* and *Aquabacterium* at early time points (T1 and T2). At later time points both genera formed minor components of the community (<1%) and therefore it is likely that such differences in OTU evenness between halite communities of different Ponds would have been minimal. Nevertheless, these results indicate one or both of the following; that (1) some aspect of the two ponds (e.g. lower water activity or certain ion concentrations) provided a more optimal environment for the growth and survival of the two genera, or (2) that, in contrast, conditions within Pond 2 were unfavourable for their growth (e.g. due to reduced concentration of certain ions, sub-optimal water activity, or competition with other organisms.).

Considering that environmental variables such as salinity, ionic composition and water activity are each inter-linked, it is not overtly clear to which extent each individual factor influenced microbial communities in this study. Based on their physico-chemical characteristics, the three Ponds can be ordered in terms of their relative “extremity” (ion concentrations and low water activity) (Figure 4.1). However, archaeal communities from Pond 3, the intermediate, were significantly less diverse than those from Ponds 1 and 3. This

may therefore indicate that, in saturated environments, decreased water activity associated with increased ion concentrations^{-} does not influence archaeal community diversity in a linear fashion. Recent multivariate analyses have shown that microbial communities at near-saturation show dynamic changes in composition that are associated with increased concentrations of specific ions (Podell *et al.*, 2014; Gomariz *et al.*, 2015; Di Meglio *et al.*, 2016). Podell *et al.* (2014) reported that the relative abundance of *Haloquadratum* in the hypersaline Lake Tyrell (Australia) was positively correlated with seasonal increases in Mg^{2+} ion concentrations, whereas the relative abundances of *Halorubrum, Haloarcula, Halonotius* and *Salinibacter*-related sequences were negatively correlated with *Haloquadratum* and the same environmental conditions.

Interestingly, the findings of this study were somewhat in contradiction to those of Podell *et al.* (2014). In comparison, *Haloquadratum* was one of several archaeal and bacterial genera (not limited to *Candidatus* Nanosalina, *Salisaeta/Longibacter*, Uncultivated Bacteria and *GpVII* Cyanobacteria) that were significantly more abundant in Pond 2 than in the more Mg^{2+} rich Ponds 1 and 3. Similarly, while *Halorubrum* formed the dominant proportion in samples from all three Ponds, the genus was significantly more relatively abundant in Pond 3 (and not significantly so in Pond 1) than in Pond 2. Similar studies to Podell *et al.* (2014) comparing seasonal changes in microbial assemblages in solar salterns have shown that individual phylotypes belonging to the same genus can have very different environmental optima (Gomariz *et al.*, 2015; Di Meglio *et al.*, 2016). Gomariz *et al.* (2015) noted that two *Salinibacter* phylotypes derived from solar salterns were plotted on opposing sides of a canonical correspondence analysis and were associated with contrasting conditions of salinity, calcium concentrations and pH values. Similarly, Di Meglio *et al.* (2016) found that one *Haloquadratum*-related sequence (Hqr-2) identified consistently in two of three in-land Argentinian salterns (Salitral Negro and Colorada Grande) was altogether absent from the third which contained higher pH values and sulfate ion concentrations.

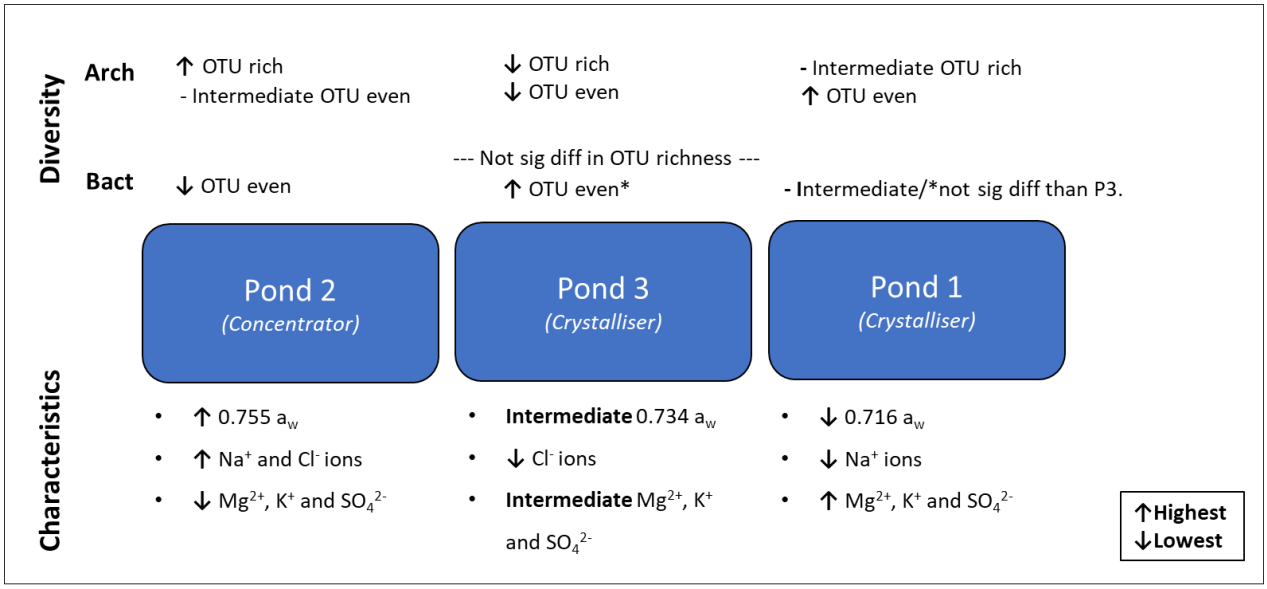

Figure 4.1: A schematic diagram grouping archaeal and bacterial diversity analyses (OTU richness and OTU evenness) with the physico-chemical characteristics of the three saltern Ponds. The three ponds are ordered in terms of their water activities and Mg^{2+}, K^+ and SO_4^{2-} ion concentrations.

In this study, the dominant *Halorubrum* phylotype in Ponds 1 and 3 differed from that of Pond 2. Trp-Arc-1 (97% similarity with *Halorubrum arcis*) formed the majority of the *Halorubrum* population in Ponds 1 and 3, whereas Trp-Arc-3 (99% similarity with *Halorubrum orientale*) dominated in Pond 2 (EAII.1). In comparison, *Haloquadratum* was dominated by a single phylotype in all three Ponds (Trp-Arc-2, 99% similar with *Haloquadratum walsbyi* strain JCM 12705) and was most abundant in Pond 2. Given that a similar inverse relationship between *Halorubrum* phylotypes and the abundance of *Haloquadratum* (Trp-Arc-2) was observed in comparisons between *in-situ* brine and halite communities, these results may indicate that the differential abundances of Trp-Arc-3 and Trp-Arc-2, as well as other OTUs with affiliation to *Candidatus* Nanosalina, *Salisaeta/Longibacter* and *GpVII_Unclass*, are due to lesser capabilities to withstand exceptional increases in salinity and the associated ion effects of brines following halite precipitation.

After halite has precipitated from seawater, continued evaporation results in the sequential formation of salts in the order $MgSO_4$, KCl and finally $MgCl_2$. At each stage in the sequence, the ionic composition of the remaining brine shifts in response to the newly formed salts (Abdel-Aal *et al.*, 2017). Subsequently, comparing the brine ionic composition of the three Ponds with those of seawater at set intervals along the evaporation process showed that while Pond 2 was approaching halite precipitation, Pond 1 was nearer the on-set of sylvite (KCl) formation (Grant, 2004; Abdel-Aal *et al.*, 2017). This is important to consider because

solutes (such as the aforementioned salts) vary in their ability to reduce water activity and can exert additional, potentially stress-inducing, effects (e.g. kosmotropic or chaotropic) on biological systems that may in turn influence the composition of microbial communities (Hallsworth *et al.*, 2007).

Microorganisms in brines with a low water availability exhibit impaired growth rates and have been shown to undergo morphological changes from rods into smaller spherical particles (Fendrihan *et al.*, 2012; Stevenson *et al.*, 2015). Stevenson *et al.* (2015) showed that, even among the most halophilic microorganisms, there existed considerable differences in their water activity minima. Stevenson *et al.* (2015) noted that while the growth of the two bacterial species *Salinibacter ruber* and *Salisaeta longa* did not extend below water activities of 0.755, the archaeaon *Haloquadratum walsbyi* was able to grow down to 0.709 a_w, and further still, two other archaeal strains (namely GN-2 and GN-5), previously cultured in bittern waters, were able to remain active in media with water activity as low as 0.635 a_w (Javor, 1984; Stevenson *et al.*, 2015). Evidently, in this study as well, some of the differential relative abundances of individual phylotypes between the three Ponds may have been, in part, due to the differences in their own water activity windows for growth.

Brines approaching KCl precipitation would have been enriched in $MgSO_4$ and like the NaCl-rich brine of Pond 2 would have elicited a similar kosmotropic (stabilising to biological macromolecules and cellular systems) activity on the surrounding environment (Cray *et al.*, 2013; Abdel-Aal *et al.*, 2017). Despite the relatively low water activity and kosmotropicity, archaeal communities from Pond 1 were the most archaeal OTU rich of the three and contained significantly greater relative abundances of *Haloplanus, Halorientalis, Halomicrobium, Natribaculum, Salinirubrum* and *Halorussus* than were found in Ponds 2 and 3. A BLAST search of abundant OTUs relating to *Halorientalis*, *Halomicrobium*, *Natribaculum* reported low sequence identity with other known strains (<96%, down to 90% for "*Natribaculum*"). Consequently, their increased abundances remain difficult to explain. Overall, the interactions between microbial communities and the solutes in their environment are exceedingly complex, and the comparisons made between ponds in this study suggest that some groups become prevalent in brines only at specific stages in the evaporative concentration of seawater.

5 Conclusion

In conclusion, the combined use of 16S rRNA gene amplicon sequencing and qPCR analyses in this study has enabled a comprehensive comparison of microbial communities (Archaea and Bacteria) in brine and halite samples derived from Trapani Salterns in Sicily. Most notably, the results of this study demonstrate that there are few compositional changes in both archaeal and bacterial communities in halite over time, and that even after 21-weeks of entombment both communities still closely represent those found in the parent brine. For both archaea and bacteria, cells are incorporated into halite, and remain at, numbers that match their abundances in brine. In-keeping with previous reports, this study shows that Archaea are significantly more abundant (~400 fold) than bacteria in both brine and halite.

Comparisons between archaeal and bacterial communities in brine and halite have shown that all genera in brine are included inside halite upon formation, however some are less capable of surviving (e.g. *Candidatus* Nanosalina). Moreover, comparison between communities from different pond origins has shown that communities in halite can vary depending on the environmental conditions (ionic composition and water activity) at the point of halite precipitation. Overall, the results of this study provide further insight into how microorganisms respond to entombment in halite, however further studies involving proteomic techniques will be needed to provide greater insight into the specific physiological responses of microorganisms to such conditions, as well as additional co-entombment experiments that further explore key interactions between community members.

6 Future Work

In general, the results of the succession experiment indicate that few dramatic compositional changes occur in communities of extremely halophilic archaea and bacteria as a consequence of their short-term (up to 21-weeks) entombment in halite. Given that time was a limiting factor throughout this project, it would be interesting to perform follow up analyses of the same experimentally entombed communities (i.e. those trapped in halite that originate from the same parent brines) at later intervals (e.g. after 6, 9 and 12 months following entombment) in order to determine whether there is a threshold period of time at which certain groups become less able to survive and are filtered out. This in turn may further highlight whether particular members of a mixed microbial group are better equipped for such conditions.

Interestingly, comparisons of archaeal abundance between time points of the succession experiment did not reveal any significant differences, suggesting that archaea were as abundant after 21-weeks of halite entombment as they were in the parent brine. However, as noted in Section 4.3, halite is known to preserve DNA and other biological macromolecules, including those derived from dead cells. Consequently, future estimations of microbial abundances in halite based on 16S rRNA gene abundance should require additional verification through microscopic examination and fluorescent staining with non-cytotoxic MitoTracker dyes or a LIVE/DEAD kit that enables the determination of live versus dead cells (Leuko *et al.*, 2004; Maslov *et al.*, 2018). Alternatively, the use of bioorthogonal non-canonical amino acid tagging (BONCAT) paired with fluorescent in-situ hybridisation (FISH) may present an efficient way of determining the metabolic activity, and therefore, viability of specific community members from dissolved halite (Hatzenpichler *et al.*, 2014).

Comparisons between *in-situ* samples showed some significant differences between archaeal and bacterial communities in brine and halite. However, it is noted in Section 4.1.1 that the precise age of the *in-situ* halite samples could not be easily determined, and therefore the microbial inhabitants of such halite may be considerably older than thought. Additionally, this raised the question of whether the differences in community composition observed between sample types were instead due to differences in the ionic compositions of the fluid brine inclusions inside halite, relative to that of the present-day brine? Previous studies have shown that archaeal community composition in particular can vary considerably alongside temporal fluctuations in ionic composition, temperature and sunlight (Podell *et al.*, 2014; Andrade *et al.*, 2015; Gomariz *et al.*, 2015; Di Meglio *et al.*, 2016). To separate the effect that halite entombment has on *in-situ* microbial communities from that of the other aforementioned environmental factors, a repeat investigation could be performed in which

multiple brine and halite samples are collected from the same positions over the course of a few days.

Lastly, this study has focussed primarily on the compositional changes that occur over time in communities of extremely halophilic archaea and bacteria following their entombment in halite. Yet, it remains unclear what specific physiological changes occur in these communities at the cellular level that may afford them the ability to survive for extended periods of time inside halite. In order to provide insight into such changes, future study should be directed towards the mechanisms underlying survival in halite. One suggestion may be that a similar laboratory experiment to that of the succession experiment in this study could be carried out whereby proteomic analyses are performed at set intervals on a model organism (e.g. *Hbt. salinarum*) that has been experimentally entombed in halite.

7 Appendix

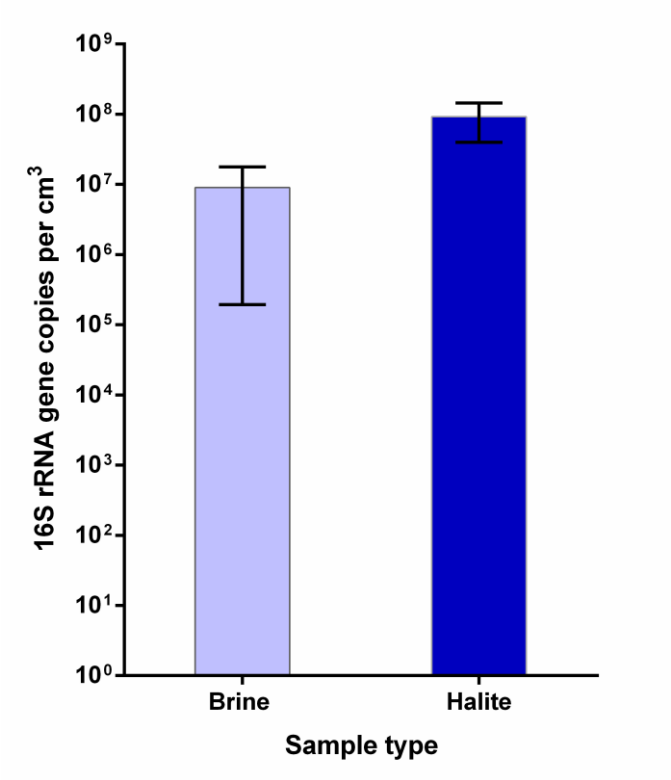

Figure A.1: The mean number of 16S rRNA gene copies per cm^3 quantified from DNA extracts taken from *in-situ* brine and halite samples. Each bar represents the mean starting quantity of three experimental replicates (*n* = 3). Error bars represent the standard error of the biological mean values. Archaeal 16S rRNA gene abundance was quantified using archaeal primers 344F and 915R (R^2 = 0.999, E = 110.4%). Values derived from 1 ml of liquid brine and 1 g of solid halite were normalised to 1 cm^3 to equate for the differences in their density. One-way ANOVA followed by Tukey's HSD ($P<0.05$) were performed to identify significant differences in abundance between brines time points.

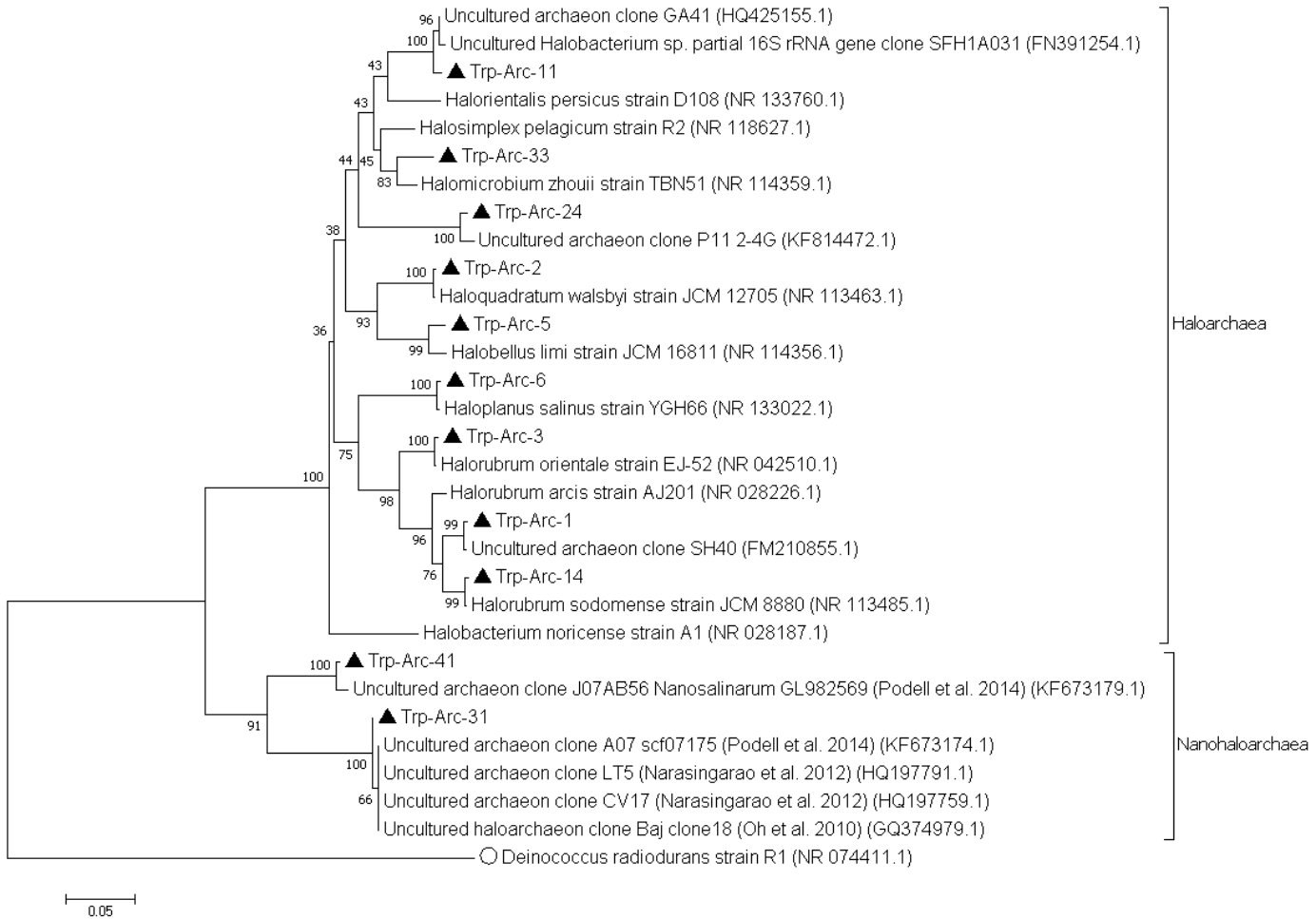

Figure A.2: Phylogenetic affiliation of the 16S rRNA archaeal sequences derived from brine and halite samples in this study. The tree was inferred using the Neighbor-Joining method and constructed based on an alignment of 340 bp. Evolutionary distances were computed using the Jukes-Cantor method. The scale bar corresponds with 0.05 substitutions per nucleotide position. Bootstrap values (%) at branching points represent the significance of branching order (500 repeats). OTUs derived from this study are indicated with ▲. The named sequences represent the closest type-strain or uncultivated relative of a specific OTU(s). The sequence of *Deinococcus Radiodurans* strain R1 served as the outgroup (O). All phylogenetic analyses were conducted in MEGA 7 (Kumar *et al.*, 2016).

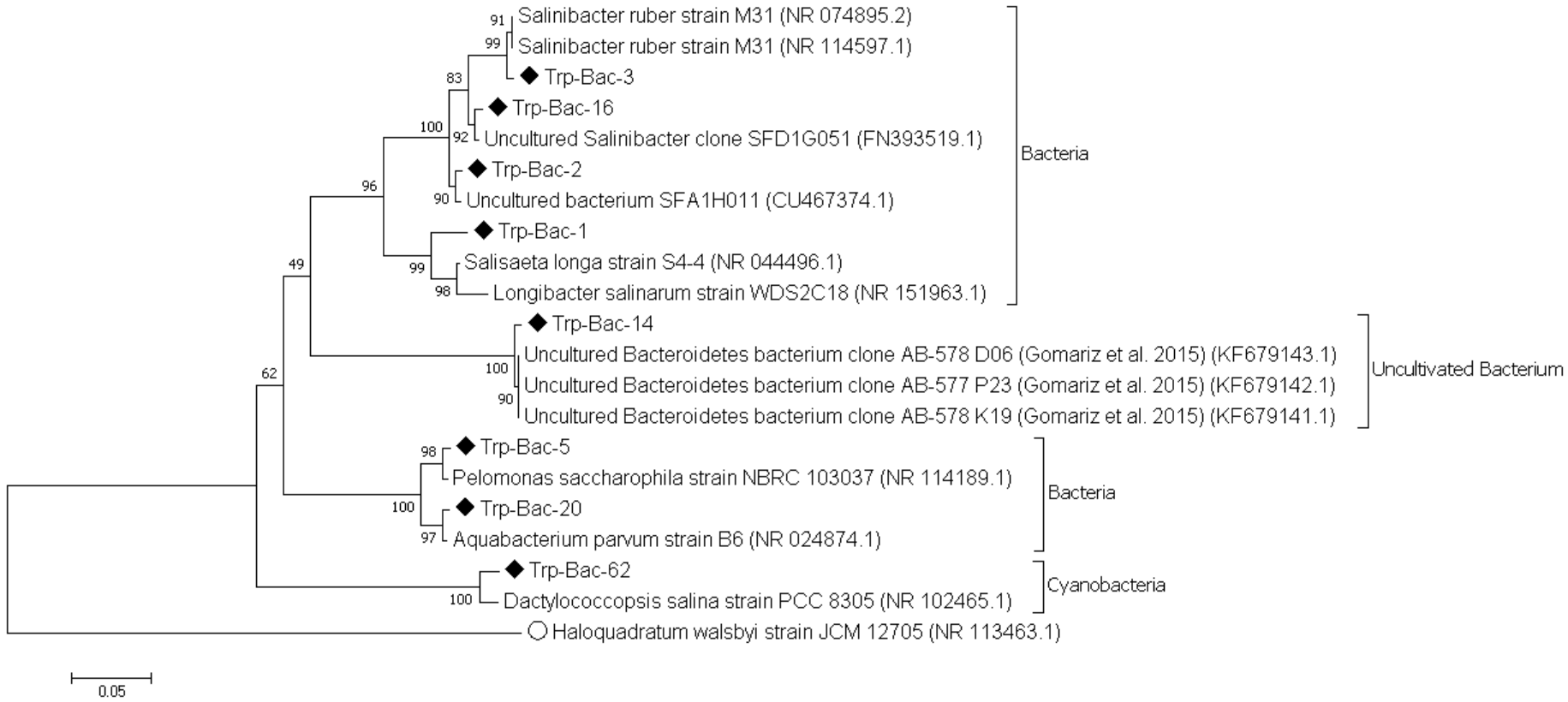

Figure A.3: Phylogenetic affiliation of the 16S rRNA bacterial sequences derived from brine and halite samples in this study. The tree was inferred using the Neighbor-Joining method and constructed based on an alignment of 468 bp. Evolutionary distances were computed using the Jukes-Cantor method. The scale bar corresponds with 0.05 substitutions per nucleotide position. Bootstrap values (%) at branching points represent the significance of branching order (500 repeats). OTUs derived from this study are indicated with ♦. The named sequences represent the closest type-strain or uncultivated relative of a specific OTU(s). The sequence of *Haloquadratum walsbyi* strain JCM 12705 served as the outgroup (O). All phylogenetic analyses were conducted in MEGA 7 (Kumar *et al.*, 2016).

Table A.1. Semi-quantitative comparison of microbial growth derived from lab-made halite crystals of 1 year in age. Halite samples that were formed in the lab and were 1 year old were inoculated into Payne's medium (20% NaCl) and checked after 2 months for turbidity: for samples from Pond 1 growth was observed in 4/5 cases, for Pond 2 in 4/5 cases and for Pond 3 in 2/5 cases. H1-3 refers to the Pond origin of the halite. Data was collected by five undergraduate project students (left).

	H1	**H2**	**H3**
Ryan	+	+++	+
Jonathan	+	++	-?
Niall	+	-?	+++
Myles	++	+	-?
Christian	-?	+++	-?

8 References

Abdel-Aal H, Zohdy K, Abdelkreem M (2017) Seawater Bittern a Precursor for Magnesium Chloride Separation: Discussion and Assessment of Case Studies. *International Journal of Waste Resources*, **7**.

Adamski JC, Roberts JA, Goldstein RH (2006) Entrapment of bacteria in fluid inclusions in laboratory-grown halite. *Astrobiology*, **6**, 552–562.

Albers S-V, Meyer BH (2011) The archaeal cell envelope. *Nature Reviews Microbiology*, **9**, 414–426.

Anderson H (1953) The Reddening of Salted Hides and Fish. *Applied Microbiology*, **2**, 64–69.

Andrade K, Logemann J, Heidelberg KB et al. (2015) Metagenomic and lipid analyses reveal a diel cycle in a hypersaline microbial ecosystem. *The ISME Journal*, **9**, 2697–2711.

Andrei AŞ, Banciu HL, Oren A (2012) Living with salt: Metabolic and phylogenetic diversity of archaea inhabiting saline ecosystems. *FEMS Microbiology Letters*, **330**, 1–9.

Antón J (2011) Compatible Solute. In: *Encyclopedia of Astrobiology*, pp. 351–352. Springer Berlin Heidelberg, Berlin, Heidelberg.

Antón J, Rosselló-mora R, Amann R, Anto J (2000) Extremely Halophilic Bacteria in Crystallizer Ponds from Solar Salterns. *Applied and Environmental Microbiology*, **66**, 3052–3057.

Antón J, Oren A, Benlloch S, Rodríguez-Valera F, Amann R, Rosselló-Mora R (2002) *Salinibacter ruber* gen. nov., sp. nov., a novel, extremely halophilic member of the Bacteria from saltern crystallizer ponds. *International Journal of Systematic and Evolutionary Microbiology*, **52**, 485–491.

Antón J, Peña A, Santos F, Martínez-García M, Schmitt-Kopplin P, Rosselló-Mora R (2008) Distribution, abundance and diversity of the extremely halophilic bacterium *Salinibacter ruber*. *Saline Systems*, **4**, 15.

Antunes A, Taborda M, Huber R, Moissl C, Nobre MF, da Costa MS (2008) *Halorhabdus tiamatea* sp. nov., a non-pigmented extremely halophilic archaeon from a deep-sea hypersaline anoxic basin of the Red Sea, and emended description of the genus Halorhabdus. *International Journal of Systematic and Evolutionary Microbiology*, **58**, 215–220.

Arahal DR, Oren A, Ventosa A (2017) International Committee on Systematics of Prokaryotes Subcommittee on the taxonomy of Halobacteria and Subcommittee on the taxonomy of Halomonadaceae. Minutes of the joint open meeting, 11 July 2017, Valencia, Spain. *International Journal of Systematic and Evolutionary Microbiology*, **67**, 4279–4283.

Aslam SN, Dumbrell AJ, Sabir JS et al. (2016) Soil compartment is a major determinant of the impact of simulated rainfall on desert microbiota. *Environmental Microbiology*, **18**, 5048–5062.

Atanasova NS, Oksanen HM, Bamford DH (2015) Haloviruses of archaea, bacteria, and eukaryotes. *Current Opinion in Microbiology*, **25**, 40–48.

Baati H, Guermazi S, Gharsallah N, Sghir A, Ammar E (2010a) Novel prokaryotic diversity in sediments of Tunisian multipond solar saltern. *Research in Microbiology*, **161**, 573–582.

Baati H, Guermazi S, Gharsallah N, Sghir A, Ammar E (2010b) Microbial community of salt crystals processed from Mediterranean seawater based on 16S rRNA analysis. *Canadian Journal of Microbiology*, **55**, 1–8.

Balashov SP, Imasheva ES, Boichenko VA, Antón J, Wang JM, Lanyi JK (2005) Xanthorhodopsin: a proton pump with a light-harvesting carotenoid antenna. *Science (New York, N.Y.)*, **309**, 2061–4.

Baliga NS, Bjork SJ, Bonneau R et al. (2004) Systems level insights into the stress response to UV radiation in the halophilic archaeon *Halobacterium* NRC-1. *Genome Research*, **14**, 1025–1035.

Ben-Amotz A, Avron M (1973) The role of glycerol in the osmotic regulation of the halophilic alga Dunaliella parva. *Plant Physiology*, **51**, 875–878.

Benlloch S, Acinas SG, Antón J, López-López A, Luz SP, Rodríguez-Valera F (2001) Archaeal Biodiversity in Crystallizer Ponds from a Solar Saltern: Culture versus PCR. *Microbial Ecology*, **41**, 12–19.

Benlloch S, López-López A, Casamayor EO et al. (2002) Prokaryotic genetic diversity throughout the salinity gradient of a coastal solar saltern. *Environmental Microbiology*, **4**, 349–360.

Bodaker I, Sharon I, Feingersch R, Rosenberg M (2009) Archaeal diversity in the Dead Sea : Microbial survival under increasingly harsh conditions. *Natural Resources and Environmental Issues*, **15**, 137–143.

Bodaker I, Sharon I, Suzuki MT et al. (2010) Comparative community genomics in the Dead Sea: an increasingly extreme environment. *The ISME Journal*, **4**, 399–407.

Bolhuis H, Palm P, Wende A et al. (2006) The genome of the square archaeon *Haloquadratum walsbyi*: Life at the limits of water activity. *BMC Genomics*, **7**, 169.

Boujelben I, Gomariz M, Martínez-García M et al. (2012) Spatial and seasonal prokaryotic community dynamics in ponds of increasing salinity of Sfax solar saltern in Tunisia. *Antonie van Leeuwenhoek, International Journal of General and Molecular Microbiology*, **101**, 845–857.

Bowers KJ, Wiegel J (2011) Temperature and pH optima of extremely halophilic archaea: a mini-review. *Extremophiles*, **98**, 119–128.

Burns DG, Camakaris HM, Janssen PH, Dyall-Smith ML (2004) Cultivation of Walsby's square haloarchaeon. *FEMS Microbiology Letters*, **238**, 469–473.

Burns DG, Janssen PH, Itoh T et al. (2007) *Haloquadratum walsbyi* gen. nov., sp. nov., the square haloarchaeon of Walsby, isolated from saltern crystallizers in Australia and Spain. *International Journal of Systematic and Evolutionary Microbiology*, **57**, 387–392.

Casamayor EO, Massana R, Benlloch S et al. (2002) Changes in archaeal, bacterial and eukaryal assemblages along a salinity gradient by comparison of genetic fingerprinting methods in a multipond solar saltern. *Environmental Microbiology*, **4**, 338–348.

Castanier S, Perthuisot JP, Matrat M, Morvan JY (1999) The salt ooids of Berre salt works (Bouches du Rhone, France): The role of bacteria in salt crystallisation. *Sedimentary Geology*, **125**, 9–21.

Castillo AM, Gutiérrez MC, Kamekura M et al. (2006) *Halorubrum orientale* sp. nov., a halophilic archaeon isolated from Lake Ejinor, Inner Mongolia, China. *International Journal of Systematic and Evolutionary Microbiology*, **56**, 2559–2563.

Clark DR, Mathieu M, Mourot L, Dufossé L, Underwood GJC, Dumbrell AJ, McGenity TJ

(2017) Biogeography at the limits of life: Do extremophilic microbial communities show biogeographical regionalization? *Global Ecology and Biogeography*, **26**, 1435–1446.

Cray JA, Russell JT, Timson DJ, Singhal RS, Hallsworth JE (2013) A universal measure of chaotropicity and kosmotropicity. *Environmental Microbiology*, **15**, 287–296.

Crits-Christoph A, Gelsinger DR, Ma B et al. (2016) Functional analysis of the archaea, bacteria, and viruses from a halite endolithic microbial community. *Environmental Microbiology*, **18**, 2064–2077.

Denner EBM, McGenity TJ, Busse H-J, Grant WD, Wanner G, Stan-Lotter H (1994) *Halococcus salifodinae* sp. nov., an Archaeal Isolate from an Austrian Salt Mine. *International Journal of Systematic Bacteriology*, **44**, 774–780.

Deole R, Challacombe J, Raiford DW, Hoff WD (2013) An extremely halophilic proteobacterium combines a highly acidic proteome with a low cytoplasmic potassium content. *Journal of Biological Chemistry*, **288**, 581–588.

Dombrowski H (1963) Bacteria from Paleozoic Salt Deposits. *Annals of the New York Academy of Sciences*, **108**, 453–460.

Elevi Bardavid R, Oren A (2008) Dihydroxyacetone metabolism in *Salinibacter ruber* and in *Haloquadratum walsbyi*. *Extremophiles*, **12**, 125–131.

Falb M, Pfeiffer F, Palm P, Rodewald K, Hickmann V, Tittor J, Oesterhelt D (2005) Living with two extremes: Conclusions from the genome sequence of *Natronomonas pharaonis*. *Genome Research*, **15**, 1336–1343.

Falb M, Müller K, Königsmaier L et al. (2008) Metabolism of halophilic archaea. *Extremophiles*, **12**, 177–196.

Fendrihan S, Bérces A, Lammer H et al. (2009) Investigating the effects of simulated martian ultraviolet radiation on *Halococcus dombrowskii* and other extremely halophilic archaebacteria. *Astrobiology*, **9**, 104–12.

Fendrihan S, Dornmayr-Pfaffenhuemer M, Gerbl FW et al. (2012) Spherical particles of halophilic archaea correlate with exposure to low water activity - implications for microbial survival in fluid inclusions of ancient halite. *Geobiology*, **10**, 424–433.

Fernandez AB, Vera-Gargallo B, Sanchez-Porro C, Ghai R, Papke RT, Rodriguez-Valera F, Ventosa A (2014) Comparison of prokaryotic community structure from Mediterranean and Atlantic saltern concentrator ponds by a metagenomic approach. *Frontiers in Microbiology*, **5**, 196.

Fish SA, Shepherd TJ, McGenity TJ, Grant WD (2002) Recovery of 16S ribosomal RNA gene fragments from ancient halite. *Nature*, **417**, 432–6.

Ghai R, Pašić L, Fernández AB et al. (2011) New Abundant Microbial Groups in Aquatic Hypersaline Environments. *Scientific Reports*, **1**, 135.

Gibbons NE (1974) *Family V. Halobacteriaceae fam. nov.* The Williams and Wilkins Co., Baltimore, 269–273 pp.

Gibtan A, Park K, Woo M et al. (2017) Diversity of extremely halophilic archaeal and bacterial communities from commercial salts. *Frontiers in Microbiology*, **8**, 799.

Gomariz M, Martínez-García M, Santos F et al. (2015) From community approaches to single-cell genomics: the discovery of ubiquitous hyperhalophilic Bacteroidetes generalists. *The ISME Journal*, **9**, 16–31.

Gomila M, Bowien B, Falsen E, Moore ERB, Lalucat J (2007) Description of Pelomonas

aquatica sp. nov. and *Pelomonas puraquae* sp. nov., isolated from industrial and haemodialysis water. *International Journal of Systematic and Evolutionary Microbiology*, **57**, 2629–2635.

Gramain A (2009) *Entombment and survival of extreme halophiles in halite.* University of Essex.

Gramain A, Díaz GC, Demergasso C, Lowenstein TK, Mcgenity TJ (2011) Archaeal diversity along a subterranean salt core from the Salar Grande (Chile). *Environmental Microbiology*, **13**, 2105–2121.

Grant WD (2001) Genus I. Halobacterium Elazari-Volcani 1957, 207, AL emend. Larsen and Grant 1989, 2222. *Bergey's Manual of Systematic Bacteriology*, **1**, 301–305.

Grant WD (2004) Life at low water activity. *Philosophical Transactions of the Royal Society B: Biological Sciences*, **359**, 1249–1267.

Grant WD, Larsen H (1989) Extremely halophilic archaeobacteria, order Halobacteriales ord. nov. *Bergey's Manual of Systematic Bacteriology*, **3**, 2216–2228.

Grant WD, Gemmell RT, McGenity TJ (1998) Halobacteria: The evidence for longevity. *Extremophiles*, **2**, 279–287.

Griffith JD, Willcox S, Powers DW, Nelson R, Baxter BK (2008) Discovery of Abundant Cellulose Microfibers Encased in 250 Ma Permian Halite: A Macromolecular Target in the Search for Life on Other Planets. *Astrobiology*, **8**, 215–228.

Griffiths RI, Whiteley AS, O'Donnell AG, Bailey MJ (2000) Rapid method for coextraction of DNA and RNA from natural environments for analysis of ribosomal DNA- and rRNA-based microbial community composition. *Applied and Environmental Microbiology*, **66**, 5488–5491.

Gruber C, Legat A, Pfaffenhuemer M, Radax C, Weidler G, Busse HJ, Stan-Lotter H (2004) *Halobacterium noricense* sp. nov., an archaeal isolate from a bore core of an alpine Permian salt deposit, classification of *Halobacterium* sp. NRC-1 as a strain of H. salinarum and emended description of H. salinarum. *Extremophiles*, **8**, 431–439.

Guixa-Boixareu N, Calderón-Paz JI, Heldal M, Bratbak G, Pedrós-Alió C (1996) Viral lysis and bacterivory as prokaryotic loss factors along a salinity gradient. *Aquatic Microbial Ecology*, **11**, 215–227.

Gupta RS, Naushad S, Baker S (2015) Phylogenomic analyses and molecular signatures for the class Halobacteria and its two major clades: A proposal for division of the class Halobacteria into an emended order Halobacteriales and two new orders, Haloferacales ord. nov. and Natrialbales ord. n. *International Journal of Systematic and Evolutionary Microbiology*, **65**, 1050–1069.

Gupta RS, Naushad S, Fabros R, Adeolu M (2016) A phylogenomic reappraisal of family-level divisions within the class Halobacteria: proposal to divide the order Halobacteriales into the families *Halobacteriaceae*, *Haloarculaceae* fam. nov., and *Halococcaceae* fam. nov., and the order Haloferacales into th. *Antonie van Leeuwenhoek, International Journal of General and Molecular Microbiology*, **109**, 565–587.

Hallsworth JE, Yakimov MM, Golyshin PN et al. (2007) Limits of life in MgCl2-containing environments: Chaotropicity defines the window. *Environmental Microbiology*, **9**, 801–813.

Harrison FC, Kennedy ME (1929) The red discolouration of cured codfish. *Transactions of the Royal Society of Canada*, 101–152.

Hatzenpichler R, Scheller S, Tavormina PL, Babin BM, Tirrell DA, Orphan VJ (2014) In situ visualization of newly synthesized proteins in environmental microbes using amino acid tagging and click chemistry. *Environmental Microbiology*, **16**, 2568–2590.

Hebsgaard MB, Phillips MJ, Willerslev E (2005) Geologically ancient DNA: Fact or artefact? *Trends in Microbiology*, **13**, 212–220.

Hechler T, Pfeifer F (2009) Anaerobiosis inhibits gas vesicle formation in halophilic Archaea. *Molecular Microbiology*, **71**, 132–145.

Henriet O, Fourmentin J, Delincé B, Mahillon J (2014) Exploring the diversity of extremely halophilic archaea in food-grade salts. *International Journal of Food Microbiology*, **191**, 36–44.

Illumina (2015) 16S Metagenomic sequencing library preparation: Preparing 16S ribosomal RNA gene amplicons for the Illumina MiSeq system. 21.

Imhoff JF, Rodriguez-Valerat F (1984) Betaine Is the Main Compatible Solute of Halophilic Eubacteria. *Journal of Bacteriology*, **160**, 478–479.

Jaakkola ST, Zerulla K, Guo Q et al. (2014) Halophilic archaea cultivated from surface sterilized middle-late Eocene rock salt are polyploid. *PLoS ONE*, **9**, 24–26.

Jaakkola ST, Ravantti JJ, Oksanen HM, Bamford DH (2016) Buried Alive: Microbes from Ancient Halite. *Trends in Microbiology*, **24**, 148–160.

Javor BJ (1984) Growth potential of halophilic bacteria isolated from solar salt environments: carbon sources and salt requirements. *Applied and Environmental Microbiology*, **48**, 352–360.

Javor B (1989) *Hypersaline Environments. Microbiology and Biogeochemistry*. Springer Berlin Heidelberg, 1–4 pp.

Jones DL, Baxter BK (2017) DNA Repair and Photoprotection: Mechanisms of Overcoming Environmental Ultraviolet Radiation Exposure in Halophilic Archaea. *Frontiers in Microbiology*, **8**, 1882.

Kellermann MY, Yoshinaga MY, Valentine RC, Wörmer L, Valentine DL (2016) Important roles for membrane lipids in haloarchaeal bioenergetics. *Biochimica et Biophysica Acta - Biomembranes*, **1858**, 2940–2956.

Kim YB, Kim JY, Song HS et al. (2018) Novel haloarchaeon Natrinema thermophila having the highest growth temperature among haloarchaea with a large genome size. *Scientific Reports*, **8**, 7777.

Kish A, Kirkali G, Robinson C, Rosenblatt R, Jaruga P, Dizdaroglu M, Diruggiero J (2009) Salt shield: Intracellular salts provide cellular protection against ionizing radiation in the halophilic archaeon, *Halobacterium salinarum* NRC-1. *Environmental Microbiology*, **11**, 1066–1078.

Klappenbach JA (2001) rrndb: the Ribosomal RNA Operon Copy Number Database. *Nucleic Acids Research*, **29**, 181–184.

Klindworth A, Pruesse E, Schweer T, Peplies J, Quast C, Horn M, Glackner FO (2013) Evaluation of general 16S ribosomal RNA gene PCR primers for classical and next-generation sequencing-based diversity studies. *Nucleic Acids Research*, **41**.

Kogej T, Stein M, Volkmann M, Gorbushina AA, Galinski EA, Gunde-Cimerman N (2007) Osmotic adaptation of the halophilic fungus *Hortaea werneckii*: Role of osmolytes and melanization. *Microbiology*, **153**, 4261–4273.

Kulakov LA, McAlister MB, Ogden KL, Larkin MJ, O'Hanlon JF (2002) Analysis of bacteria contaminating ultrapure water in industrial systems. *Applied and Environmental Microbiology*, **68**, 1548–1555.

Kumar S, Stecher G, Tamura K (2016) MEGA7: Molecular Evolutionary Genetics Analysis Version 7.0 for Bigger Datasets. *Molecular Biology and Evolution*, **33**, 1870–1874.

Kurt-Kızıldoğan A, Abanoz B, Okay S (2017) Global transcriptome analysis of *Halolamina* sp. to decipher the salt tolerance in extremely halophilic archaea. *Gene*, **601**, 56–64.

Kushner D (1978) *Life in high salt and solute concentrations: halophilic bacteria*.

Lee CK, Herbold CW, Polson SW, Wommack KE, Williamson SJ, McDonald IR, Cary SC (2012) Groundtruthing Next-Gen Sequencing for Microbial Ecology-Biases and Errors in Community Structure Estimates from PCR Amplicon Pyrosequencing (ed Gilbert JA). *PLoS ONE*, **7**, e44224.

Leuko S, Legat A, Fendrihan S, Stan-Lotter H (2004) Evaluation of the LIVE/DEAD BacLight Kit for Detection of Extremophilic Archaea and Visualization of Microorganisms in Environmental Hypersaline Samples. *Applied and Environmental Microbiology*, **70**, 6884–6886.

Lopez-Cortes A, Ochoa J-LL, Vazquez-Duhalt R, Vazquezduhalt R (1994) Participation of halobacteria in crystal formation and the crystallization rate of NaCl. *Geomicrobiology Journal*, **12**, 69–80.

López-López A, Benlloch S, Bonfá M, Rodríguez-Valera F, Mira A (2007) Intragenomic 16s rDNA divergence in Haloarcula marismortui is an adaptation to different temperatures. *Journal of Molecular Evolution*, **65**, 687–696.

de los Ríos A, Valea S, Ascaso C et al. (2010) Comparative analysis of the microbial communities inhabiting halite evaporates of the Atacama Desert. *International Microbiology*, **13**, 79–89.

Louca S, Doebeli M, Parfrey LW (2018) Correcting for 16S rRNA gene copy numbers in microbiome surveys remains an unsolved problem. *Microbiome*, **6**, 41.

Luk A, Williams T, Erdmann S, Papke R, Cavicchioli R (2014) Viruses of Haloarchaea. *Life*, **4**, 681–715.

Maslov I, Bogorodskiy A, Mishin A et al. (2018) Efficient non-cytotoxic fluorescent staining of halophiles. *Scientific Reports*, **8**, 2549.

McGenity T, Oren A (2012) Hypersaline Environments. In: *Life at Extremes: Environments, Organisms, and Strategies for Survival* (ed Bell E), pp. 402–437.

McGenity TJ, Gemmell RT, Grant WD, Stan-Lotter H (2000) Origins of halophilic microorganisms in ancient salt deposits. *Environmental Microbiology*, **2**, 243–250.

McGenity TJ, Hallsworth JE, Timmis KN (2007) Connectivity between 'ancient' and 'modern' hypersaline environments, and the salinity limits of life.

Di Meglio L, Santos F, Gomariz M, Almansa C, López C, Antón J, Nercessian D (2016) Seasonal dynamics of extremely halophilic microbial communities in three Argentinian salterns (ed Olson J). *FEMS Microbiology Ecology*, **92**, fiw184.

Mesbah NM, Cook GM, Wiegel J (2009) The halophilic alkalithermophile *Natranaerobius thermophilus* adapts to multiple environmental extremes using a large repertoire of Na +(K+)/H+ antiporters. *Molecular Microbiology*, **74**, 270–281.

Morita RY (1998) Bacteria in oligotrophic environments. Starvation-Survival lifestyle.

Limnology and Oceanography, **43**, 1021–1022.

Mormile MR, Biesen MA, Gutierrez MC, Ventosa A, Pavlovich JB, Onstott TC, Fredrickson JK (2003) Isolation of *Halobacterium salinarum* retrieved directly from halite brine inclusions. *Environmental Microbiology*, **5**, 1094–1102.

Munoz R, Rosselló-Móra R, Amann R (2017) Revised phylogeny of Bacteroidetes and proposal of sixteen new taxa and two new combinations including Rhodothermaeota phyl. nov. *Systematic and Applied Microbiology*, **40**, 190.

Narasingarao P, Podell S, Ugalde JA et al. (2012) De novo metagenomic assembly reveals abundant novel major lineage of Archaea in hypersaline microbial communities. *The ISME Journal*, **6**, 81–93.

Ng WV, Kennedy SP, Mahairas GG et al. (2000) Genome sequence of Halobacterium species NRC-1. *Proceedings of the National Academy of Sciences*, **97**, 12176–12181.

Norton C, Grant W (1988) Survival of Halobacteria Within Fluid Inclusions in Salt Crystals. *Journal of General Microbiology*, **134**, 1365–1.

Norton C, McGenity T, Grant W (1993) Archaeal halophiles (halobacteria) from two British salt mines. *Journal of General Microbiology*, **139**, 1077–1081.

Oh D, Porter K, Russ B, Burns D, Dyall-Smith M (2010) Diversity of Haloquadratum and other haloarchaea in three, geographically distant, Australian saltern crystallizer ponds. *Extremophiles*, **14**, 161–169.

Orellana M V., Pang WL, Durand PM, Whitehead K, Baliga NS (2013) A Role for Programmed Cell Death in the Microbial Loop. *PLoS ONE*, **8**.

Oren A (1999) Bioenergetic Aspects of Halophilism. *Microbiology and Molecular Biology Reviews*, **63**, 334–48.

Oren A (2002) Molecular ecology of extremely halophilic Archaea and Bacteria. *Fems Microbiology Ecology*, **39**, 1–7.

Oren A (2006) The Order Halobacteriales. In: *The Prokaryotes - Volume 3: Archaea. Bacteria: Firmicutes, Actinomycetes*, pp. 1050–1079.

Oren A (2008) Microbial life at high salt concentrations: phylogenetic and metabolic diversity. *Saline Systems*, **4**, 2.

Oren A (2009a) Microbial diversity and microbial abundance in salt-saturated brines: Why are the waters of hypersaline lakes red? *Natural Resources and Environmental Issues*, **15**, 247–255.

Oren A (2009b) Saltern evaporation ponds as model systems for the study of primary production processes under hypersaline conditions. In: *Aquatic Microbial Ecology*, Vol. 56, pp. 193–204.

Oren A (2011) Thermodynamic limits to microbial life at high salt concentrations. *Environmental Microbiology*, **13**, 1908–1923.

Oren A (2013) Life at high salt concentrations, intracellular KCl concentrations, and acidic proteomes. *Frontiers in Microbiology*, **4**, 315.

Oren A (2014a) Taxonomy of halophilic Archaea: current status and future challenges. *Extremophiles*, **18**, 825–834.

Oren A (2014b) The ecology of Dunaliella in high-salt environments. *Journal of Biological Research (Greece)*, **21**, 23.

Oren A, Gurevich P (1994) Production of D-lactate, acetate, from glycerol in communities of in the Dead Sea and in saltern and pyruvate halophilic archaea crystallizer ponds. *FEMS Microbiology Ecology*, **14**, 147–156.

Oren A, Gurevich P (1995) Dynamics of a bloom of halophilic archaea in the Dead Sea. *Hydrobiologia*, **315**, 149–158.

Oren A, Shilo M (1982) Population dynamics of *Dunaliella parva* in the Dead Sea. *Limnology and Oceanography*, **27**, 201–211.

Oren A, Ventosa A (2016) International committee on systematics of Prokaryotes subcommittee on the taxonomy of halobacteriaceae and subcommittee on the taxonomy of *Halomonadaceae*. Minutes of the joint open meeting, 23 may 2016, San Juan, Puerto Rico. *International Journal of Systematic and Evolutionary Microbiology*, **66**, 4291–4295.

Oren A, Gurevich P, Anati DA, Barkan E, Luz B (1995) A Bloom of Dunaliella-Parva in the Dead-Sea in 1992 - Biological and Biogeochemical Aspects. *Hydrobiologia*, **297**, 173–185.

Oren A, Ventosa A, Grant WD (1997) Proposed Minimal Standards for Description of New Taxa in the Order Halobacteriales. *International Journal of Systematic Bacteriology*, **47**, 233–238.

Park JS, Vreeland RHR, Cho BC, Lowenstein TK, Timofeeff MN, Rosenzweig WD (2009) Haloarchaeal diversity in 23, 121 and 419 MYA salts. *Geobiology*, **7**, 515–523.

Parks DH, Tyson GW, Hugenholtz P, Beiko RG (2014) STAMP: Statistical analysis of taxonomic and functional profiles. *Bioinformatics*, **30**, 3123–3124.

Pašić L, Bartual SG, Ulrih NP, Grabnar M, Velikonja BH (2005) Diversity of halophilic archaea in the crystallizers of an Adriatic solar saltern. *FEMS Microbiology Ecology*, **54**, 491–498.

Podell S, Emerson JB, Jones CM et al. (2014) Seasonal fluctuations in ionic concentrations drive microbial succession in a hypersaline lake community. *The ISME Journal*, **8**, 979–90.

Poretsky R, Rodriguez-R LM, Luo C, Tsementzi D, Konstantinidis KT (2014) Strengths and Limitations of 16S rRNA Gene Amplicon Sequencing in Revealing Temporal Microbial Community Dynamics. *PLoS ONE*, **9**, e93827.

Purdy KJ, Cresswell-Maynard TD, Nedwell DB, McGenity TJ, Grant WD, Timmis KN, Embley TM (2004) Isolation of halarchaea that grow at low salinites. *Environmental Microbiology*, **6**, 591–595.

Quadri I, Hassani II, l'Haridon S, Chalopin M, Hacène H, Jebbar M (2016) Characterization and antimicrobial potential of extremely halophilic archaea isolated from hypersaline environments of the Algerian Sahara. *Microbiological Research*, **186**, 119–131.

Radax C, Gruber C, Stan-Lotter H (2001) Novel haloarchaeal 16S rRNA gene sequences from Alpine Permo-Triassic rock salt. *Extremophiles*, **5**, 221–228.

Ramana CV, Srinivas A, Subhash Y, Tushar L, Mukherjee T, Kiran PU, Sasikala C (2013) *Salinicoccus halitifaciens* sp. nov., a novel bacterium participating in halite formation. *Antonie van Leeuwenhoek, International Journal of General and Molecular Microbiology*, **103**, 885–898.

Ranjan R, Rani A, Metwally A, McGee HS, Perkins DL (2016) Analysis of the microbiome: Advantages of whole genome shotgun versus 16S amplicon sequencing. *Biochemical*

and Biophysical Research Communications, **469**, 967–77.

Reiser R, Tasch P (1960) Investigation of the viability of osmophile bacteria of great geological age. *Transactions of the Kansas Academy of Science. Kansas Academy of Science*, **63**, 31–34.

Roberts MF, Galinski E, Martin D et al. (2005) Organic compatible solutes of halotolerant and halophilic microorganisms. *Saline Systems*, **1**, 5.

Robinson CK, Webb K, Kaur A et al. (2011) A major role for nonenzymatic antioxidant processes in the radioresistance of Halobacterium salinarum. *Journal of Bacteriology*, **193**, 1653–1662.

De Rosa M, Gambacorta A, Nicolaus B, Grant WD (1983) A C25,C25 Diether Core Lipid from Archaebacterial Haloalkaliphiles. *Microbiology*, **129**, 2333–2337.

Sankaranarayanan K, Timofeeff MN, Spathis R, Lowenstein TK, Lum JK (2011) Ancient microbes from halite fluid inclusions: Optimized surface sterilization and DNA extraction (ed Ouzounis CA). *PLoS ONE*, **6**, e20683.

Sankaranarayanan K, Lowenstein TK, Timofeeff MN, Schubert B a, Lum JK (2014) Characterization of ancient DNA supports long-term survival of Haloarchaea. *Astrobiology*, **14**, 553–60.

Sato Y, Kimura H (2019) Temperature-dependent expression of different guanine-plus-cytosine content 16S rRNA genes in Haloarcula strains of the class Halobacteria. *Antonie van Leeuwenhoek, International Journal of General and Molecular Microbiology*, **112**, 187–201.

Satterfield CL, Lowenstein TK, Vreeland RH, Rosenzweig WD, Powers DW (2005) New evidence for 250 Ma age of halotolerant bacterium from a Permian salt crystal. *Geology*, **33**, 265–268.

Savage KN, Krumholz LR, Oren A, Elsahed MS (2007) *Haladaptatus paucihalophilus* gen. nov., sp. nov., a halophilic archaeon isolated from a low-salt, sulfide-rich spring. *International Journal of Systematic and Evolutionary Microbiology*, **57**, 19–24.

Schubert BA, Lowenstein TK, Timofeeff MN, Parker MA (2009a) How do prokaryotes survive in fluid inclusions in halite for 30 k.y.? *Geology*, **37**, 1059–1062.

Schubert BA, Lowenstein TK, Timofeeff MN (2009b) Microscopic identification of prokaryotes in modern and ancient halite, Saline Valley and Death Valley, California. *Astrobiology*, **9**, 467–482.

Schubert BA, Timofeeff MN, Lowenstein TK, Polle JEW (2010a) *Dunaliella* Cells in Fluid Inclusions in Halite: Significance for Long-term Survival of Prokaryotes. *Geomicrobiology Journal*, **27**, 61–75.

Schubert BA, Lowenstein TK, Timofeeff MN, Parker MA (2010b) Halophilic archaea cultured from ancient halite, Death Valley, California. *Environmental Microbiology*, **12**, 440–454.

Seckbach J, Oren A, Stan-Lotter H (2015) Polyextremophiles and the Constraints for Terrestrial Habitability. In: *Polyextremophiles : Life Under Multiple Forms of Stress*. Springer.

Shahmohammadi HR, Asgarani E, Terato H et al. (1998) Protective roles of bacterioruberin and intracellular KCl in the resistance of Halobacterium salinarium against DNA-damaging agents. *Journal of Radiation Research*, **39**, 251–62.

Soppa J (2013) Evolutionary advantages of polyploidy in halophilic archaea. *Biochemical Society transactions*, **41**, 339–43.

Sorokin DY, Berben T, Melton ED, Overmars L, Vavourakis CD, Muyzer G (2014) Microbial diversity and biogeochemical cycling in soda lakes. *Extremophiles*, **18**, 791–809.

Sorokin DY, Kublanov I V., Yakimov MM, Rijpstra WIC, Sinninghe Damsté JS (2016a) *Halanaeroarchaeum sulfurireducens* gen. nov., sp. nov., the first obligately anaerobic sulfur-respiring haloarchaeon, isolated from a hypersaline lake. *International Journal of Systematic and Evolutionary Microbiology*, **66**, 2377–2381.

Sorokin DY, Kublanov I V, Gavrilov SN et al. (2016b) Elemental sulfur and acetate can support life of a novel strictly anaerobic haloarchaeon. *The ISME Journal*, **10**, 240–252.

Sorokin DY, Messina E, Smedile F et al. (2017) Discovery of anaerobic lithoheterotrophic haloarchaea, ubiquitous in hypersaline habitats. *The ISME Journal*, **11**, 1245–1260.

Sowers KR, Gunsalus RP (1995) Halotolerance in *Methanosarcina* spp.: Role of N-Acetyl-β-Lysine, α-Glutamate, Glycine Betaine, and K+ as Compatible Solutes for Osmotic Adaptation. *Applied and Environmental Microbiology*, **61**, 4382–4388.

Speelmans G, Poolman B, Konings WN (1995) Na+ as coupling ion in energy transduction in extremophilic Bacteria and Archaea. *World Journal of Microbiology & Biotechnology*, **11**, 58–70.

Stan-Lotter H, McGenity TJ, Legat A, Denner EBM, Glaser K, Stetter KO, Wanner G (1999) Very similar strains of *Halococcus salifodinae* are found in geographically separated Permo-Triassic salt deposits. *Microbiology*, **145**, 3565–3574.

Stan-Lotter H, Pfaffenhuemer M, Legat A, Busse HJ, Radax C, Gruber C (2002) *Halococcus dombrowskii* sp. nov., an archaeal isolate from a Permian alpine salt deposit. *International Journal of Systematic and Evolutionary Microbiology*, **52**, 1807–1814.

Stevenson A, Cray JA, Williams JP et al. (2015) Is there a common water-activity limit for the three domains of life. *ISME Journal*, **9**, 1333–1351.

Swanson J, Reed D, Ams D, Norden D (2012) Status report on the microbial characterization of halite and groundwater samples from the WIPP.

Tadeo X, López-Méndez B, Trigueros T, Laín A, Castaño D, Millet O (2009) Structural basis for the aminoacid composition of proteins from halophilic archea (ed Petsko GA). *PLoS Biology*, **7**, e1000257.

Ugalde JA, Podell S, Narasingarao P, Allen EE (2011) Xenorhodopsins, an enigmatic new class of microbial rhodopsins horizontally transferred between archaea and bacteria. *Biology Direct*, **6**, 52.

Uritskiy G, Diruggiero J (2019) Applying Genome-Resolved Metagenomics to Deconvolute the Halophilic Microbiome.

Vaisman N, Oren A (2009) *Salisaeta longa* gen. nov., sp. nov., a red, halophilic member of the Bacteroidetes. *International Journal of Systematic and Evolutionary Microbiology*, **59**, 2571–2574.

Valentine DL (2007) Adaptations to energy stress dictate the ecology and evolution of the Archaea. *Nature Reviews Microbiology*, **5**, 316–323.

Viver T, Orellana L, González-Torres P et al. (2018) Genomic comparison between members of the *Salinibacteraceae* family, and description of a new species of Salinibacter (*Salinibacter altiplanensis* sp. nov.) isolated from high altitude hypersaline environments of the Argentinian Altiplano. *Systematic and Applied Microbiology*.

van de Vossenberg JL, Driessen a J, Grant WD, Konings WN (1999) Lipid membranes from halophilic and alkali-halophilic Archaea have a low H+ and Na+ permeability at high salt

concentration. *Extremophiles*, **3**, 253–7.

Vreeland RH, Rosenzweig WD, Powers DW (2000) Isolation of a 250 million-year-old halotolerant bacterium from a primary salt crystal. *Nature*, **407**, 897–900.

Vreeland RH, Jones J, Monson A et al. (2007) Isolation of live Cretaceous (121-112 million years old) halophilic Archaea from primary salt crystals. *Geomicrobiology Journal*, **24**, 275–282.

Werner J, Ferrer M, Michel G et al. (2014) Halorhabdus tiamatea: Proteogenomics and glycosidase activity measurements identify the first cultivated euryarchaeon from a deep-sea anoxic brine lake as potential polysaccharide degrader. *Environmental Microbiology*, **16**, 2525–2537.

Williams JP, Hallsworth JE (2009) Limits of life in hostile environments: no barriers to biosphere function? *Environmental Microbiology*, **11**, 3292–3308.

Williams TJ, Allen MA, DeMaere MZ, Kyrpides NC, Tringe SG, Woyke T, Cavicchioli R (2014) Microbial ecology of an Antarctic hypersaline lake: genomic assessment of ecophysiology among dominant haloarchaea. *The ISME Journal*, **8**, 1645–58.

Winters YD, Lowenstein TK, Timofeeff MN (2015) Starvation-Survival in Haloarchaea. *Life (Basel, Switzerland)*, **5**, 1587–609.

Xia J, Dunlap CA, Flor-Weiler L, Rooney AP, Chen GJ, Du ZJ (2016) *Longibacter salinarum* gen. nov., sp. nov., isolated from a marine solar saltern. *International Journal of Systematic and Evolutionary Microbiology*, **66**, 3287–3292.

Xu XW, Wu YH, Zhang H Bin, Wu M (2007) *Halorubrum arcis* sp. nov., an extremely halophilic archaeon isolated from a saline lake on the Qinghai-Tibet Plateau, China. *International Journal of Systematic and Evolutionary Microbiology*, **57**, 1069–1072.

Yancey PH (2005) Organic osmolytes as compatible, metabolic and counteracting cytoprotectants in high osmolarity and other stresses. *The Journal of experimental biology*, **208**, 2819–2830.

Youssef NH, Savage-Ashlock KN, McCully AL, Luedtke B, Shaw EI, Hoff WD, Elshahed MS (2014) Trehalose/2-sulfotrehalose biosynthesis and glycine-betaine uptake are widely spread mechanisms for osmoadaptation in the Halobacteriales. *The ISME Journal*, **8**, 636–49.

Zenke R, Gronau S von, Bolhuis H, Gruska M, Pfeiffer F, Oesterhelt D (2015) Fluorescence microscopy visualization of halomucin, a secreted 927 kDa protein surrounding Haloquadratum walsbyi cells. *Frontiers in Microbiology*, **6**, 249.

Zerulla K, Soppa J (2014) Polyploidy in haloarchaea: Advantages for growth and survival. *Frontiers in Microbiology*, **5**, 274.

Zhou J, Liu H-C, Xiang H, Chen S (2016) *Haloparvum sedimenti* gen. nov., sp. nov., a member of the family Haloferacaceae. *International Journal of Systematic and Evolutionary Microbiology*, **66**, 2327–2334.